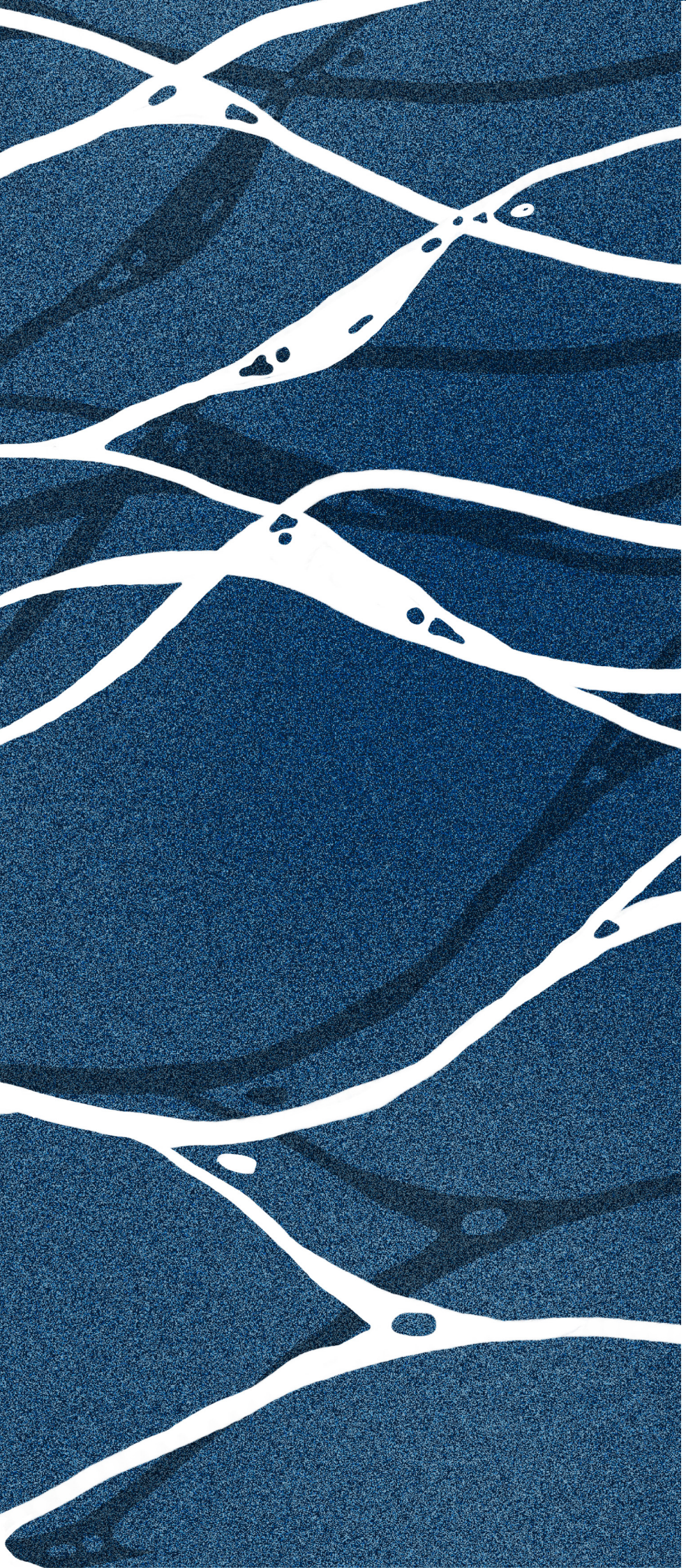

Grounded Resilience

a Rainwater Simulation Framework for Improving Building Flood Resilience through Blue-Green Infrastructure Design Strategies

Vadya Dzauqiah
6184030

Graduation Project

MSc Building Technology
Faculty of Architecture
and the Built Environment TU Delft

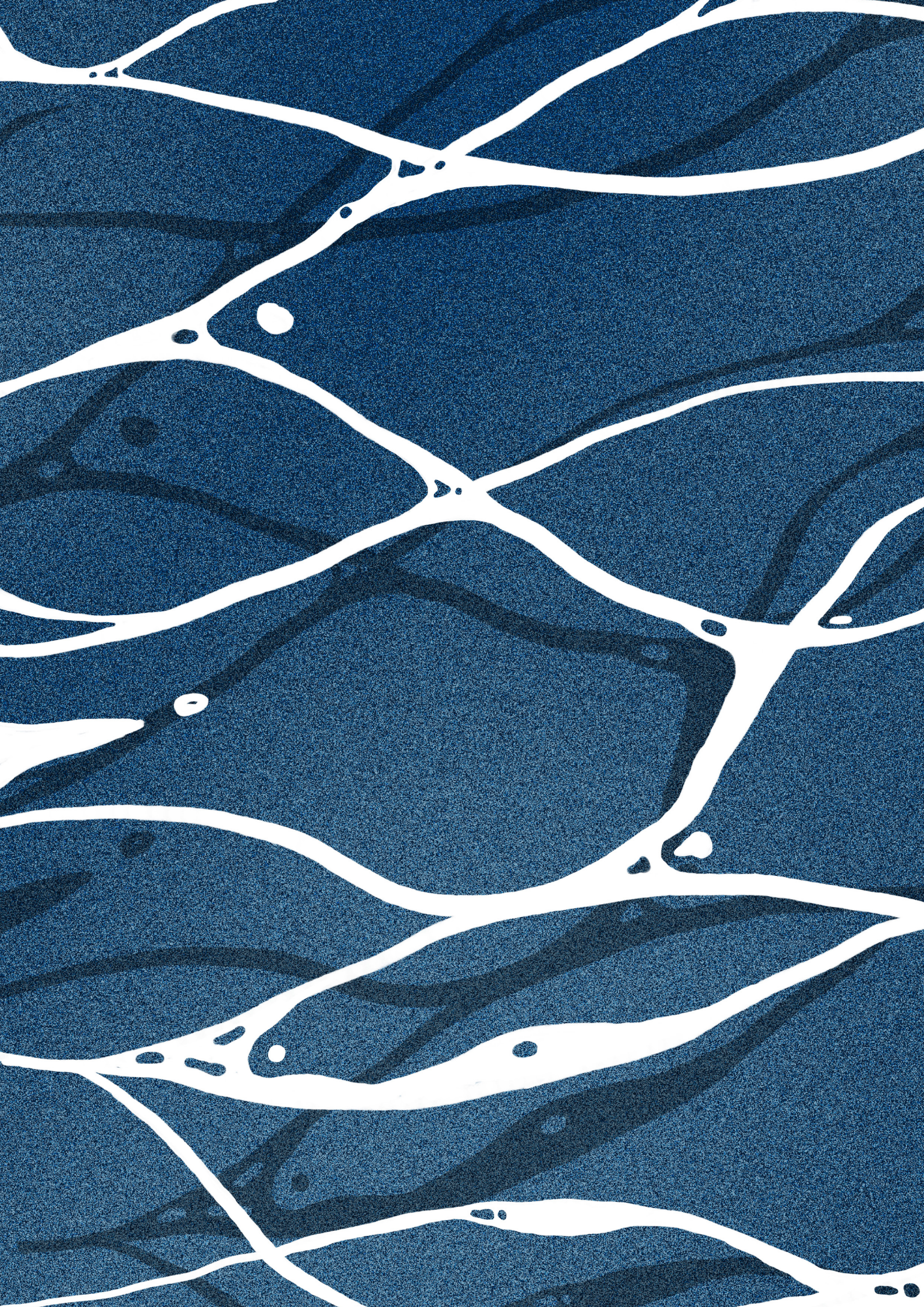

Grounded Resilience

a Rainwater Simulation Framework for Improving Building Flood Resilience through Blue-Green Infrastructure Design Strategies

Author
Vadya Dzauqiah
6184030

First Mentor
Dr. Simona Bianchi
Assistant Professor of the ReStruct Group

Second Mentor
Dr. Daniele Cannatella
Assistant Professor of Urban Data for Design

Delegate
Ir. Henri van Bennekom
MSc Coordinator of Architecture Department

Delft University of Technology
Faculty of Architecture and the Built Environment
MSc Architecture, Urbanism and Building Sciences | Track Building Technology

This thesis was funded by
Indonesia Endowment Fund for Education (LPDP Scholarship)

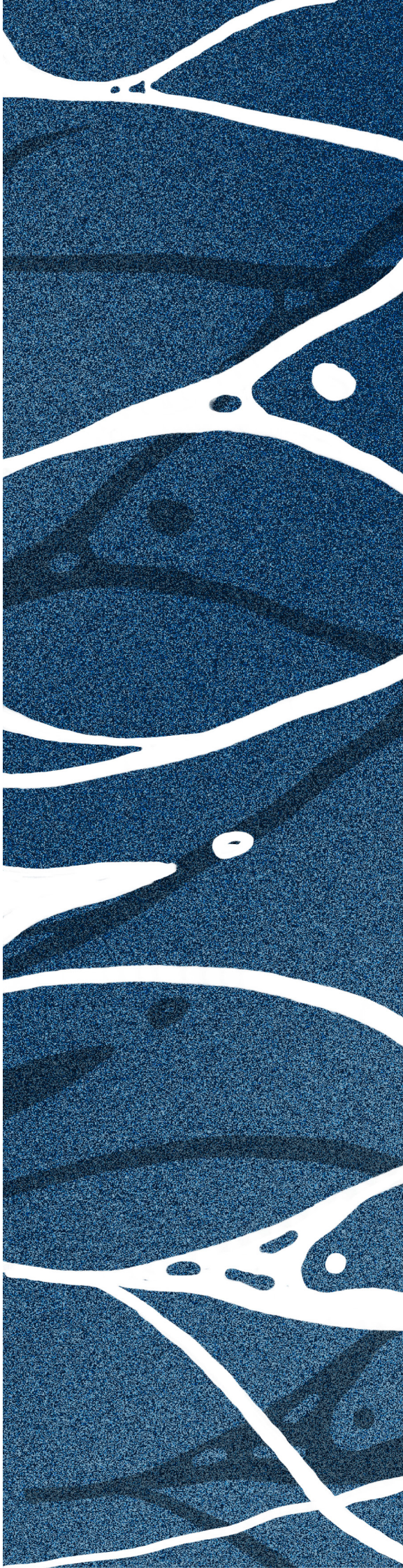

Disclaimer
Unless stated otherwise, all images, photographs, diagrams, and visual materials included in this report were created or captured by the author. Any external visual content has been clearly credited to its original source in accordance with academic and ethical standards.

Artificial Intelligence (AI) tools were used in a limited and responsible manner during the preparation of this report. These tools supported tasks such as language refinement, idea development, restructuring of text, and improving readability. All AI-generated suggestions were critically reviewed, edited, and verified by the author before inclusion. The research findings, interpretations, conclusions, and overall academic responsibility remain entirely the author's own. Care was taken to ensure accuracy, originality, and proper attribution throughout the report.

Acknowledgement

I would like to begin by expressing my gratitude to my parents, grandparents, little sister, and my big family for their unwavering support in allowing me to pursue what I love. I am forever grateful to have been raised in a family that has always prioritised education first and foremost.

I would also like to thank my mentors, Simona Bianchi and Daniele Cannatella, for their guidance, patience, and trust throughout this thesis journey. Thank you for giving me the opportunity to explore a topic that is slightly unusual, combining two domains that have always been close to my interests: architecture and urbanism. This research was only possible because you believed in the idea from the beginning and encouraged me to keep developing it.

I am also grateful to Rob van Houten for helping me understand Grasshopper at an urban scale and introducing me to the Kangaroo Solver, which became an important part of this research workflow. My thanks also go to G. A. Ken Arroyo Ohori for helping me with questions related to image processing and for offering his insights when I was trying to understand unfamiliar technical challenges.

This master's journey was made possible through the support of the LPDP Scholarship, which granted me the opportunity to pursue my studies at TU Delft.

To Pak Donny Koerniawan and Pak Agus Suharjono Ekomadyo, thank you for your support throughout my master's degree journey. I would also like to thank my colleagues in Indonesia: Pak Muhammad Sagitha, Bu Anggi Paramitha, Rio, Vira, and Rendi, who have shaped the way I understand architecture and practice.

To Febricetta and Rizqi, thank you for your support as friends, and especially for helping me navigate coding, data processing, and technical challenges that were beyond my own knowledge.

Last but not least, I am grateful to the people who made my time in Delft far more meaningful than I had expected: Rafif, Celia, Emmanouela, Janvi, Krishna Koushik, Purvi, Sana, Thalia, Thanassis, and my fellow Building Technology 2024 cohort; my Indonesian friends, Thoriq, Ammar, Grase, and Andika Hadi; and the Indelftnesia team: Rifa, Ovi, Maulvi, Muktitika, Yogan, and Garry. Thank you for making the past two years worth remembering.

Fondazione Querini Stampalia by Carlo Scarpa (Author, 2025)

Motivation

Water has always fascinated me, not only as a natural element, but also as something that shapes the way people experience, inhabit, and move through space. In architecture and spatial design, water has often been approached as both an experiential and aesthetic component. It reflect, guide movement, create atmosphere, and define the relationship between people and their surroundings. This can be seen, for example, in the work of Carlo Scarpa, whose architecture often becomes more alive through the presence of water.

Today, technological developments allow environmental conditions to be understood through more data-driven approaches. These technologies create opportunities for designers to engage with water not only intuitively, but also analytically and systematically as part of the design process. For me, this opens an important question of how spatial design can be supported by data without losing its sensitivity to place, experience, and people.

Growing up in Indonesia, particularly within dense urban environments, I became aware of how fragile and inconsistent water management systems can be. Flooding, poor infrastructure, and unequal access to quality public spaces were recurring realities that shaped my everyday experience. Rather than viewing these issues solely as engineering problems, I believe they should also be addressed spatially and socially. Designers, architects, and urban practitioners all have a role in shaping environments that respond more responsibly to water-related challenges.

The Netherlands, with its long history of living with water and its well-developed culture of spatial and environmental data, provides a valuable context for me to learn from. Through this thesis, I see an opportunity not only to develop a computational design-support workflow, but also to reflect on how data-driven methods can become more accessible to designers. In this sense, this research is also part of a larger personal intention: to learn from the Dutch context, translate this knowledge through my own perspective, and eventually bring something meaningful back home.

Abstract

As populations continue to grow, cities also continue to densify and expand. In this process, natural surfaces are increasingly replaced by impervious surfaces, which reduce the ability of rainwater to infiltrate into the ground. This increases pluvial flood risk and shows the need to rethink how urban areas are built. One way to do this is by making room for more natural areas within the urban fabric. However, in dense cities where space is limited, these areas also need to perform multiple functions. Blue-Green Infrastructure offers this form of spatial adaptation by combining rainwater regulation with other urban benefits. While some BGI strategies are applied at the building scale, this research focuses on ground-based BGI adaptation: strategies applied to open spaces and ground surfaces at the urban scale.

Ground-based BGI adaptation is often evaluated through its ability to reduce flood hazard in general. However, when adaptation resources and available urban space are limited, it becomes important to ask where adaptation can create the most meaningful improvement. This is why a more targeted receptor-based perspective matters. Among the many urban receptors affected by flooding, this research focuses on buildings and examines how building flood-resilience improvement can be understood through an urban adaptation lens. Reflecting the idea of Grounded Resilience, the research explores how building-level flood-resilience assessment can be used to ground the spatial design of ground-based BGI adaptation strategies. To do this, the research develops a Grasshopper-based rainwater simulation workflow that links BGI adaptation with building-level flood-resilience assessment. The workflow connects particle-based runoff simulation, BGI absorption logic, flood-depth estimation, and building-level resilience scoring within one design environment.

The workflow is tested in the Lijnbaan area in Rotterdam using terrain data, 3D building geometry, building attributes, rainfall input, and selected BGI scenarios. The results show that BGI effectiveness is not determined by storage capacity or adapted area alone, but also by its position in relation to runoff pathways, accumulation areas, and affected buildings. Therefore, BGI adaptation should not only be evaluated through general flood-depth reduction, but also through its ability to reduce flood impact where building resilience is most affected. The workflow enables scenario comparison through absorbed volume, flood-depth changes, resilience-score differences, movement-path visualisation, and indicative implementation cost.

The research shows that the developed workflow is most useful as an early-stage comparative design-support framework, rather than as a fully calibrated hydraulic or damage-prediction model. Its value lies in connecting site runoff behaviour with building resilience outcomes, helping designers identify where BGI adaptation may create meaningful local improvement and where adaptation is most needed.

The Grasshopper custom components, workflow examples, and supporting scripts developed for this thesis are available in the project repository.

github.com/vadyadzauqiah/Grounded-Resilience

Table of Contents

Case Study

Discussion

Conclusion

01
Context

Background

Problem Definition

Research Question

Methodology

1.1 | Background

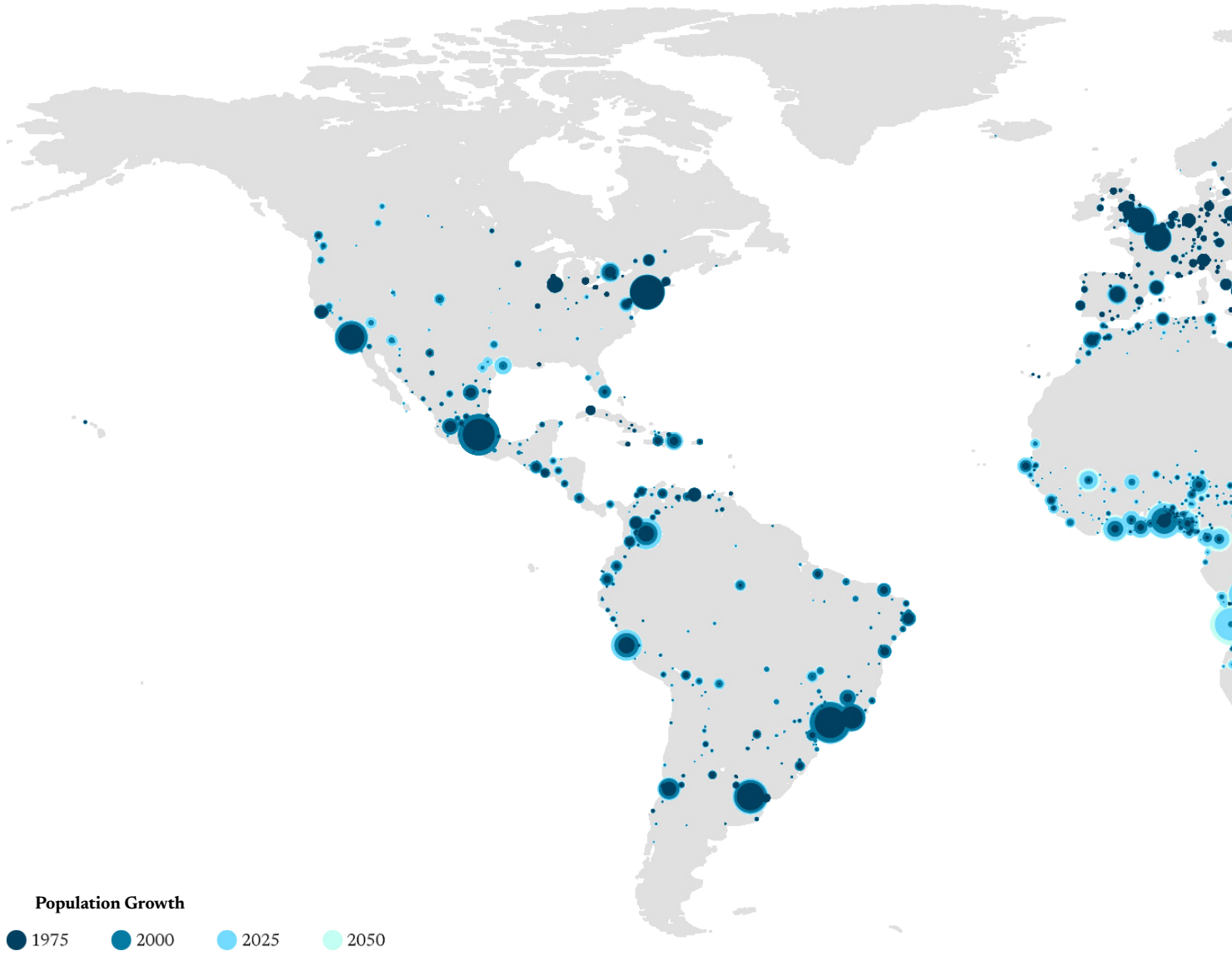

Figure 1. Global urban agglomeration populations (1975–2050) (LumiNocity visualization based on United Nations World Urbanization Prospects 2025)

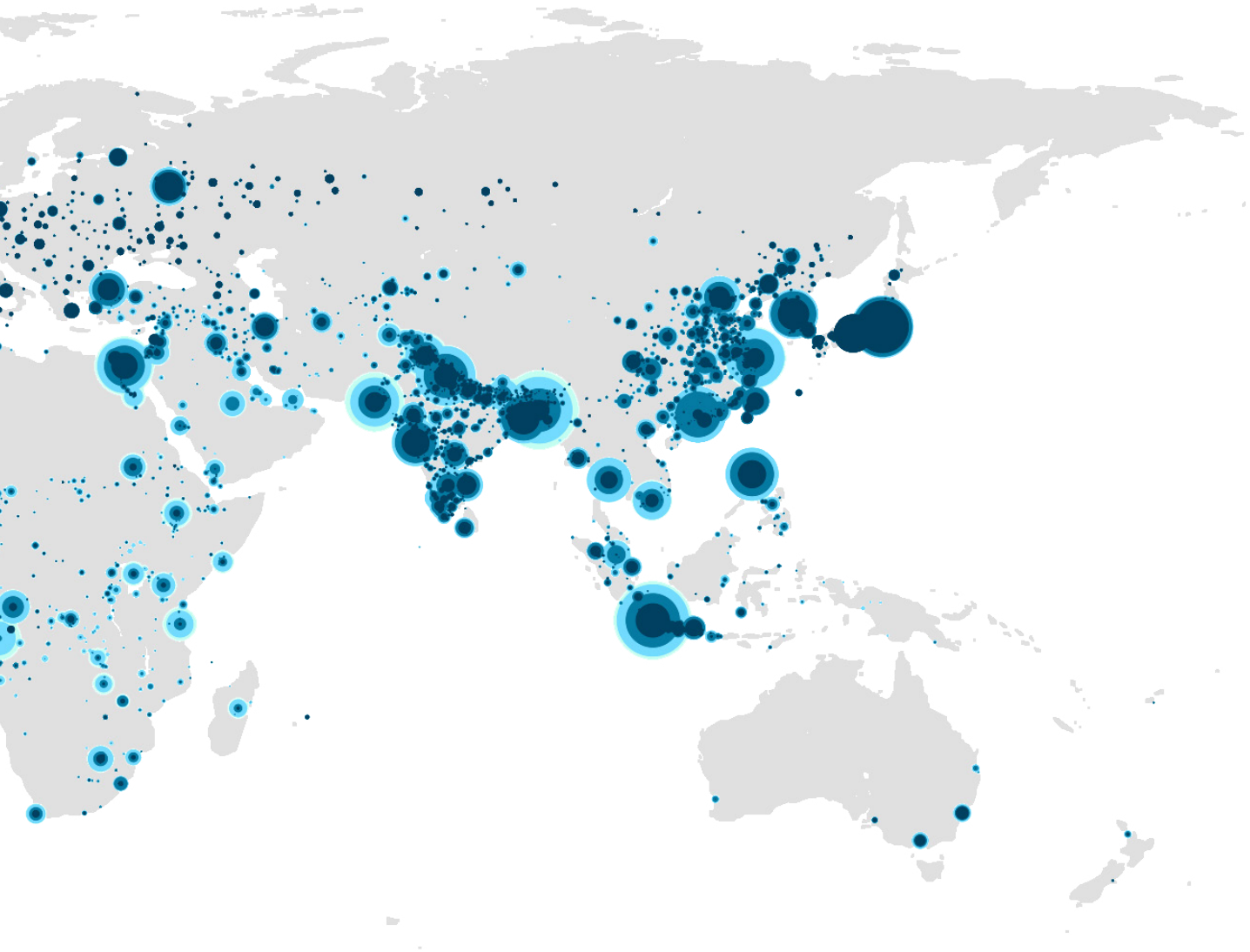

The More We Grow, The More We Build

According to the United Nations' World Urbanization Prospects 2025, nearly half of the world's population now lives in urban areas, with this proportion expected to continue growing in the coming decades. This is a testament to what is inevitable: as population growth expands, so is our cities. As urban areas continue to develop, natural landscapes are increasingly replaced by dense built environments, roads, and other impermeable surfaces that alter the natural movement and absorption of water.

Figure 2. Collage of urban flood impacts around the world (Left to Right: (Oregon Public Broadcasting, 2024), (Al-Jazeera, 2025), (CNN, 2021), (CNN, 2023), (CNN, 2023), (CNN, 2023), (The Guardian, 2019), New Straits Times (2026), (The Guardian, 2019)

The More We Build, The Less We Absrob

Urbanization intensifies floods by increasing impermeable surfaces and modifying flow paths (Bertilsson et al., 2019). At the same time, climate change further increases the pressure on urban water systems by exposing more people to extreme weather events. The Intergovernmental Panel on Climate Change (2022) highlights that climate change threatens water security, particularly in areas with existing socioeconomic vulnerabilities. In the context of rapid urbanization, this creates a critical challenge: as cities expand, the combination of altered hydrological cycles, increasing surface runoff, and densifying built environments significantly heightens the risk of flood-related failures within urban systems and infrastructure.

A Shift in The Way We Build

To mitigate localized inundation, the increased amount of rainwater flowing over urban surfaces, known as surface runoff, due to land-cover change cannot be addressed only through conventional drainage infrastructure. Instead, it requires a more integrated approach that combines engineered systems with natural and spatial strategies (Watson & Adams, 2011). This reflects a broader shift in urban water management: from a purely defensive, "fail-safe" approach toward a more resilient "fail-to-safe" design paradigm, where urban spaces are expected not only to resist flooding, but also to absorb, adapt to, and recover from it (Ahern, 2011).

Within this shift, rainwater management is no longer seen as the sole responsibility of civil engineers. It has become an integrated design concern, reflected in concepts such as Water Sensitive Urban Design (WSUD) in Australia, Low Impact Development (LID) in the United States and New Zealand, and Sustainable Urban Drainage Systems (SUDS) in the United Kingdom (Burns et al., 2012). These approaches commonly rely on Blue-Green Infrastructure (BGI), which uses nature-based and multifunctional urban spaces to manage water closer to its source. In this way, urban spaces can take on different roles under different conditions: functioning as public amenities during dry periods, while also providing retention, infiltration, or conveyance capacity during heavy rainfall events. For architects, landscape architects, and urban designers, this means that water management needs to be considered from the early design stages. Early integration allows spatial decisions, building layouts, public spaces, and BGI strategies to be coordinated before design opportunities are lost or conflicts emerge between building structures and rainwater management systems (Chen et al., 2016).

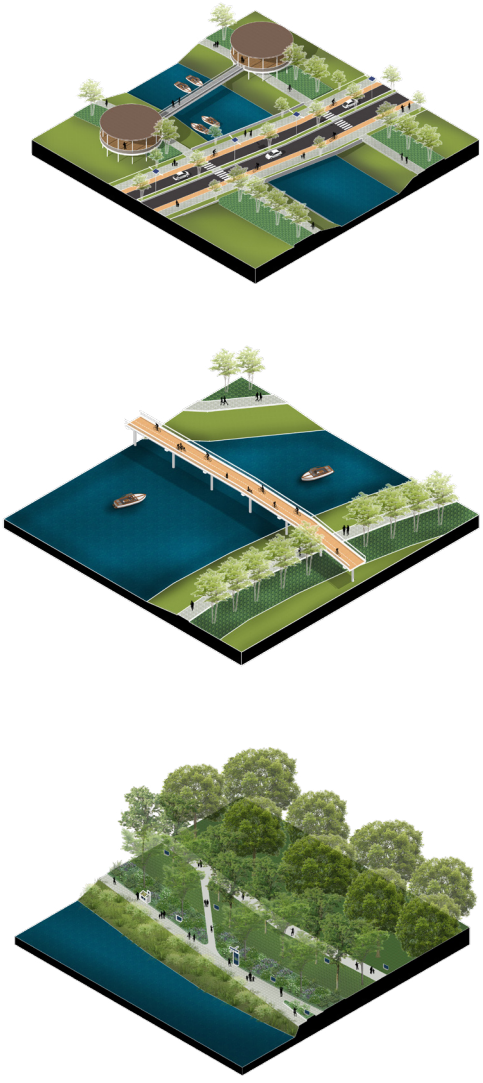

Figure 3. Blue Green Infrastructure

Data Driven Decision

As design software evolves, data and simulation are increasingly used to support early-stage architectural and urban design decisions. In flood-related design, this allows designers to move beyond general assumptions and explore how rainfall, terrain, land cover, and built form may influence surface runoff and flood impact. For BGI adaptation, the effect of a strategy depends not only on how much water it can store, but also on where it is placed and how runoff moves across the site.

A data-driven workflow can therefore support design decisions by linking spatial design inputs with flood-related performance indicators before adaptation strategies are finalised. During early design stages, when spatial layouts, public spaces, building edges, and BGI locations are still flexible, simulation can help make these relationships more visible. This allows designers to compare adaptation options and understand their potential consequences more systematically.

State of the Art

Previous studies show that computational tools can support early-stage rainwater analysis by translating terrain, land cover, and rainfall input into runoff-related outputs. More detailed hydraulic or hydrological software can represent spatially varied infiltration, drainage behaviour, and sewer-network interactions more accurately. However, these tools are often data-intensive, technically demanding, less accessible, and separated from the design environment. For architects, landscape architects, and urban designers, this can create barriers during early-stage exploration, where design alternatives change frequently.

This research therefore focuses on workflows developed within Rhinoceros 3D and Grasshopper, because Grasshopper allows simulation logic to be embedded within a familiar parametric design environment. Within this environment, rainfall, terrain, BGI, and building-related inputs can be adjusted and evaluated more interactively. This makes Grasshopper relevant for exploring BGI adaptation at the early design stage, especially when different BGI areas need to be assigned their own performance parameters.

The following subsections review relevant Grasshopper-based workflows and rainwater assessment precedents. The review is organised into two parts: first, existing tools and workflows are discussed; second, the remaining gaps are identified.

Existing Grasshopper Based Plugin & Workflow

Groundhog

Groundhog (www.groundhog.philipbelesky.com) is a Grasshopper plugin and documentation platform developed to support computational design methods in landscape architecture, providing components and reference workflows for analysing and representing landscape features. Groundhog provides several hydrology-related components that allow users to explore how water may move and accumulate across a terrain surface. Its workflow is mainly based on terrain-driven analysis, where a mesh surface is used as the main input. Components such as flow path, flow catchment, and flow saturation can then be used to trace possible surface water movement, identify catchment areas, and estimate relative saturation patterns across the landscape.

One relevant feature of Groundhog is that it translates terrain geometry into simplified hydrological indicators. The Flow Path (Figure 4) component traces possible runoff movement across the terrain, while Flow Catchments (Figure 5) groups these paths according to their approximate end locations and expresses the result as a relative volume percentage. This means that Groundhog can indicate which parts of the landscape are likely to receive more accumulated runoff, even though it does not calculate exact flood volume or depth. The Flow Saturation component further extends this by applying a start volume and segment loss value along the flow paths, allowing users to estimate relative saturation patterns across the terrain.flow paths, allowing users to estimate relative saturation patterns across the terrain.

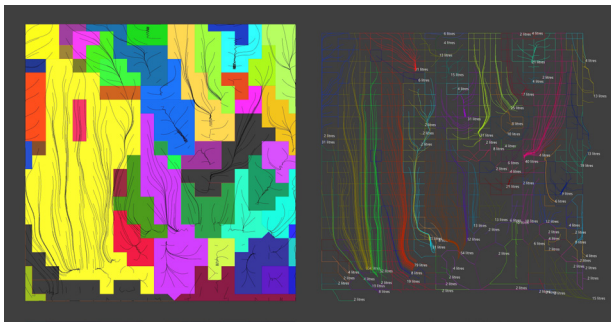

Figure 4. Groundhog flow path feature (groundhog.philipbelesky.com)

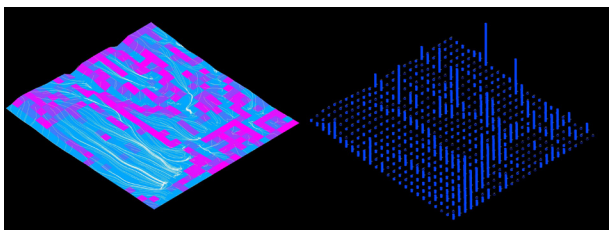

Figure 5. Groundhog flow catchment feature (groundhog.philipbelesky.com)

However, Groundhog remains limited for the purpose of this research because its hydrology-related outputs are primarily relative indicators rather than direct flood-depth values. In addition, Groundhog's saturation logic applies a single Segment Loss value to the whole analysed mesh. This means that if the entire site is simulated as one mesh, the same infiltration or water-loss value is applied across the whole area. To assign different values to different site patches, the mesh would need to be divided and analysed separately, making the workflow less straightforward for spatially varied BGI assessment. Therefore, while Groundhog provides a relevant precedent for Grasshopper-based terrain-driven water analysis, further workflow development is needed to connect BGI-specific absorption behaviour with flood-depth estimation and building-level resilience assessment.

Kangaroo

Developed by Daniel Piker, Kangaroo is a live physics engine for interactive simulation, form-finding, optimization, and constraint solving. In Grasshopper, Kangaroo works by applying forces and constraints to geometry and iteratively updating their positions until a balanced state is reached. Although Kangaroo is not specifically developed as a hydrological simulation tool, several previous studies have adapted it to represent rainwater movement by treating water as particles moving across a terrain surface. These workflows primarily rely on the Kangaroo Solver component in Grasshopper, which receives the particles, forces, and constraints as inputs and iteratively updates the particle positions during the simulation process, as illustrated in Figure 6.

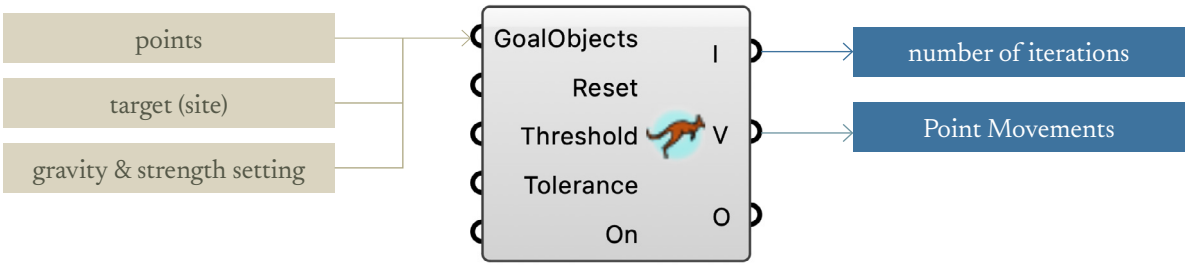

Figure 6. Kangaroo Solver component

A related Kangaroo-based workflow can also be found in the Spatial Resilience Toolbox – Flooding (SRTF) developed by Morschek et al. (2019) (Figure 7). The toolbox was developed in Grasshopper to integrate flood-related simulation and analysis into the urban planning process, allowing users to evaluate spatial layouts according to their flood resilience status. Its rain-runoff simulation uses Kangaroo to represent rainfall through particles with mass and gravitational force, allowing them to move downward across 3D geometry and accumulate around bottlenecks or depressions. The evaluation also considers buildings as urban receptors by counting the number of particles located within a defined range around each building and dividing this value by the building footprint area to estimate inundation risk. However, the resulting inundation risk is mainly derived from the density of accumulated particles around buildings and street segments. Buildings surrounded by more particles are assigned a higher risk value, while buildings with fewer nearby particles are considered less exposed. This makes the assessment useful for visualizing flood-prone areas within a spatial layout, but the risk value is not directly based on flood-depth values or building-specific data. In addition, the rain-runoff simulation does not explicitly model green-space-specific hydrological behaviour, such as infiltration or absorption capacity. Instead, different spatial elements influence runoff behaviour mainly through their geometry and position within the 3D layout, which may redirect, obstruct, or affect particle movement. Therefore, the workflow remains limited for assessing BGI as an adaptation strategy and for linking flood exposure to data-driven building-level resilience assessment.

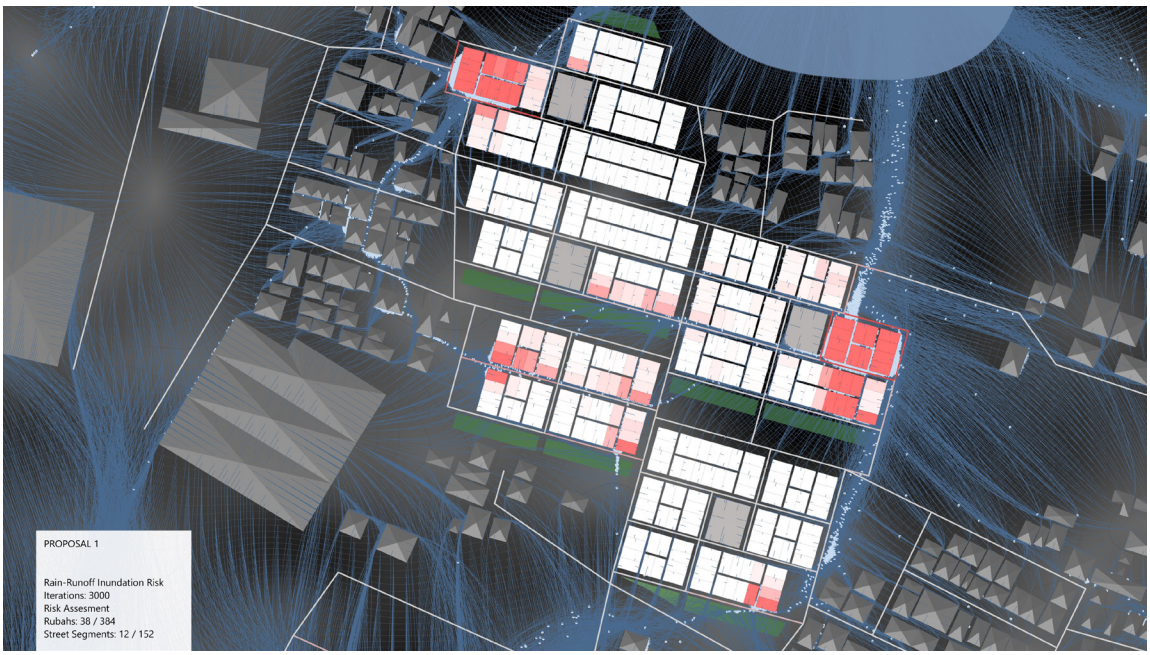

Figure 7. Spatial Resilience Toolbox Flood Analysis

Another related study is conducted by Jia et al. (2022, 2024), who used Kangaroo to simulate runoff movement, terrain interaction, and water accumulation across urban surfaces. Their workflow demonstrates how particle movement can be used to represent runoff direction and accumulation within a design environment. Compared with SRTF, Jia et al. more explicitly address land-cover interaction by distinguishing between Urban Green Space (UGS) and artificial surfaces. However, the land-cover logic in their model remains relatively simplified. The site is mainly classified into UGS and artificial surfaces, where UGS is assumed to retain stormwater while artificial surfaces are treated as non-absorptive. This creates a binary distinction between absorptive and non-absorptive surfaces, which limits the ability to represent more spatially varied BGI performance. The workflow is illustrated in Figure 8.

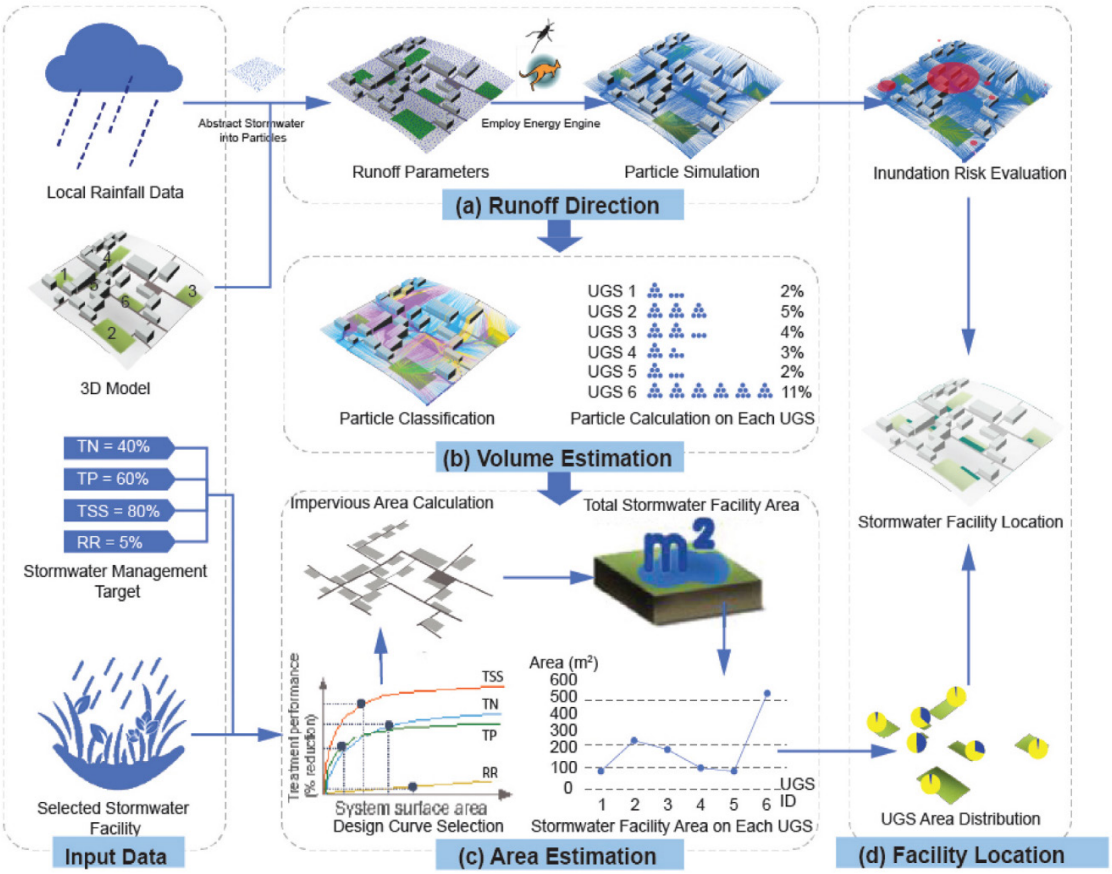

Figure 8. Runoff management workflow using Kangaroo (Jia et all., 2024)

Similarly, Luo et al. (2020) used a different Grasshopper plug-in, HoopSnake, to iteratively move rainwater particles along the steepest slope of a terrain mesh. Although the plug-in differs, the underlying principle remains similar: rainwater movement is approximated through particle behaviour across terrain geometry.

Gap Identification

While these workflows demonstrate the potential of computational tools for rainwater analysis, many design-oriented approaches still focus primarily on runoff movement and accumulation. This becomes limiting when the aim is not only to understand where water moves, but also to evaluate how flood conditions affect exposed urban receptors, including buildings. Andriessen et al. (2024) highlight this issue by arguing that existing flood models often lack detailed information about the urban environment beyond geometry and infiltration rates, making it difficult to identify direct and indirect effects on infrastructure and inhabitants. This aligns with the broader disaster-risk framing in the GAR Special Report (United Nations, 2024), which emphasises that hazard events become disasters when exposed people, assets, or ecosystems are also vulnerable.

This connection also marks the shift from identifying flood risk toward assessing flood resilience. REDi for Floods frames resilience-based flood design as a process that mitigates flood risk to enable swift recovery after flood events (Hogan et al., 2023). In this sense, buildings cannot be treated as identical exposed objects: their function, components, recovery needs, and surrounding site conditions influence how flood impact translates into resilience outcomes.

A further gap concerns how BGI performance is represented within current Grasshopper-based runoff workflows. In many design-oriented simulations, infiltration or absorption is either neglected or applied as a general condition across the whole site rather than assigned to specific land-use or BGI areas. This becomes limiting when multiple BGI strategies are applied within the same site, because different BGI types do not have the same water-management behaviour.

Together, these gaps reveal a missing link between building-level vulnerability and BGI adaptation strategies. Building-level approaches often focus on structural adaptation, damage, or recovery, while BGI strategies usually aim to reduce inundation more generally. Treating these separately overlooks the potential for BGI adaptation to be used more strategically: not only to manage runoff across the site, but also to contribute to building-specific resilience improvement before more intrusive building retrofits are required. Therefore, a more integrated Grasshopper-based workflow is needed to connect BGI performance assessment with building-level flood resilience evaluation within one design environment.

> “ Existing flood models are currently incapable of identifying the direct and indirect effects of a flood on a city’s infrastructure and its inhabitants as they are missing important information on the urban environment itself that goes beyond the geometries and infiltration rates used for standard flood simulation models. ”
>
> –Andriessen et al., 2024

Figure 9. Rainwater inundation entering residential lawns and affecting building surroundings (The Guardian, 2019)

1.2 | Problem Definition

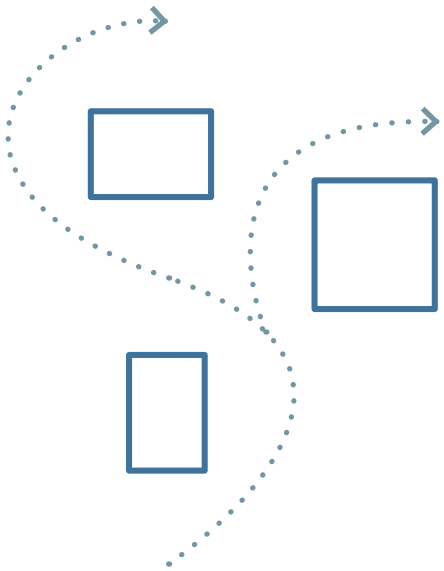

A critical missing link lies in bridging the divide between building resilience and site adaptation.

REDi for Flood frames site resilience around the capacity of buildings and site to withstand, adapt to, and recover from flood events (Hogan et al., 2023). However, these dimensions are often addressed separately in practice: building-level approaches tend to focus on structural adaptation, damage, or recovery, while BGI strategies applied at the site mainly aim to reduce inundation more generally. This separation overlooks the potential for BGI adaptation to be used more strategically, not only to manage runoff across the site, but also to contribute to building-specific resilience improvement.

Primary Objective

Building on this gap, this research develops a Grasshopper-based rainwater simulation workflow that connects building flood vulnerability with Blue-Green Infrastructure adaptation, particularly BGI strategies applied at the site scale. In this research, these are referred to as ground-based BGI adaptations, meaning adaptations applied to open spaces and ground surfaces within the site. The workflow integrates particle-based runoff simulation, BGI performance assessment, flood-depth estimation, and building-level resilience evaluation within one design environment. Through this integration, the research explores how spatial BGI adaptation can be used not only to manage runoff across the site, but also to support building-specific resilience improvement. This objective is broken down into three components:

Sub Objectives

Building Scale Resilience Assessment	Evaluation of Ground Based Blue–Green Infrastructure Performance	Simulation-Based Design Decision Support Workflow

Relevance

Existing Grasshopper-based workflows demonstrate the potential of particle-based rainwater simulation, yet they generally do not estimate actual flood depth values or link simulation outcomes to the vulnerability of specific receptors, which in this research are buildings. By connecting rainwater simulation, spatially varied BGI performance modelling, and building-level resilience scoring within a single data-driven design environment, this research offers an approach that has not previously been realised in existing tools. Rather than treating building and site adaptation as separate concerns, this research positions ground-based BGI strategies as the primary means of improving building flood resilience. This makes the workflow particularly relevant for architects and urban designers working at the neighbourhood scale during early design stages, when spatial decisions are still flexible.

Beyond its technical contribution, the workflow is designed to respond to three practical challenges faced by designers working on flood resilience at the neighbourhood scale:

Targeted Impact Over Total Coverage

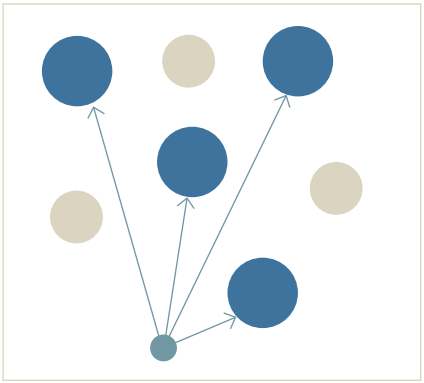

Shifts flood resilience from protecting maximum land area to prioritizing high-impact, consequence-driven adaptation.

Efficient Use of Limited Resources

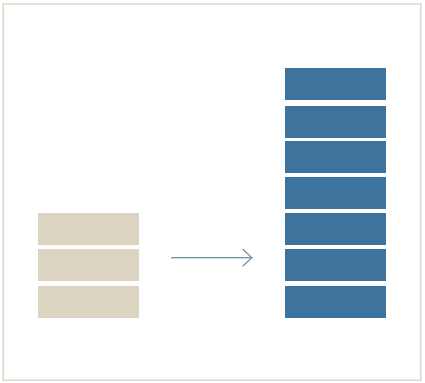

Supports data-driven decision-making for the strategic allocation of constrained budgets and scarce urban space.

Bridging the Gap Between Disciplines

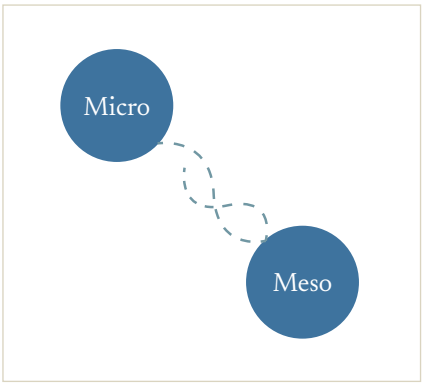

While regular building protection simulations focus on interventions on individual structures, this simulation approach leverages ground-based BGI strategies to directly enhance the flood resilience of buildings.

Scope

Research Focus

This research develops a data-driven design-support simulation environment to assess how BGI can improve building flood resilience at the neighbourhood scale. The environment integrates spatial data, rainwater simulation, BGI performance assessment, and building-level resilience calculation to compare different BGI scenarios.

Grasshopper is used for the main simulation and design process, including scenario modelling and retrieving results. QGIS is used to obtain and prepare spatial data for the case study, while Python supports preprocessing and post-processing, including data matching, calculation, result processing.

Plugin dependency in Grasshopper is kept limited, with priority given to plugins that are accessible on both Windows and macOS. The main required plugins are Kangaroo, for the particle-based simulation, and CityJSON, for obtaining and structuring Dutch 3D city-model data. Other custom components are developed by the author using Python 3 for Grasshopper.

Flood Type

The workflow focuses on pluvial flooding. Zhu et al. (2024) drawing on Falconer et al. (2009), define pluvial flooding as flooding that occurs when rainfall generates overland flow and ponding before runoff can enter the drainage system. Pluvial flooding is particularly relevant for urban-scale and neighbourhood-scale design because it is strongly influenced by local surface conditions, including the relationship between pervious and impervious surfaces, surface morphology, topography, and drainage capacity.

As Watson & Adams (2011) suggest, runoff mitigation should be addressed as close as possible to the source of runoff. This makes pluvial flooding a spatial design issue, where the location, distribution, and performance of BGI strategies directly affect how runoff is intercepted, slowed, stored, or redirected within the neighbourhood.

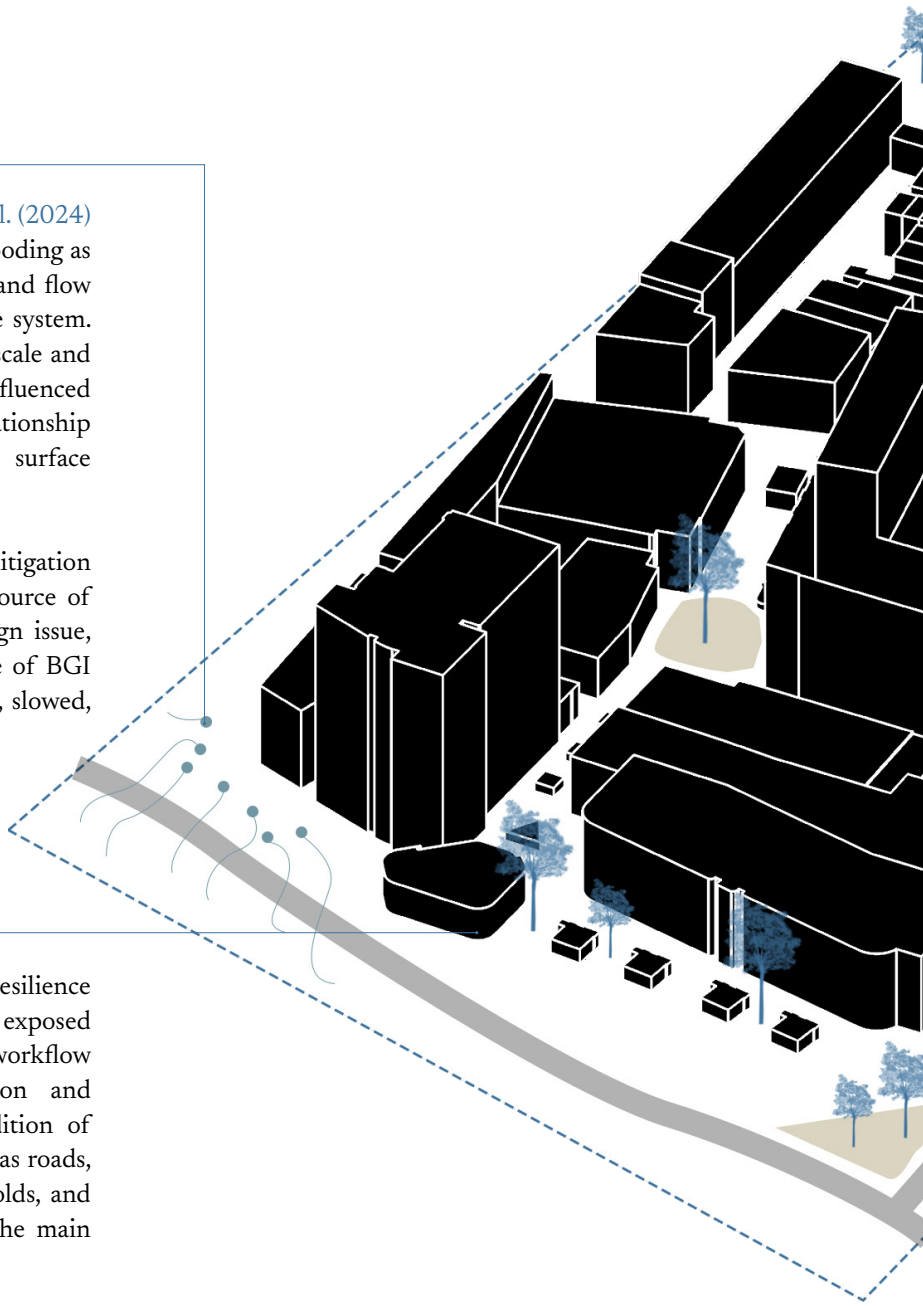

Assessment Focus

This research focuses on building-level flood resilience assessment, with buildings treated as the main exposed receptors within the neighbourhood. The workflow evaluates how changes in runoff accumulation and estimated flood depth affect the resilience condition of different building categories. Other receptors such as roads, critical infrastructure, social vulnerability, households, and evacuation accessibility, are not assessed within the main scope of this research.

Spatial Scale

The workflow is developed for neighbourhood-scale assessment, where spatial strategies, surface conditions, open-space distribution, and BGI placement can still be explored during early-stage design. This scale is relevant to architectural and urban design practice, while also allowing the assessment to capture variation between building types, urban surfaces, and site conditions. To test the workflow, it is applied to an approximately 18-hectare case study area in Rotterdam, the Netherlands. However, the purpose of the case study is to demonstrate and evaluate the workflow, rather than to provide a final design recommendation or definitive adaptation strategy for the area.

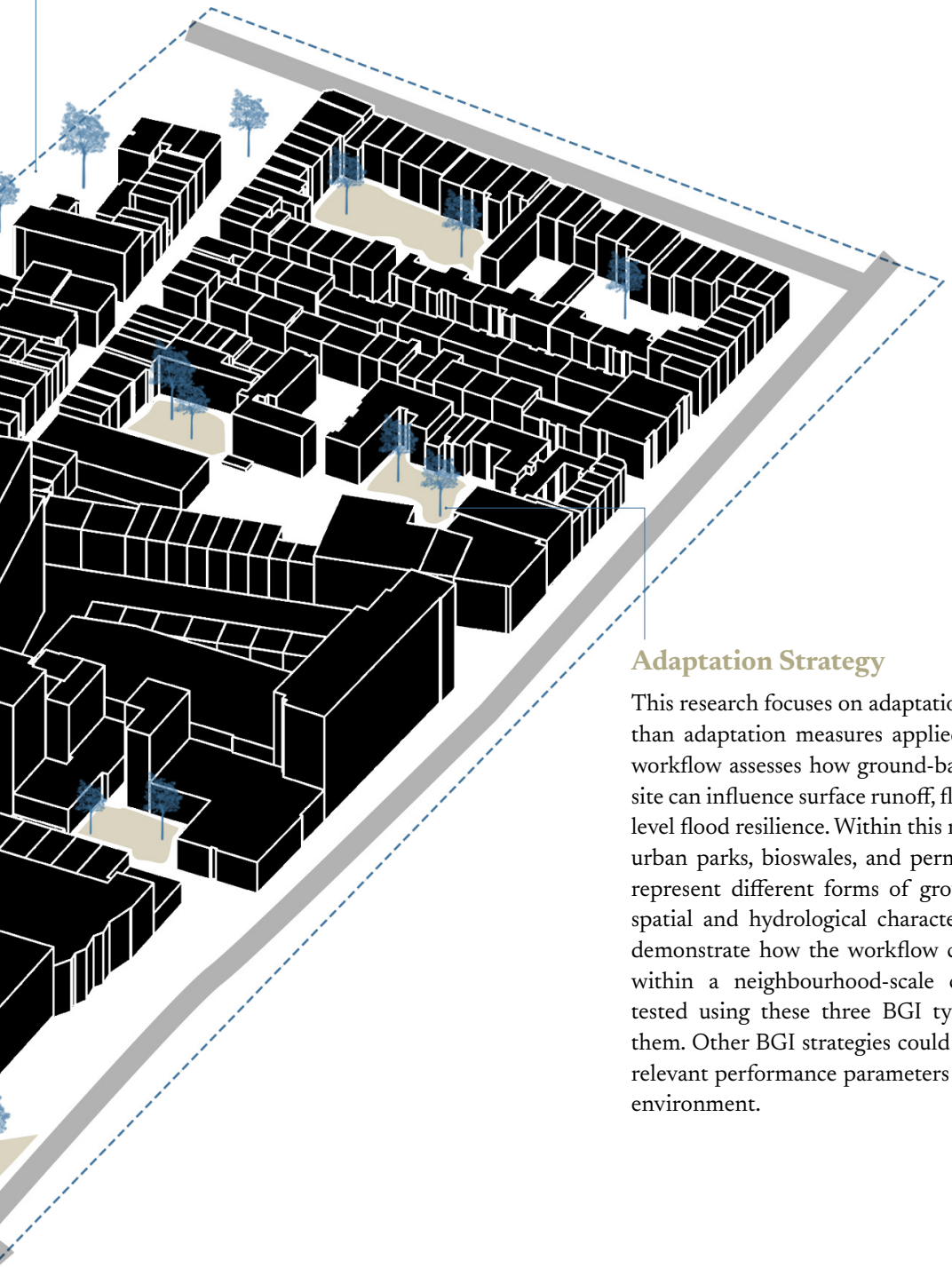

Adaptation Strategy

This research focuses on adaptation strategies applied at the site, rather than adaptation measures applied directly to the building itself. The workflow assesses how ground-based BGI strategies placed within the site can influence surface runoff, flood-depth distribution, and building-level flood resilience. Within this research, three BGI types are selected: urban parks, bioswales, and permeable pavements. These are used to represent different forms of ground-based adaptation with different spatial and hydrological characteristics. The selection is intended to demonstrate how the workflow can compare different BGI strategies within a neighbourhood-scale context. Although the workflow is tested using these three BGI types, the approach is not limited to them. Other BGI strategies could also be incorporated, as long as their relevant performance parameters can be defined within the simulation environment.

Boundary Conditions

Simulation Resolution

Because the workflow is applied at the neighbourhood scale, the level of simulation refinement is limited by the need to maintain computational efficiency. The outputs are therefore interpreted as comparative design-support indicators for evaluating BGI scenarios, rather than precise hydraulic flood predictions at the scale of individual surface details.

Deterministic Rainfall Scenario

The rainfall input is treated as a predetermined scenario rather than a probabilistic range of rainfall events. This means the workflow is used to compare BGI strategies under the same fixed rainfall condition, rather than to predict the probability of flooding. The deterministic setup supports consistent comparison between design scenarios.

Simplified Hydrological Representation

The workflow adopts a simplified hydrological representation to support early-stage design assessment within Grasshopper. Runoff is represented primarily as surface-water accumulation rather than as a detailed hydraulic process. Under this simplified no-drainage assumption, the simulation focuses on how runoff particles move across the terrain and accumulate in lower areas. Rainfall scenarios are therefore interpreted mainly through cumulative rainfall depth, meaning that scenarios with the same total precipitation are treated as producing comparable runoff accumulation patterns.

Although BGI can involve other hydrological functions, the simulation focuses only on its runoff-reduction capacity represented through infiltration. This simplification is made because the research aims to compare how different ground-based BGI adaptations influence the amount of runoff remaining on the surface, which may then contribute to ponding and flood-depth formation, rather than to reproduce the full physical behaviour of each BGI system.

Detailed drainage response, flow timing, intensity-dependent infiltration changes, soil processes, evapotranspiration, vegetation growth, maintenance conditions, and long-term seasonal changes are therefore outside the scope of the model. The results should be interpreted as comparative design-support indicators for assessing BGI scenarios, rather than precise hydraulic flood predictions.

Building Resilience Assessment

The building resilience assessment in this research focuses primarily on depth–damage relationships, as the current workflow evaluates how estimated flood depth affects building-level flood impact and resilience. The damage curve used in the workflow is adopted as a generic inundation-based reference, rather than a curve specifically developed for pluvial flooding, because pluvial-specific building damage data is currently limited and not directly accessible within the scope of this research. As a result, the assessment should be understood as a framework-based evaluation rather than a fully calibrated prediction of building damage. The resulting resilience scores are therefore more useful for comparing relative differences between the current and adapted scenarios than for interpreting absolute score values as exact damage predictions. In this sense, the workflow supports design decisions by showing whether, where, and to what extent BGI adaptation improves building-level resilience under the same assessment assumptions. If more specific pluvial flood damage curves, local building vulnerability data, or detailed recovery parameters become available, these inputs can be replaced or updated within the same workflow structure.

1.3 | Research Question

Main Research Question

How can a rainwater data-driven simulation framework be developed to improve building flood resilience through Blue-Green Infrastructure design strategies at the neighbourhood scale?

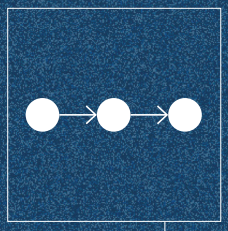

Grasshopper
Simulation Environment

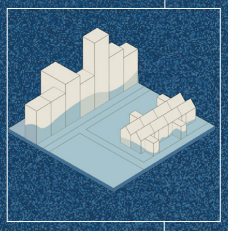

Building Level
Flood Resilience

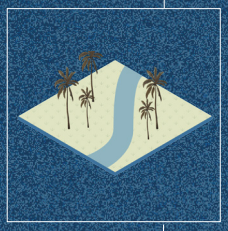

Blue-Green Infrastructure
Strategies

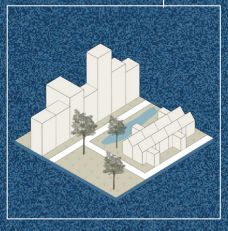

Application to the
Neighbourhood Scale

Sub Research Questions (SQ)

Building Resilience

1 How can pluvial flood resilience be defined and quantified at the building scale?

2 How can pluvial flood impact be simulated in Grasshopper to support building resilience scoring?

Blue Green Infrastructure

3 What defines the selection and rainwater regulation performance of BGI types for flood adaptation?

4 How can the selected BGI types be modelled in Grasshopper to evaluate their impact on building flood resilience?

Application to the Neighbourhood Scale

5 How can the simulation environment be applied to design and compare BGI strategies at the neighbourhood scale?

6 What insights can be gained from the simulation environment regarding the impact of BGI strategies on building flood resilience?

1.4 | Research Methodology

This research methodology builds on the connection between building resilience, computational workflow, and Blue-Green Infrastructure. Rather than treating these domains as separate topics, the methodology combines building-scale resilience assessment with the evaluation of ground-based BGI performance in a simulation-based design decision-support workflow. The literature review first establishes the research gap between flood resilience, flood simulation, and flood adaptation. This gap is then translated into the theoretical framework, where the resilience scoring components, flood simulation approach, and BGI performance indicators are defined.

These components are then developed into a Grasshopper-based workflow that connects the different domains through particle-based rainwater simulation, BGI performance assessment, flood-depth estimation, and building-level resilience scoring. The workflow is applied in the case study to test different BGI adaptation scenarios and compare their effects on flood depth, building resilience scores, BGI configuration, and indicative cost. The final evaluation reflects on the resilience outcomes, workflow usability, and insights gained from the tested BGI configurations. The overall structure of the methodology and its relation to the thesis chapters are illustrated in the Figure on the right.

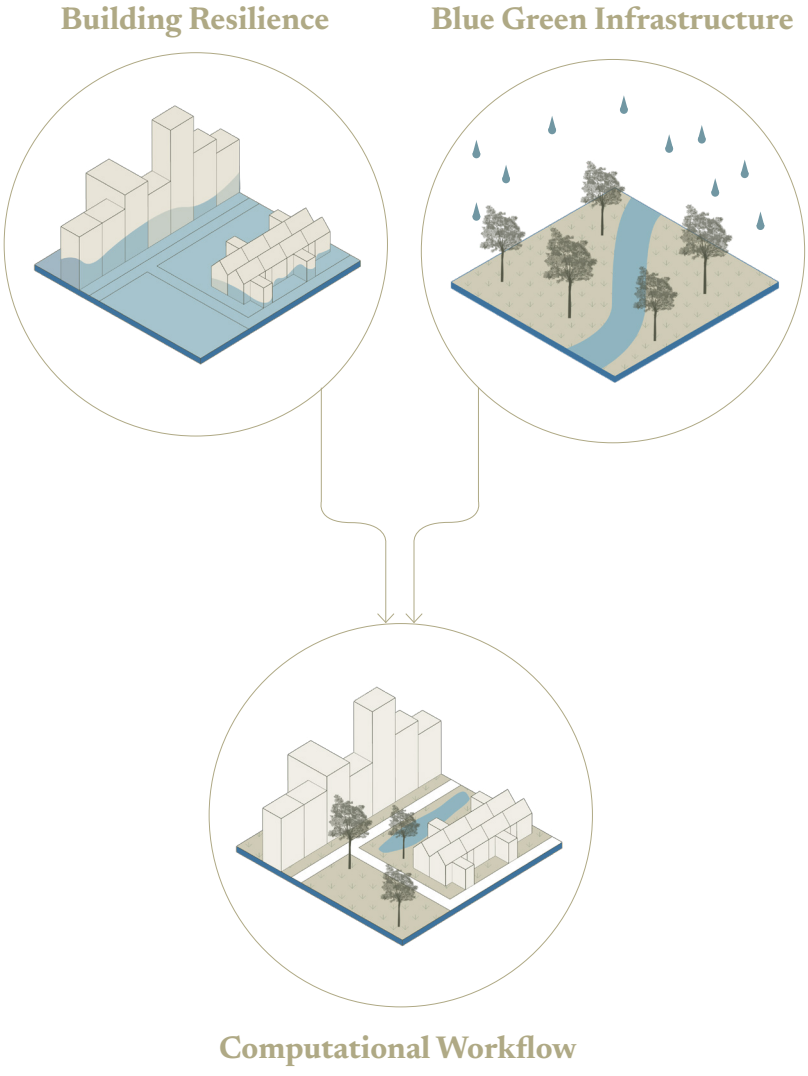

Chapter 1: Context
Chapter 2: Approach
Chapter 3: Case Study
Chapter 4: Discussion
Chapter 5: Conclusion

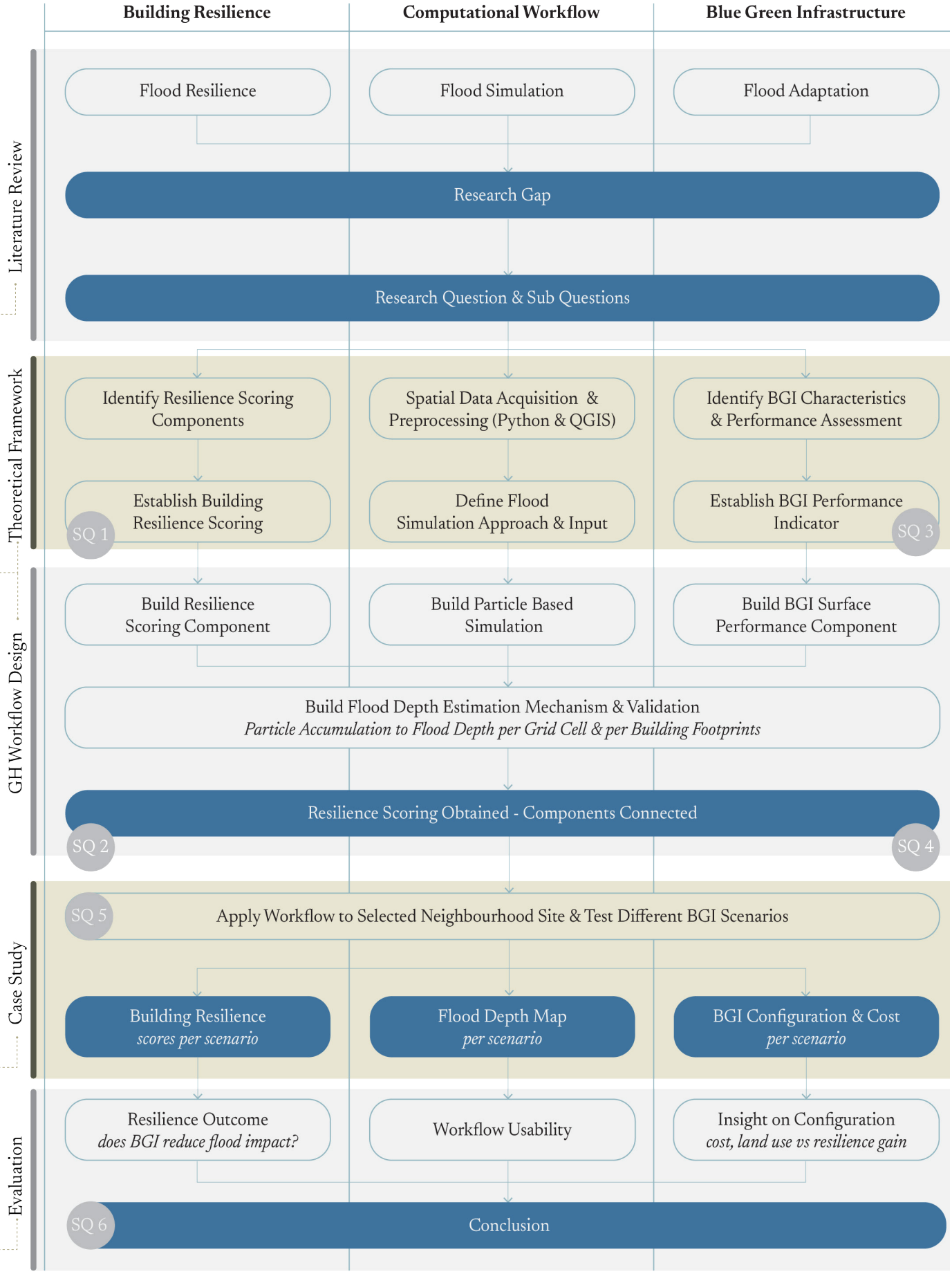

Figure 10. Research Methodology Diagram

02
Approach

Building Level Flood Resilience

Blue Green Infrastructure

Computational Workflow

2.1 | Building Level Flood Resilience

This section discusses building-level flood resilience as the theoretical basis for the resilience assessment used in the proposed workflow. It first explains how pluvial flood impact on buildings can be understood through hazard, exposure, and vulnerability, before introducing resilience as the ability to retain and recover functionality after disruption. These concepts are then translated into a building-level assessment framework using flood depth, damage ratio, remaining functionality, recovery time, and a quantitative resilience score.

Flood Impact on Building

Before building-level flood resilience can be assessed, the flood impact on buildings first needs to be understood. This requires situating building impact within the broader concept of flood risk. As Barsley (2020) notes, 'flood risk is inherently site-specific', meaning that no two places experience flooding in exactly the same way and that any adaptation should respond to the particular flood-risk context of the site. Flood risk is conventionally understood as a function of hazard, exposure, and vulnerability (Intergovernmental Panel On Climate Change, 2023) (Figure 11).

Figure 11. Flood Risk Component

Hazard

Hazard refers to the physical source of flood impact, which in this context is the flood event itself. Sayers (2013) defines flood hazard as the potential for inundation that may threaten life, health, property, and the vital functions of natural floodplain resources. However, flood hazard is not determined only by the presence of water. Barsley (2020) identifies several hazard characteristics that influence the degree of flood risk:

> **Depth and Velocity of Flood Water**
> Flood depth and velocity both influence the severity of flood hazard. Barsley notes that the depth and velocity of floodwater can be major contributing factors to the level of risk it poses. These two variables work in combination: depth indicates the level of inundation, while velocity indicates the force and movement of water. Even shallow water can become dangerous when it moves at high velocity, while deeper water can increase pressure on buildings, limit access, and increase the likelihood of damage.

> **Type of Flooding**
> This characteristic is relevant to urban areas because pluvial flooding is closely related to rainfall intensity and duration. When rainfall intensity exceeds the capacity of the ground surface, local infiltration processes, or drainage system, runoff can accumulate on the surface and form localised ponding. The duration of rainfall also matters because longer rainfall events can increase the total runoff volume and prolong inundation, even when the rainfall intensity is not extreme throughout the whole event.

> **Duration**
> Flood duration refers to how long floodwater remains in an area. Barsley explains that duration can vary depending on the type of flooding, topography, rainfall volume, ground conditions, and compounding factors. Surface-water or pluvial flooding often lasts for shorter durations compared with groundwater flooding, but it can still cause disruption and damage when water accumulates around ground floors, entrances, basements, or access routes.

> **Contamination**
> Floodwater may also contain hazardous substances or debris. Barsley (2020) notes that floodwater can carry pollutants, fuel, sewage, chemicals, sharp objects, or other dangerous materials. These contaminants can increase health risks, complicate clean-up, and extend recovery. Although contamination is not explicitly modelled in this workflow, it is acknowledged as an additional hazard factor that may affect real-world building recovery.

Exposure

Exposure refers to the receptors that are located within a hazard zone and are therefore susceptible to potential loss. These receptors may include people, buildings, infrastructure networks, habitats, or other urban assets (Sayers, 2013; Watson & Adams, 2011). In the context of building-level flood resilience, exposure concerns whether buildings are located in areas that may come into contact with floodwater.

Barsley (2020) further explains that exposure depends on the probability of a flood event and the position of the receptor in relation to the hazard, both horizontally and vertically. However, exposure is not always easy to determine from proximity alone. A building located far from a river, for example, may still be exposed to surface-water flooding if intense rainfall causes runoff to accumulate along roads, low-lying spaces, or blocked flow paths. This is particularly relevant for pluvial flooding, where water can spread quickly through the urban surface and affect areas that are not traditionally perceived as flood-prone.

Therefore, in urban pluvial flooding, exposure should be understood spatially rather than only through distance from a watercourse. Buildings may become exposed when their location, elevation, or surrounding surface conditions place them within the path or accumulation zone of runoff. However, being located along a runoff path does not necessarily mean that the building experiences measurable flood impact, as impact depends on whether water accumulates to a level that can affect the building.

Vulnerability

Vulnerability refers to the susceptibility of exposed receptors to experience damage or loss when affected by a hazard. It is a multi-dimensional condition shaped by physical, economic, and social factors, and it also influences the capacity of a property or community to recover after a flood event (Sayers, 2013; Tingsanchali, 2012). While exposure determines whether a building may come into contact with floodwater, vulnerability determines how severely that building may be affected once exposed.

In the built environment, vulnerability can be related to building characteristics such as construction type, building function, presence of basements, and material sensitivity. This is reflected in flood loss estimation methods such as Hazus (Federal Emergency Management Agency, 2025), where building damage estimation considers parameters including occupancy type, number of stories, foundation type, flood depth, flood hazard type, and appropriate damage functions. Hazus also incorporates basement condition in its damage-function assignment and adjustment, particularly for residential structures, indicating that below-grade spaces can influence expected flood damage. As a result, two buildings exposed to the same flood depth may experience different levels of physical damage, disruption, or recovery needs. Vulnerability therefore provides the basis for understanding why flood impact is not only determined by the hazard itself, but also by the characteristics of the exposed building.

Concept of Resilience

Sayers (2013) defines resilience as "the ability of an individual, community, city or nation to resist, absorb or recover from a shock," such as an extreme flood, and to adapt to changing conditions in a timely and efficient manner. In the built environment, this means that resilience is not only about whether flooding occurs, but also about how far a building is physically affected and how much of its function is disrupted after the event. For this research, physical damage becomes the main entry point for translating building-level flood resilience into the workflow. This follows the logic of REDi for Floods, where designing buildings to sustain less damage is identified as a key component of resilience-based flood design (Hogan et al., 2023).

The REDi Rating System further explains that recovery is not determined only by the physical repair process, but also by delays that may impede the initiation and progress of repair and restoration. These delays, referred to as impeding factors, include uncertainties related to financing, regulatory processes, inspections, resource availability, and other logistical constraints that can prolong recovery time. During this impeding period, functionality remains at a reduced level.

Quantifying Building Flood Resilience

To understand how flood impact and recovery unfold over time, building-level flood resilience is translated into a simplified functionality–time curve, as illustrated in Figure 12. Before the flood event, the building is assumed to operate at full functionality. Once flooding occurs, functionality is assumed to drop immediately according to the estimated damage level. In reality, functionality loss may occur more gradually depending on flood duration, water ingress, access disruption, emergency response, and building operation. However, an instantaneous drop is adopted here as a simplification to support a clear and consistent early-stage assessment. After the initial drop, functionality remains reduced during the impeding period, before gradually recovering throughout the restoration period.

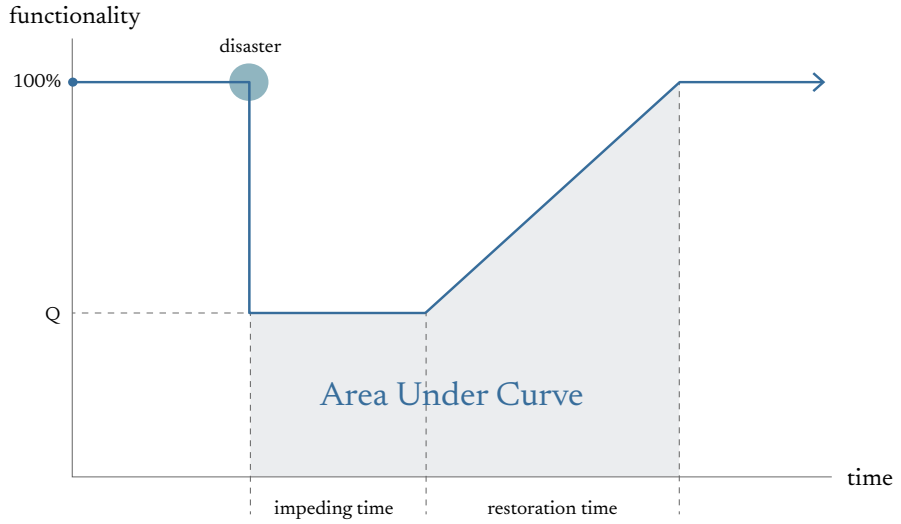

Figure 12. Flood Resilience Graph

This approach is adapted from the performance-over-time logic proposed by Bruneau et al., (2003), originally developed in the context of seismic resilience. Although their framework focuses on earthquake impacts, the underlying logic is transferable to flood resilience because both involve a disruption that reduces system performance, followed by a recovery process over time. Bruneau et al. conceptualise resilience through the change in system performance **Q(t)** after a disruptive event. In their framework, system performance ranges from 0% to 100%, where 100% represents no degradation in service and 0% represents no available service. A disaster causes an abrupt reduction in performance, followed by gradual restoration over time. Bruneau et al. define loss of resilience as the area above the performance curve, meaning that greater performance degradation and longer recovery time result in higher resilience loss.

In this research, the same performance-over-time logic is used, but the scoring direction is inverted to make the result more intuitive for design assessment. Instead of calculating resilience loss as the area above the curve, the resilience score is calculated as the normalised area under the functionality–time curve. This means that a higher score represents better retained functionality and/or faster recovery, while a lower score represents greater functionality loss and/or longer recovery. This interpretation is also consistent with Bianchi et al. (2025), who develop building Resilience Readiness rating system on a 0–1 scale where values closer to 1 indicate higher resilience. Therefore, in this workflow, a resilience score of 1 represents full retained functionality over the assessed period, while a score closer to 0 represents severe functionality loss and slow recovery. This relationship is then expressed through the following equation:

$$\text{Resilience} = \frac{\text{Area Under Curve}}{\text{Perfect Area}}$$

Which is then translated into:

$$\text{Resilience} = \frac{Q \cdot t_{imp} + 1/2\,(Q+1) \cdot t_{res}}{t_{imp} + t_{res}}$$

Q = funcitonality
timp = impeding time
tres = restoration time

The resilience score is therefore composed of three main components: remaining functionality, impeding time, and restoration time. Each component is explained in the following subsection.

Functionality (Q)

Remaining functionality describes the extent to which a building can continue to operate after flood impact. In quantitative flood-impact assessment, functionality can be approximated by first estimating the level of building damage. A building with limited physical damage is more likely to retain its usability, while a building with severe damage is more likely to experience functional disruption. Figure 13 illustrates common flood-related damage impacts on buildings.

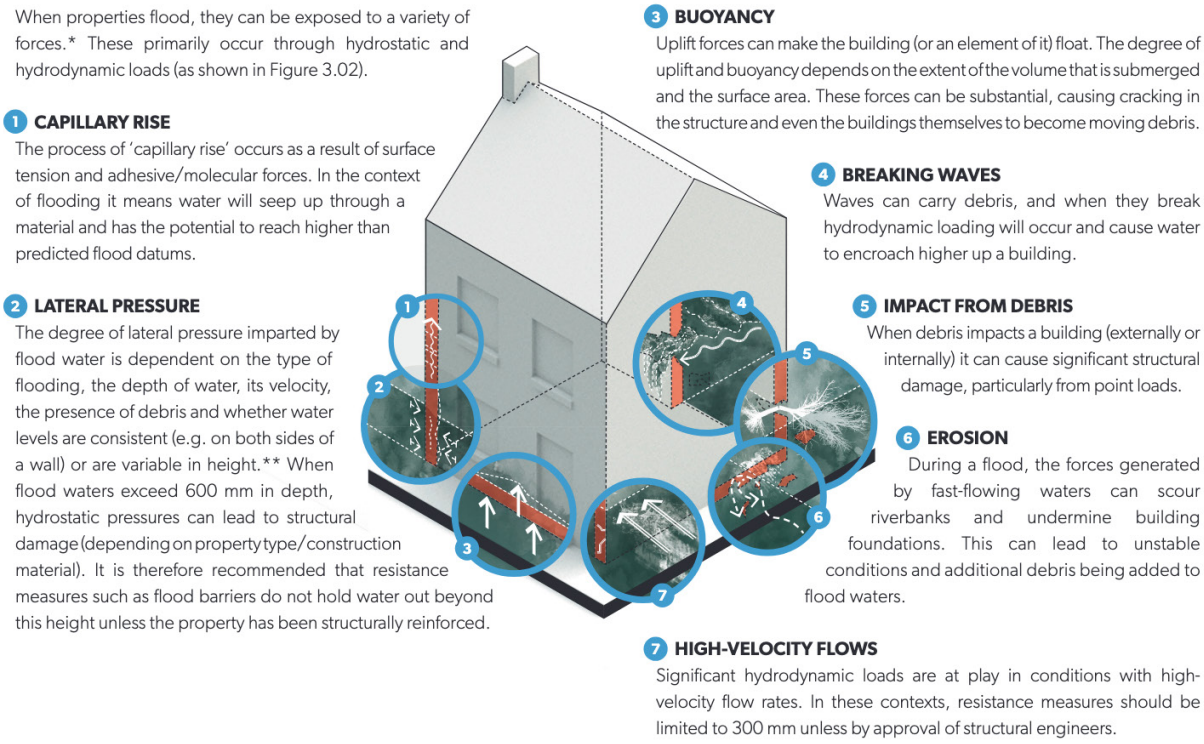

Figure 13. Common flood-related damage impact on building (Barsley, 2020)

Depth-Damage Approach

However, current flood damage assessment methods predominantly rely on the depth–damage approach, which remains one of the most established quantitative methods for estimating flood-related losses. Although various factors such as flow velocity, contamination, building materials, and duration of inundation may also influence damage severity, many existing models primarily focus on the relationship between inundation depth and expected damage. The Joint Research Centre developed the Global Flood Depth-Damage Functions (Huizinga, J. et al., 2017) which are commonly used to estimate potential losses under varying flood depths across different damage categories at both building and landscape scales. The method currently accounts for three primary building typologies: residential, commercial, and industrial. The figure below illustrated this function as a curve.

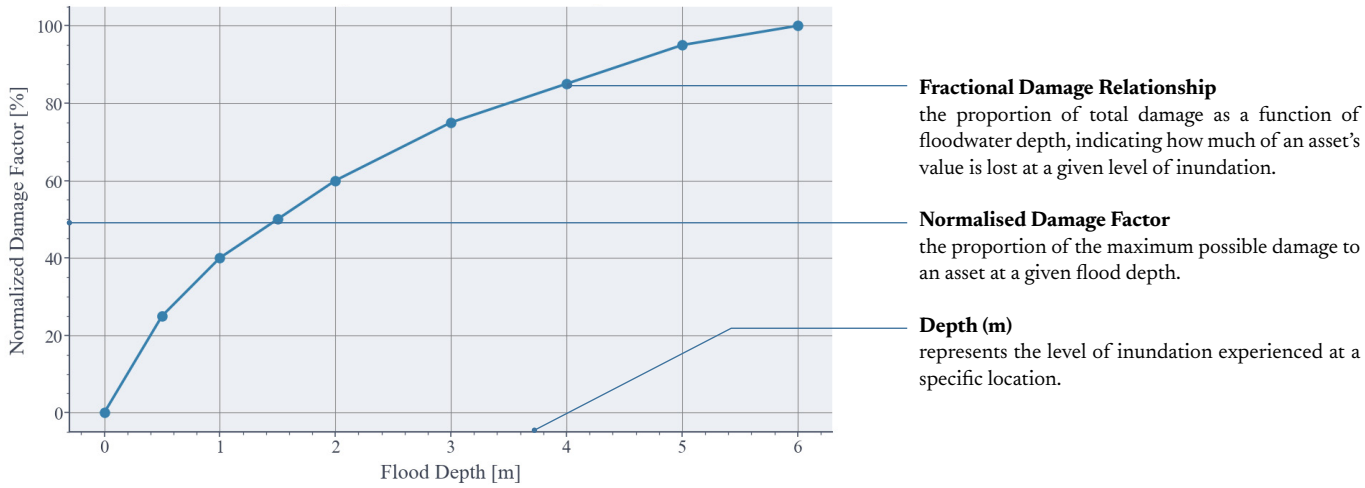

Figure 14. Component of Depth - Damage Curve

The JRC depth–damage methodology was selected as the baseline curve because it is designed as a generic inundation model and is not associated with one specific flood type. Huizinga et al. (2017) state that the functions were constructed from both fluvial and marine flood data and can initially be used for the damage assessment of a generic inundation event. This makes the JRC curves suitable as a flexible baseline for exploratory assessment of pluvial flooding scenarios, especially where pluvial-specific damage curves are limited.

In contrast, the Dutch SSM2015 methodology developed by Deltares (De Bruijn et al., 2015) is primarily designed to assess flood impacts from large-scale floods from the main water bodies in the Netherlands. Therefore, although SSM2015 provides a more context-specific Dutch flood damage assessment method, its original application context is less aligned with the exploratory neighbourhood-scale pluvial flood assessment developed in this research.

Nevertheless, the broader logic of the SSM methodology remains relevant because it distinguishes between different forms of flood impact, including physical damage and interruption-related impacts. In this research, this logic is conceptually incorporated into the JRC depth–damage approach through adjustment factors, allowing the estimated physical damage ratio to be translated into indicative functionality loss and recovery-related disruption. A limitation of this approach is that neither the JRC nor SSM2015 methodologies were specifically developed for building-level pluvial flood resilience assessment, particularly under shallow urban flooding conditions. However, the generic and internationally derived nature of the JRC database makes it easier to adapt across different geographic and urban contexts, which supports the exploratory and transferable aim of the proposed workflow. Figure 15-17 illustrate Depth-Damage Curve for residential, commercial, and industrial.

From the selected depth–damage curve, the inundation depth is translated into a damage ratio D, ranging from 0 to 1. A value of 0 represents no estimated damage, while a value of 1 represents maximum damage. This damage ratio is then used to estimate remaining functionality.

$$Q = 1 - D$$

where Q represents remaining functionality and D represents the estimated damage ratio. In this way, higher flood damage results in lower remaining functionality.

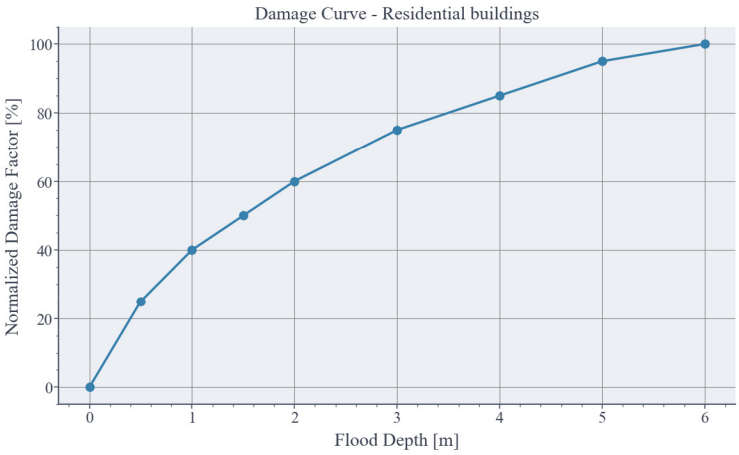

Figure 15. Depth-Damage Curve for Residential Buildings

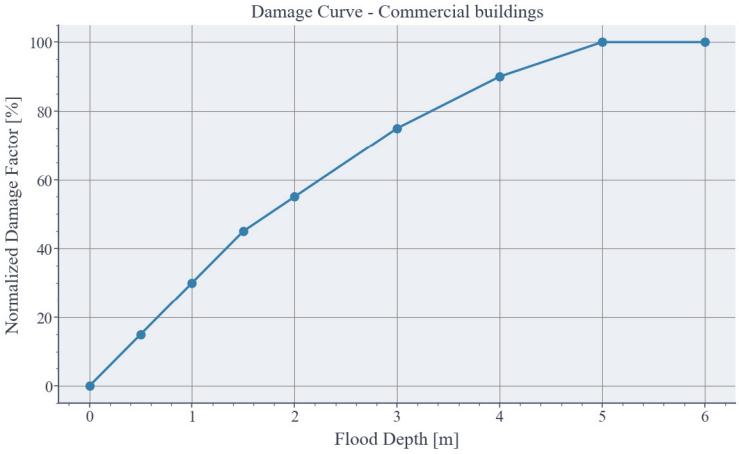

Figure 16. Depth-Damage Curve for Commercial Buildings

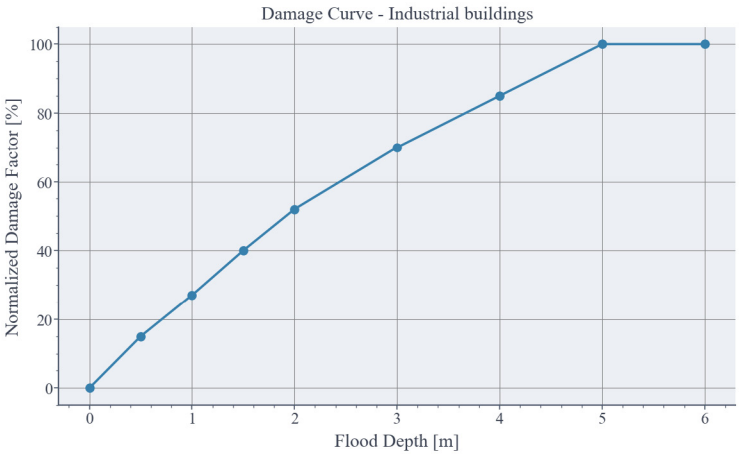

Figure 17. Depth-Damage Curve for Industrial Buildings

Floor - Level Shift

Before the damage ratio D is derived from the selected depth–damage curve, the inundation depth can be adjusted according to the floor level affected by the floodwater. This adjustment follows the floor-level differentiation approach in SSM2015, which proposes that the damage function for upper-floor apartments should be shifted by one floor height per floor level. De Bruijn et al. (2015) use a standard Dutch floor-to-ceiling height of 2.5 m, meaning that the effective depth used in the damage function is reduced by 2.5 m for each higher floor level.

This adjustment reflects the physical reality that upper-floor dwellings are only exposed to flood damage when water rises above their floor level. It also corrects the overestimation in the original HIS-SSM method, where all residential units within a building were treated as equally exposed regardless of their vertical position. By applying this floor-level correction, the damage calculation better reflects which part of the building is actually inundated.

Table 1 summarises how the highest affected floor level and corresponding effective depth are determined.

Floor Level	Condition	Effective Depth
dry	depth $\leq$ 0	0 m
ground	depth $\leq$ 2.5 m	depth
first	2.5 m $<$ depth $\leq$ 5 m, floors $\geq$ 2	depth - 2.5 m
higher	depth $>$ 5, floor $\geq$ 3	depth - 5 m

Note for pluvial flooding
In typical shallow pluvial flooding conditions, particularly when flood depths remain under 1 m range, the affected floor level will remain the ground floor because the inundation depth does not exceed the 2.5 m threshold. Therefore, the floor-level differentiation has limited influence on most pluvial scenarios in this research. However, the logic is included for methodological completeness and to keep the assessment adaptable to deeper inundation scenarios.

Table 1. Floor level shift data

Basement Adjustment Factor

A second adjustment concerns the presence of basements. Basements can increase flood-related building damage because below-grade spaces may be affected before floodwater reaches the ground-floor level. Hazus 7.0 modifies selected residential structure damage functions with basements by adding damage associated with basement components that may be affected at negative flood depths, meaning water levels below the first-floor elevation. The excluded basement component costs include floor finishes, wall finishes, ceiling components, electrical elements, heating ductwork, ceiling suspension systems, and light fixtures. Hazus estimates that 7% additional damage occurs at -4 ft, with a further 4% added at -1 ft, resulting in a total basement-related addition of 11% of total structure replacement cost.

Based on this logic, this research applies a simplified basement adjustment by adding 0.11 to the estimated damage ratio when a building has a basement. The adjusted damage ratio is capped at 1.0 to avoid exceeding total damage:

$$\text{Adjusted Damage} = \min(\text{Damage} + 0.11,\ 1.0)$$

However, this adjustment should be interpreted as an indicative correction rather than a direct transfer of the Hazus method. The 0.11 factor in Hazus was originally developed to modify FIA-based damage functions by accounting for basement components excluded from insurance coverage, while this research applies it to JRC depth–damage curves. Therefore, the basement adjustment is included to represent the increased vulnerability of buildings with basements, but it remains a simplified assumption and should be refined when local basement damage data or pluvial-specific evidence is available.

Impeding Time (t*imp*)

As mentioned in the resilience section, the time required to recover from a flood event is not determined solely by the repair process itself, but also by the time needed for assessment, inspections, financing, approvals, and other recovery-related procedures. During this period, the condition and functionality of the building often remain relatively unchanged before restoration activities can begin. The REDi Rating System framework (Hogan et al., 2023) categorizes these impeding factors into five categories, all represented in units of days, as shown in Table 2.

Impeding Factor	Subcategory	Median	Dispersion
Duration and recession of floodwaters	-	2 days	0.5
Restoration mobilization and cleanup	On contract, unlimited budget	2 days	0.5
	Not on contract, unlimited budget	12 days	0.8
	On contract, limited budget	3 weeks	0.5
	Not on contract, limited budget	1 month	0.3
Engineering mobilization and permitting	On contract	7 weeks	0.4
	Not on contract	12 weeks	0.5
Financing	Pre-arranged credit line	1 week	0.5
	Private loans	15 weeks	0.7
	SBA-backed loans	6.5 months	0.5
	Insurance	6 weeks	0.5
Contractor bidding and mobilization	GC on contract	1.5 weeks	0.5
	GC not on contract	6 weeks	0.5

Table 2. Impeding Time based on diferent scenario (Hogan et al., 2023)

Based on the REDi assessment framework, different impeding times were assigned to each building class in this study according to various possible building conditions and flood impact scenarios. To represent variation in recovery conditions, a dispersion approach was adopted using three levels: Medium as the baseline value, Low calculated as 0.5× the baseline value, and High calculated as 1.5× the baseline value. The resulting impeding times, expressed in days, are presented in Table 3. These parameters will serve as input options within the workflow.

Impeding Factor	Days	Reason
RESIDENTIAL		
Duration and recession of floodwaters	2	Pluvial water drains quickly
Restoration mobilization and cleanup	30	Not on contract, limited budget
Engineering mobilization and permitting	2	Based Assumption
Financing	18	Insurance
Contractor bidding and mobilization	42	GC not on contract
TOTAL DAYS	**94**	
COMMERCIAL		
Duration and recession of floodwaters	2	Pluvial water drains quickly
Restoration mobilization and cleanup	21	On contract, limited budget
Engineering mobilization and permitting	7	On contract
Financing	45	Private loans
Contractor bidding and mobilization	10,5	GC on contract
TOTAL DAYS	**85,5**	
INDUSTRIAL		
Duration and recession of floodwaters	2	Pluvial water drains quickly
Restoration mobilization and cleanup	21	On contract, limited budget
Engineering mobilization and permitting	12	
Financing	45	Private loans
Contractor bidding and mobilization	10,5	GC on contract
TOTAL DAYS	**90,5**	

Table 3. Impeding Time mapping for each building class

Restoration Time (t*res*)

Restoration time represents the duration required for a building to return to full functionality after a flood event. In this research, restoration time is also derived from the Hazus 7.0 Flood Model Technical Manual. The restoration-time values are based on occupancy-specific estimates provided in Tables 6-4, 6-8, and 6-11 of the manual, as shown in Table 4. These tables relate flood depth to expected restoration duration for different building categories.

Building Class	Minimum Depth (m)	Maximum Depth (m)	Restoration Days	Source
Residential Buildings	-1,219	0	180	Hazus 7.0 Table 6-4
	0	1,219	360	Hazus 7.0 Table 6-4
	1,219	2,438	450	Hazus 7.0 Table 6-4
	2,438	7,315	720	Hazus 7.0 Table 6-4
Commercial Buildings	-1,219	0	180	Hazus 7.0 Table 6-8
	0	1,219	540	Hazus 7.0 Table 6-8
	1,219	2,438	630	Hazus 7.0 Table 6-8
	2,438	3,658	720	Hazus 7.0 Table 6-8
	3,658	7,315	900	Hazus 7.0 Table 6-8
Industrial Buildings	-1,219	0	0	Hazus 7.0 Table 6-11
	0	7,315	210	Hazus 7.0 Table 6-11

Table 4. Restoration Time mapping for each building class

As shown in Table 4, restoration time differs by building category and flood depth. Commercial buildings generally require longer restoration periods than residential buildings at equivalent flood depths, reflecting the additional complexity of restoring business operations compared with reoccupying a dwelling. All depth values from the Hazus tables are converted from feet to metres using 1 ft= 0.3048 m.

For the restoration-time lookup, the raw ground-surface flood depth is used rather than the floor-adjusted effective depth. This is because restoration time describes the recovery condition of the building as a whole, while the floor-level adjustment is used specifically to estimate damage at the inundated floor level. The negative depth values in Hazus are relevant for buildings with basements, because basement components may already be affected before floodwater reaches the ground-floor level. However, In typical pluvial flooding scenarios inundation depth is generally interpreted from 0 m upward at ground level.

Key Parameter Summary

Based on the resilience framework discussed above, building-level flood resilience in this workflow is represented through a simplified functionality–time curve. The curve summarises how building functionality changes before, during, and after a flood event. Before flooding, the building is assumed to operate at full functionality. Once flooding occurs, functionality drops according to the estimated physical damage level. Although functionality loss may occur more gradually in reality, an immediate drop is adopted in this workflow to support a clear and consistent early-stage assessment. After this initial drop, functionality remains reduced during the impeding period, before gradually recovering throughout the restoration period. The key parameters used to construct this curve are summarised in Table 5.

<table>
<tr><th>Parameter</th><th>Source</th><th></th><th colspan="3">Output</th></tr>
<tr><td>Maximum Inundation depth (m) per building</td><td>Flood Data</td><td>→</td><td rowspan="4">Functionality = 1 - Damage (0-100%)</td><td rowspan="4">→</td><td rowspan="6">Resilience Score [0-1]</td></tr>
<tr><td>Building Class (clustered into Residential / Commercial / Industrial)</td><td>Building Data</td><td>→</td></tr>
<tr><td>Number of floors</td><td>Building Data</td><td>→</td></tr>
<tr><td>Presence of Basement</td><td>Building Data</td><td>→</td></tr>
<tr><td>Impeding Time in Days per Building Class</td><td>REDi Database</td><td colspan="3">→</td></tr>
<tr><td>Restoration Time in Days per Building Class</td><td>Hazus Database</td><td colspan="3">→</td></tr>
</table>

Table 5. Key Parameter Summary of Building Resilience

2.2 | Blue Green Infrastructure

Urban Water Cycle

Imagine rainfall falling onto a forest floor compared to a dense urban street. In natural landscapes, water is gradually absorbed into the soil, evaporated through vegetation, or slowly released into surrounding waterways. In contrast, urban environments rapidly channel rainfall across impervious surfaces such as concrete and asphalt, limiting infiltration and significantly increasing surface runoff. As a result, the urban water cycle differs fundamentally from the natural water cycle (Watson & Adams, 2011; Eisenberg & Polcher, 2019). Under the same precipitation conditions, natural landscapes typically exhibit high levels of evaporation and infiltration and low surface runoff, whereas urban environments are characterised by reduced infiltration, limited evaporation, and increased runoff due to the dominance of impervious surfaces. This is illustrated in the figure below.

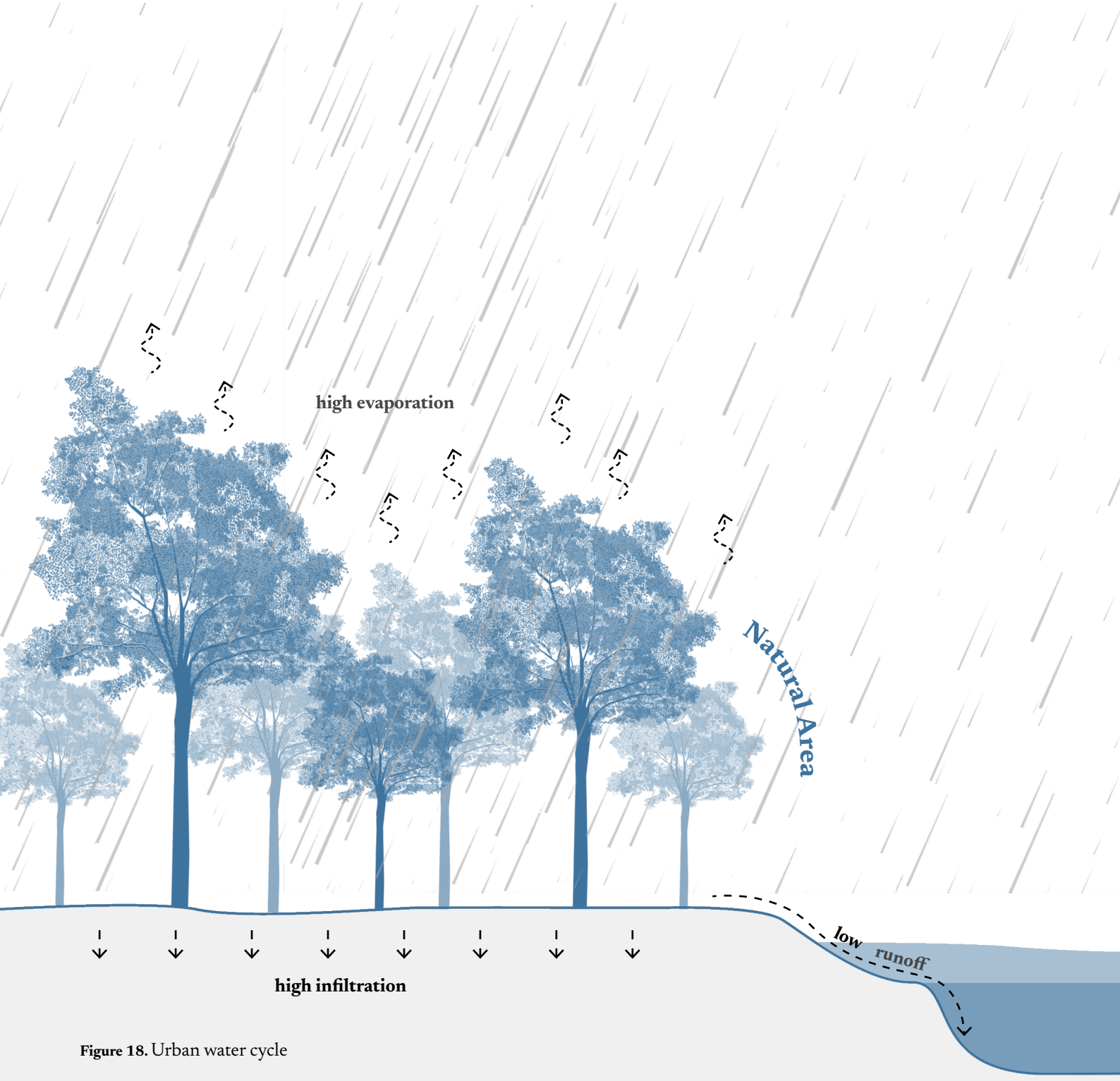

Figure 18. Urban water cycle

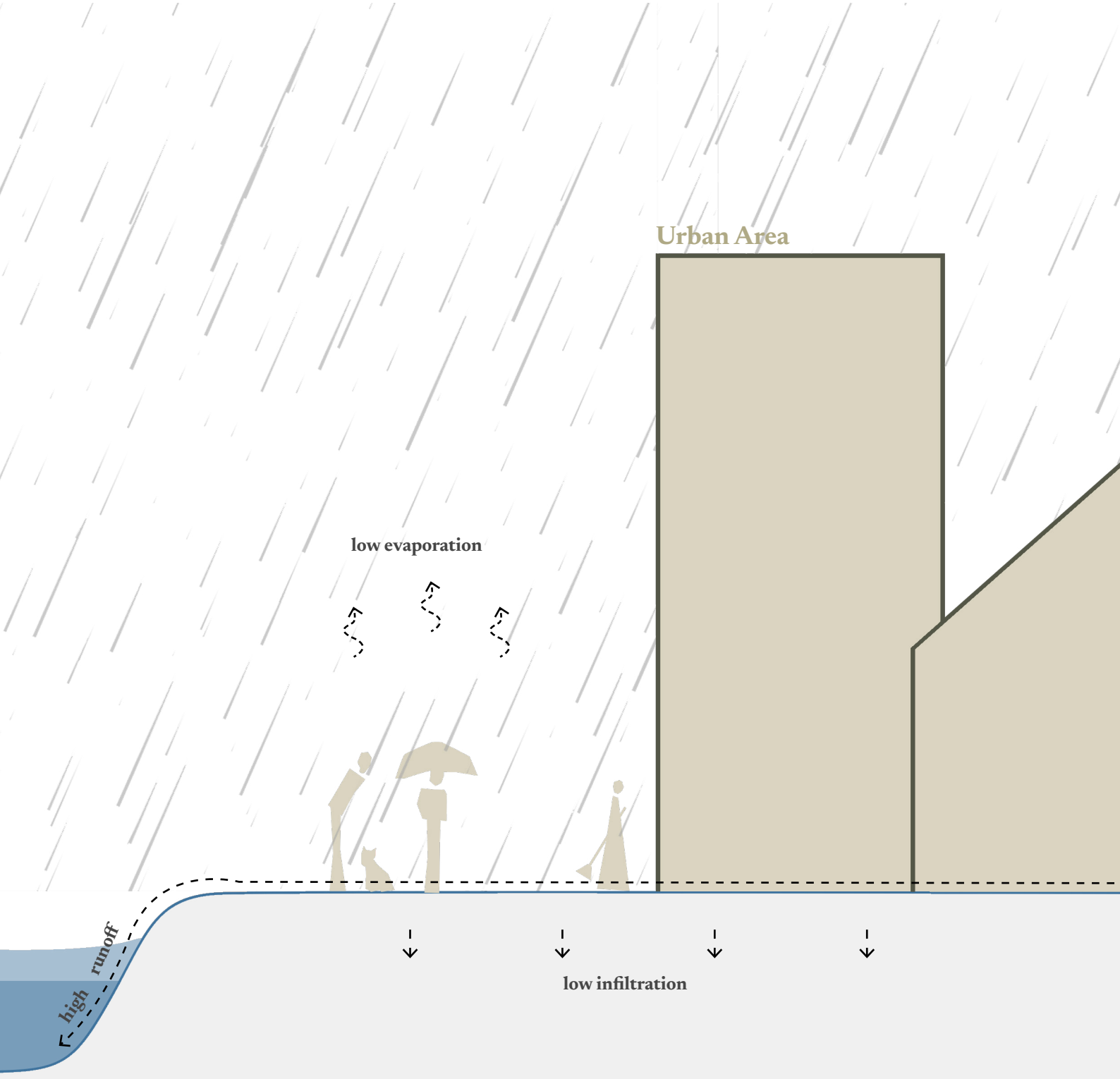
Urban Area
low evaporation
high runoff
low infiltration

BGI for Urban Water Management

One approach to managing pluvial flooding at the urban spatial scale is through BGI. BGI is closely related to the broader concept of Nature-Based Solutions (NBS), which refers to actions that use, support, or are inspired by natural processes to address environmental, social, and economic challenges (Eisenberg & Polcher, 2019). As shown in Figure 19, NBS acts as an umbrella concept for several related approaches, including ecosystem-based adaptation, green infrastructure, blue infrastructure, ecological engineering, sustainable urban drainage systems, and ecosystem services. BGI can therefore be understood as part of this broader NBS thinking, but with a more specific focus on the role of water, vegetation, soil, and open space within urban environments.

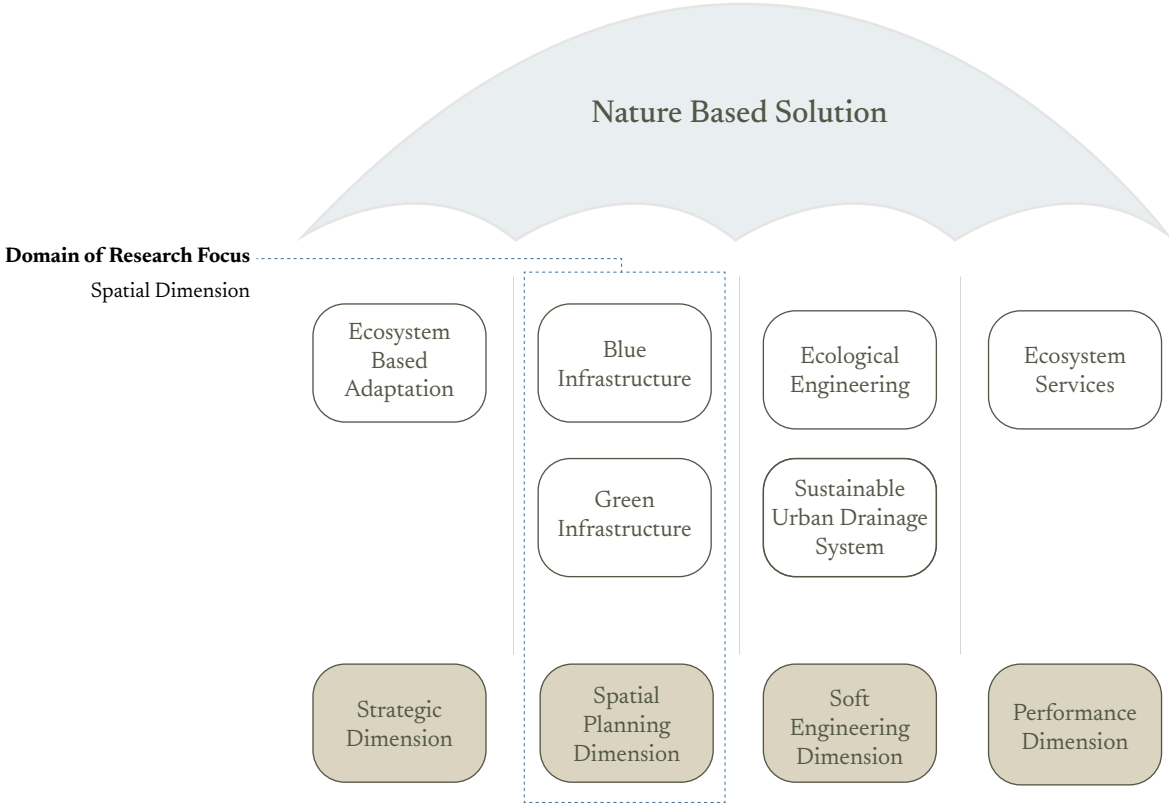

Figure 19. Nature Based Solution domain according to Eisenberg & Polcher

In urban water management, this way of thinking is also reflected in established planning and design frameworks, including Water Sensitive Urban Design (WSUD) in Australia, Low Impact Development (LID) in the United States and New Zealand, and Sustainable Urban Drainage Systems (SUDS) in the United Kingdom (Burns et al., 2012). Although these approaches differ in terminology and context of application, they reflect a broader shift in urban drainage thinking from simply conveying runoff away from urban areas toward managing runoff closer to where it falls (Fletcher et al., 2015). The terminology around BGI, NBS, GI, SUDS, LID, and WSUD is therefore not always clearly separated in the literature. These terms emerge from different disciplinary and geographical contexts, but they often overlap in practice because they share a similar aim: to manage runoff through a combination of water, vegetation, soil, and spatial systems. In this research, the term 'Blue-Green Infrastructure' is used as the main framing concept because it best reflects the focus on both water-related processes and spatial green adaptation at the site scale.

Within this shared approach, runoff should not only be transported away as quickly as possible, but should also be slowed, conveyed, stored, infiltrated, retained, or reused within the urban landscape. This reflects the water-balance regulation function of NBS, which includes processes such as water conveyance, infiltration, retention, storage, and reuse (Eisenberg & Polcher, 2019). Through these processes, BGI can reduce surface runoff, support peak-flow control, and help manage pluvial flood impacts closer to the source. This is particularly relevant in urban areas, where impervious surfaces limit infiltration and increase the speed and volume of runoff during heavy rainfall.

Each of these are explained more as follows:

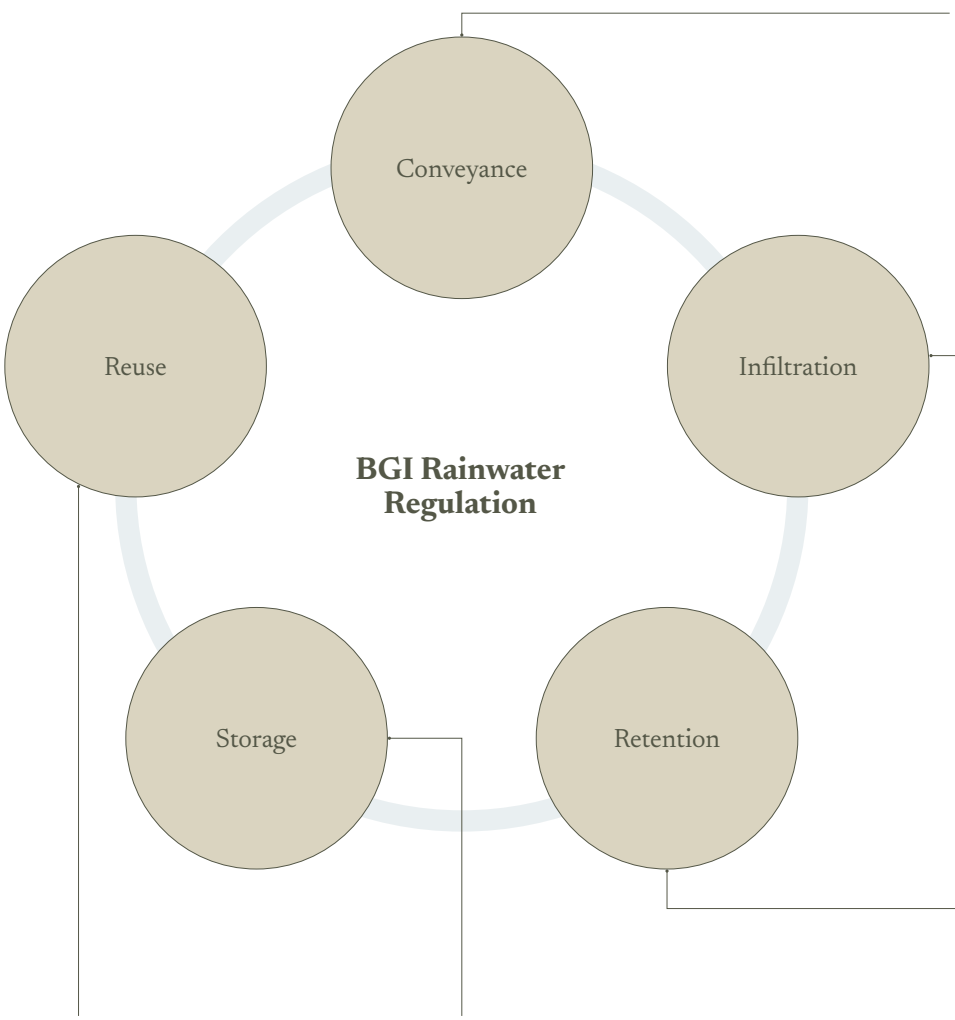

movement of runoff from one place to another. In BGI, conveyance does not only mean removing water quickly, but also guiding runoff through the landscape so that it can reach areas where it may infiltrate, slow down, or be temporarily stored. For example, swales are commonly used to convey runoff while also supporting water treatment and other hydrological functions (Ekka et al., 2021).

movement of water from the surface into soil or permeable ground layers. In BGI, this process reduces surface runoff by allowing water to enter vegetated soil, permeable pavement, or other absorptive layers. Permeable paving, for example, allows runoff to infiltrate through gaps between paving units and into an underlying stone layer before entering the soil or drainage system.

holding runoff within the site instead of immediately discharging it into the drainage system. In BGI, this reduces the amount of runoff leaving the site by keeping water in elements such as bioretention areas, green roofs, porous paving, or retention ponds. Chen et al. (2016) explain that LID strategies manage rainwater close to its source, with bioretention retaining large runoff volumes and green roofs retaining a large percentage of rainfall.

temporary collection of runoff within the site during or after rainfall. In BGI, storage helps delay runoff movement by holding water before it is gradually released, infiltrated into the soil, or conveyed elsewhere.

collecting runoff or rainwater so it can be used later. In BGI, this is often done through rainwater harvesting, where rainwater is collected and stored on site for reuse. Joshi et al. (2024) describe rainwater harvesting as the "collection and storage of on-site rain for reuse," with benefits including reduced runoff, flood reduction, and reduced water demand.

Multifunctionality of BGI

While BGI has an important hydrological function, its relevance in urban design extends beyond runoff management. Traditional flood-management approaches, such as seawalls, embankments, and sluices, can be effective in reducing flood risk, but (Crowe et al. (2025) note that they have also been criticised for causing environmental harm, negatively affecting place quality, and overlooking the social, environmental, and cultural factors that contribute to resilient and liveable communities. This aligns with broader NBS literature, which emphasises working with nature to address environmental, social, and economic goals simultaneously (Science for Environment Policy, 2021). Together, these perspectives have led to growing interest in BGI as a flood-adaptation approach that can deliver multiple benefits beyond water management.

This multifunctional character is important because BGI adaptations are not expected to deliver only one outcome. Drawing on wider NbS literature, Bona et al. (2023) highlight that recognising NBS as measures that provide multiple benefits is important to ensure that they deliver broader benefits rather than only single-purpose outcomes. In relation to pluvial flooding, P et al. (2024) also argue that BGI planning should not focus only on outcome-based variables such as runoff, flood depth, and duration, but should also consider spatial-planning criteria such as capacity, connectivity, and diversity.

On this basis, the BGI strategies selected for this workflow are considered not only as hydrological measures, but also as different forms of spatial adaptation. Their wider spatial, ecological, and urban-design qualities are not directly quantified in the simulation workflow, but they provide the rationale for selecting three representative ground-based BGI strategies: urban parks, bioswales, and permeable pavements. These strategies represent different forms of ground-based adaptation, ranging from larger multifunctional urban green space, to linear vegetated runoff systems, and hardscape-based permeable surfaces.

A contemporary example of this multifunctional approach can be seen in Tebet Eco Park, Jakarta (Figure 20), where public open space is combined with water-management functions.

BGI focus on this Research

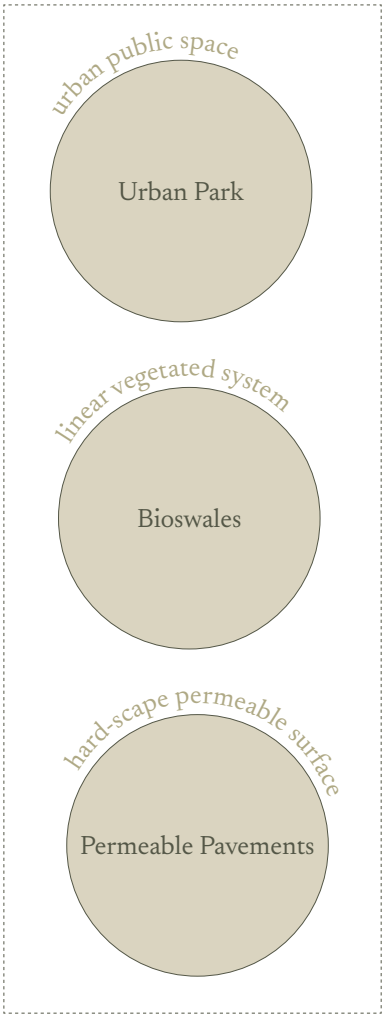

Types of BGI

Various types of BGI can be applied in urban flood adaptation. In this research, ground-based BGI adaptation refers to BGI strategies that are applied directly to the ground surface or open spaces within the site. This includes vegetated areas, planted runoff systems, and permeable surface materials that can influence how rainwater moves, accumulates, infiltrates, or is temporarily stored at the site level. This research focuses on ground-based BGI adaptations because the aim is to evaluate how spatial changes at the site level influence runoff movement, water accumulation, and building-level flood resilience. Therefore, three selected strategies are discussed in more depth: urban parks, bioswales, and permeable pavements. These strategies are selected as representative examples of different ground-based BGI typologies. Other ground-based BGI strategies are mentioned more briefly to provide a broader overview of possible approaches. Building-integrated BGI adaptations, such as green roofs, are excluded from this research because they are more closely related to building-level design than to ground-based spatial adaptation. The following section discusses each selected BGI strategy in relation to its spatial characteristics, rainwater performance, and relevance for flood adaptation.

Figure 20. Tebet Eco Park (www.archdaily.com)

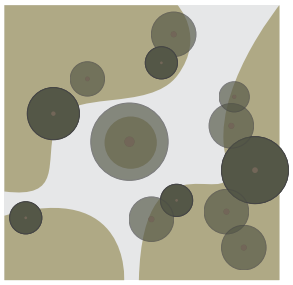

Urban Park

Among the selected BGI strategies, urban parks represent larger multifunctional green-space adaptations at the site or neighbourhood scale. They are a key component of urban green infrastructure, serving nearby residential areas as accessible spaces for nature-based recreation while also delivering environmental functions. Eisenberg & Polcher (2019) emphasises that to function effectively, parks should contain a high proportion of vegetated surfaces (>50%), particularly trees, which support climate regulation and ecological performance.

In relation to rainwater management, urban parks can contribute to runoff reduction through vegetated and permeable surfaces that allow infiltration into the soil. Grass surfaces can theoretically eliminate almost all surface runoff under ideal conditions (Armson et al., 2013). However, real urban park conditions, including soil compaction from footfall and mixed surface types, usually result in more moderate runoff performance. For example, Son and Kwon (2022) reported a runoff coefficient of 0.245 for urban park surfaces in South Korean case studies, suggesting that urban parks can substantially reduce runoff but do not necessarily absorb or retain all rainfall.

Beyond runoff reduction, urban parks also have strong multifunctional potential because they operate as public open spaces. Their contribution is therefore not limited to hydrological performance, but can also include recreational, social, ecological, and placemaking values. This is supported by Crowe et al. (2025), who discuss how BGI and placemaking can contribute to wider themes such as health and wellbeing, people and communities, active travel, economic value, and biodiversity. In the context of urban parks, these qualities are particularly relevant because parks are spaces that people can access, use, and experience directly. Recent climate-adaptive park projects further demonstrate how public-space qualities can be combined with water-management functions. The Kokkedal Climate Adaptation Project in Copenhagen (Figure 21 and 22), for example, is based on this approach, in which the urban landscape is shaped to retain and store rainwater locally, upstream, and on the surface. Rather than treating runoff as something to be hidden or removed as quickly as possible, the project uses a sequence of landscape spaces to guide, absorb, retain, and temporarily store water while also creating aesthetic, recreational, and educational qualities in the public realm (Jørgensen et al., 2022).

Figure 21. Aerial view of Kokkedal Climate Adaptation Project (www.realdania.org)

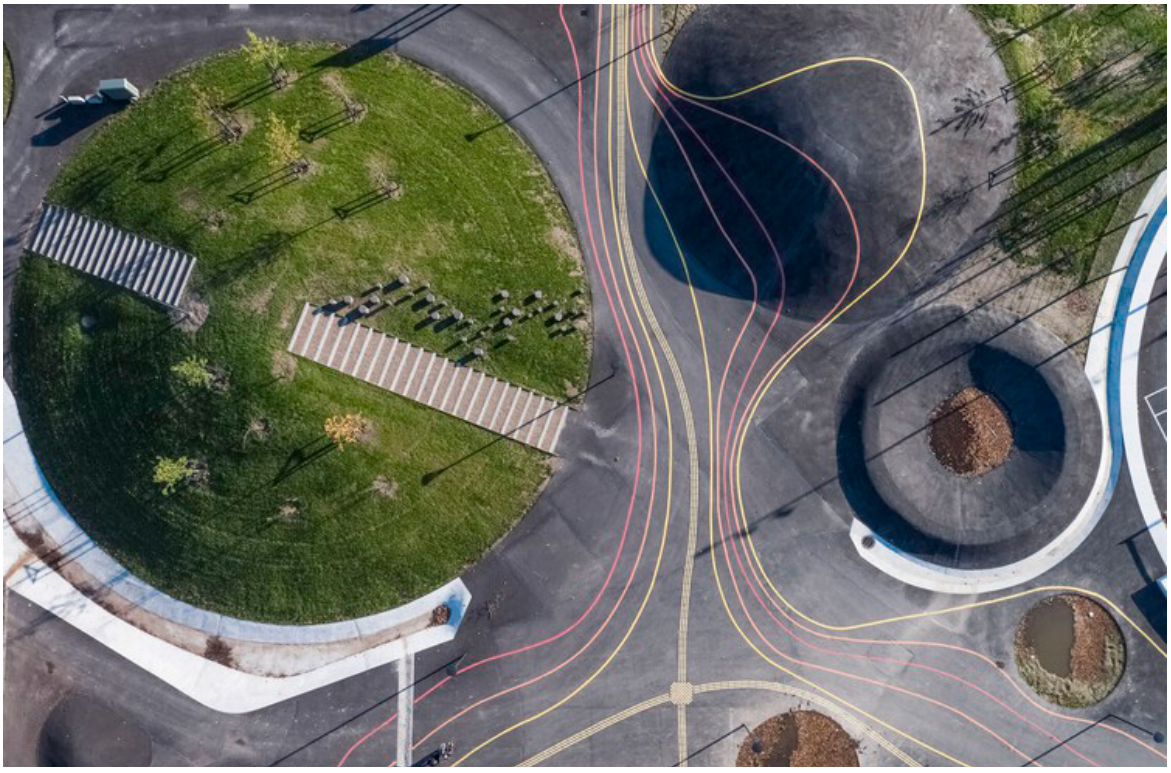

Figure 22. Top view of Kokkedal Climate Adaptation Project public space (www.realdania.org)

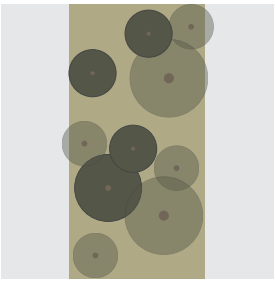

Bioswale

Among the selected BGI strategies, bioswales (Figure 24) represent linear vegetated runoff systems. They are typically located in low-lying or gently sloped areas, often adjacent to roads and paved surfaces, where they can intercept runoff from impervious urban surfaces. Bioswales manage surface runoff by slowing, conveying, temporarily storing, and infiltrating water into the ground. Through vegetation and soil media, they can also support water-quality improvement by filtering sediments and pollutants (Eisenberg & Polcher, 2019).

The performance of bioswales is strongly influenced by site-specific conditions, design configuration, and saturation behaviour. In this context, saturation behaviour refers to how the infiltration capacity of a bioswale changes as its soil and storage layers become increasingly wet or filled with water. Dutch guidelines for bioswales, or wadis, recommend an infiltration rate of at least 0.6 m/day and an emptying time of 24 hours (Boogaard et al., 2006); for a 30 cm deep swale, this emptying-time requirement corresponds to a minimum infiltration rate of approximately 0.3 m/day (Kondratenko et al., 2024). However, full-scale infiltration tests show that actual bioswale performance can vary substantially. Kondratenko et al report that infiltration rates in their Riga case studies ranged from 0.1 to 7.7 m/day and decreased by 30–58% after saturation. Their wider comparison of international full-scale tests also shows considerable variation in bioretention infiltration rates, with decreases after repeated filling and emptying. This suggests that bioswale performance is measurable but highly context-dependent, and that simplified assumptions are needed when translating bioswale performance into an early-stage design assessment workflow.

Figure 23. Bioswale-based green streets (Church, 2015)

As vegetated linear systems, bioswales contribute to runoff management while also improving ecological and streetscape quality. They are not primarily recreational spaces like urban parks, but they can be integrated into streets, sidewalks, parking areas, and road verges as visible landscape elements. For example, Acosta and Haroon (2021) describe a modular design that combines bioswales and street trees within road space previously used for parking, highlighting their potential contribution to flood reduction, air-quality improvement, green-cover expansion, and more inclusive urban design (Figure 23). Church (2015) also shows that bioswale-based Green Streets can make stormwater management more visible and support public awareness, while Lemieux et al. (2025) found that bioswales within street right-of-way spaces can improve perceived comfort, safety, attractiveness, and sustainability for walking and cycling. Therefore, the multifunctionality of bioswales is more specialised toward rainwater regulation, ecological performance, environmental awareness, and streetscape integration, rather than direct public recreation.

Figure 24. Example of a bioswale (www.maristem.co.uk)

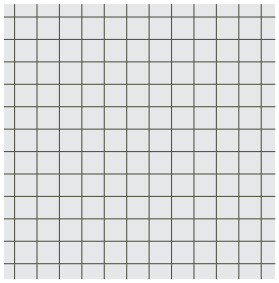

Permeable Pavement

Permeable pavement is a type of load-bearing pavement system that allows rainwater to infiltrate through gaps, joints, or porous surfaces into the underlying structure. Kuruppu et al. (2019) describe permeable pavement systems as structures designed to promote rainwater infiltration through the permeable surface and underlying layers. These systems can capture water on the pavement surface, filter and treat it as it passes through aggregate layers, and temporarily store or infiltrate it into the ground. Permeable pavements can therefore combine the function of a hard urban surface with an infiltration and detention system. They can be applied to footpaths, roads, playgrounds, car parks, pedestrian areas, and other paved surfaces, although their suitability depends on traffic load, speed, and site conditions. The working mechanism of permeable pavement is illustrated in Figure 24.

Permeable pavement provides a means of accommodating necessary hardscape functions while maintaining partial rainwater-regulation capacity. Unlike conventional impervious paving, the permeable surface and engineered sub-base system allow water to pass through the pavement and be temporarily stored or infiltrated below the surface, thereby reducing surface runoff. As previously discussed in relation to urban parks, Son and Kwon (2022) reported a runoff coefficient of 0.245 for vegetated park surfaces. In the same study, they reported a higher runoff coefficient of 0.583 for permeable sidewalks, but this was still substantially lower than the values reported for some pervious sidewalks and impervious sidewalks. Their comparison suggests that permeable sidewalks perform less effectively than vegetated areas, but can still reduce runoff compared with more impervious paved surfaces. Therefore, permeable pavement does not replace the hydrological role of green space, but can improve runoff performance in areas that need to remain paved. Due to this functional flexibility and compatibility with urban circulation systems, permeable pavement can be implemented in various contexts, including parking areas, sidewalks, pedestrian spaces, and low-traffic streets.

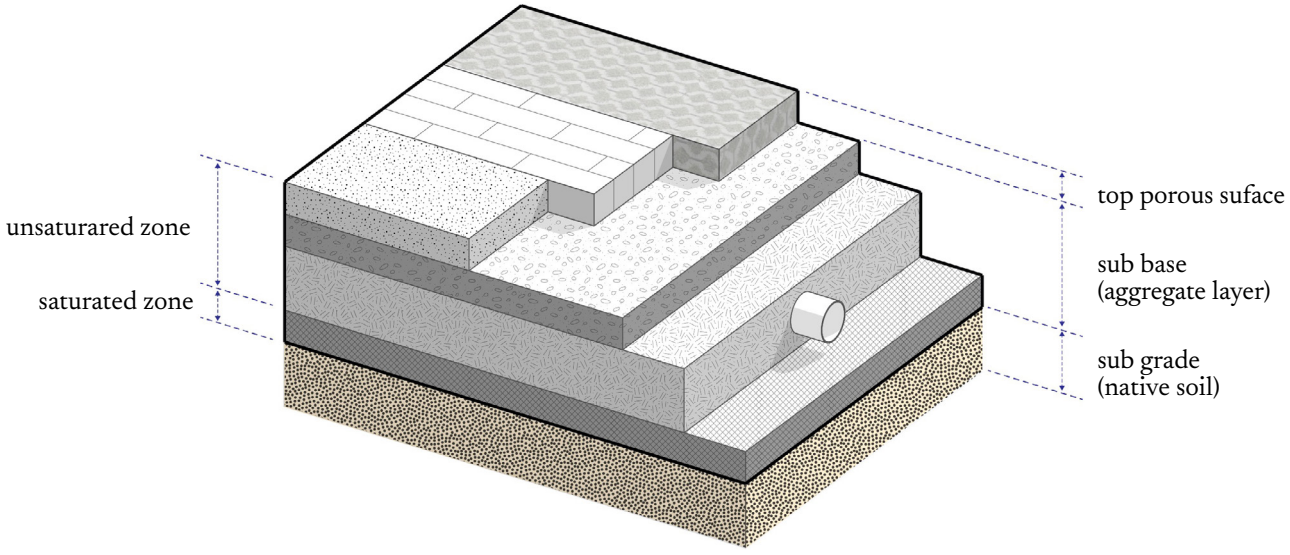

Figure 25. Layers of permeable pavement

Other Types of BGI

Besides these three BGI types, Eisenberg and Polcher (2019) also classify other BGI elements that are relevant to site rainwater management. These are briefly introduced here to provide a broader overview of possible strategies beyond the three adaptations discussed more in depth.

Infiltration Basin

An infiltration basin is a shallow, flat, grassed area designed to temporarily store surface runoff and allow water to infiltrate into the ground following heavy rainfall events (Eisenberg and Polcher, 2019). Under normal conditions, the basin remains dry, filling with water only during storm events, after which the collected runoff gradually infiltrates through underlying soil layers. Infiltration basins primarily rely on natural filtration processes within the soil to reduce runoff volumes and improve water quality. Their effectiveness depends on site conditions, including available space, soil permeability, and local rainfall intensity. Design requirements typically include placement below surrounding ground level, a level basin floor to ensure uniform infiltration, and the ability to infiltrate a significant portion of stored water within a short time frame.

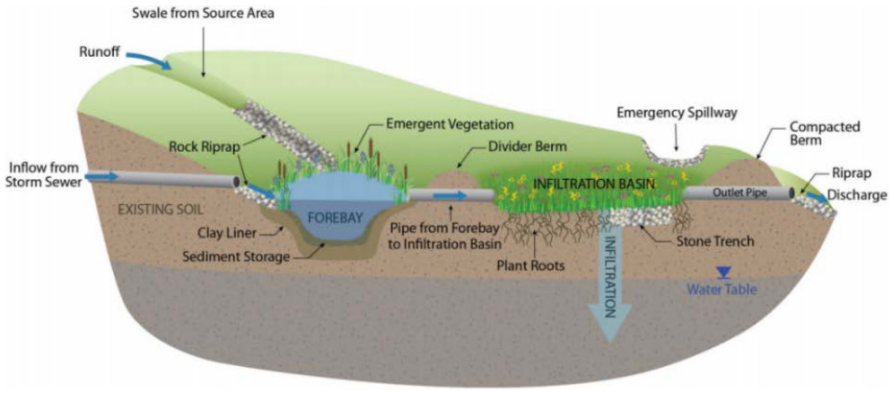

Figure 26. Infiltration Basin (Eisenberg and Polcher, 2019)

Dry Detention Pond

Figure 27. Dry Pond with Sand Filter (www.ecodesignsd.com)

A dry detention pond is a surface storage basin designed to temporarily retain stormwater during heavy rainfall events and release it gradually into the downstream drainage system (Eisenberg and Polcher, 2019).

In contrast to infiltration basins, which reduce runoff by allowing water to soak into the ground, detention ponds primarily function by storing water and reducing peak flows, with limited reliance on soil permeability. Under normal conditions, dry detention ponds remain empty and can be used as green or recreational space, while during storm events they temporarily flood before slowly draining. This makes detention ponds suitable in areas where infiltration capacity is limited but peak flow control is required.

Wet Detention Pond

Figure 28. Wet Retention Pond (www.aqualisco.com)

A wet retention pond is a permanent water body designed to continuously store stormwater, remaining filled even during dry periods (Eisenberg and Polcher, 2019). It reduces flood risk by retaining runoff and improving water quality through natural processes such as sedimentation and infiltration. Wet retention ponds are typically located at low points within a site and integrated into parks or open spaces, but their permanent water level limits alternative recreational uses.

Constructed Wetland

Figure 29. Constructed Wetland (The Wetland Conservancy)

Constructed wetlands are engineered landscape systems designed to store, treat, and regulate stormwater by mimicking the hydrological and ecological processes of natural wetlands (Eisenberg and Polcher, 2019). They use shallow basins, vegetation, soil, and microbial activity to slow water flow, promote sedimentation, and remove pollutants through filtration and biological uptake. In addition to reducing flood risk and improving water quality, constructed wetlands can support biodiversity, provide recreational value, and supply treated water for uses such as irrigation. Their implementation typically requires relatively large, gently sloped sites and is most suitable where sufficient space is available.

Biofilter (Water Purification)

Figure 30. Biofilter at Monash University (Eisenberg and Polcher, 2019)

Biofilters are engineered systems designed to collect, treat, and purify stormwater by passing it through layers of vegetation, soil, and filter media that support microbial activity (Eisenberg and Polcher, 2019). Pollutants such as nutrients, metals, sediments, and organic contaminants are removed through biological degradation, filtration, and adsorption processes. In addition to improving water quality, biofilters temporarily store stormwater and regulate runoff, allowing treated water to be reused or discharged more safely into the environment. Their effectiveness depends on appropriate filter media, vegetation selection, and sufficient space for installation.

Rainwater Regulation Performance Assessment

To model the rainwater performance of the selected BGI types, this research focuses on how BGI reduces surface runoff accumulation and, consequently, flood-depth formation. This is relevant because the building-level resilience assessment is linked to the depth–damage relationship, where changes in flood depth affect the estimated impact on buildings. Following the simplified calculation logic applied in Rainwater+ by Chen et al. (2016), runoff-reduction performance can be represented through the relationship between BGI coverage area and depth-based storage. In this research, these depth-based parameters are simplified into the term **storage depth**, which refers to the assumed depth of rainwater that a BGI patch can infiltrate and absorb per unit area. **In practical terms, the potential storage volume of a BGI patch is calculated as its surface area multiplied by its assigned storage depth.**

The main difference from Rainwater+ is that Chen et al. use these parameters within a calculation-based framework, while this workflow uses storage depth as an input to the particle-based simulation. The spatial movement, spreading, and accumulation of runoff are handled later in Grasshopper, while the storage-depth value defines how much water each BGI patch can absorb or retain when runoff reaches it. This approach also differs from Jia et al. (2022), who treated green space as fully absorptive in the runoff simulation. By introducing BGI-specific storage depths, this study enables differentiated performance representation across urban parks, bioswales, and permeable pavements before these values are translated into the Grasshopper simulation workflow.

As discussed in the previous section, urban parks, bioswales, and permeable pavements have different spatial and hydrological characteristics. The following subsections explain how these values are derived or adopted before they are translated into the Grasshopper simulation workflow.

Urban Park

Urban parks require a different storage-depth derivation because they are represented as vegetated and soil-based surfaces. For this type of surface, one widely applied baseline for representing this capacity is the SCS-CN method (Al-Ghobari et al., 2020; Soulis, 2021). The SCS-CN method is a well-established conceptual approach for estimating direct runoff volumes from a given rainfall event. Developed in the late 1950s by the U.S. Department of Agriculture, now the Natural Resources Conservation Service, it was originally intended to assess runoff in small agricultural watersheds. In this method, each surface condition is assigned a Curve Number (CN), which reflects its runoff potential based on land cover and soil type. A higher CN indicates lower infiltration and higher runoff, while a lower CN indicates greater retention capacity and lower runoff.

In this research, the CN method is used only to calculate default storage-depth values for urban park surfaces, rather than as a full runoff calculation method. This responds to the concern raised by Jia et al., who note that NRCS-based methods can still require designers to engage with hydrological data input and soil infiltration analysis. By carrying out the CN-based calculation during the parameter-definition stage, the workflow provides storage-depth values that can be directly used as default inputs for urban park surfaces. These values can still be adjusted when more specific soil, vegetation, or infiltration data is available. The CN values used for this calculation are retrieved from the open-source CN tables provided by the Hydrologic Engineering Center, as shown in Table 6.

	Curve Numbers for Soil Group			
Cover type and hydrologic condition	**A**	**B**	**C**	**D**
Poor condition (grass cover < 50%)	68	79	86	89
Fair condition (grass cover 50% to 75%)	49	69	79	84
Good condition (grass cover > 75%)	39	61	74	80

Table 6. CN Number for different grass-covered soil groups

Since urban parks are recommended to contain more than 50% vegetated surface, this research uses two grass-cover conditions: 50–75% vegetation cover and more than 75% vegetation cover. Hydrologic Soil Group C is selected as a simplified and conservative assumption, as it represents relatively low infiltration capacity and is considered suitable for an urbanised context where soil compaction and surrounding impervious surfaces may reduce infiltration performance. A similar assumption is also used by Chen et al. (2016). If more detailed soil or infiltration data is available, the storage-depth value can be adjusted accordingly. The calculation process used to derive the urban-park storage-depth values is shown below.

Fair Condition 0.068 m ← CN = 79 $S = \frac{100}{CN} - 10$ CN = 74 → **Good Condition** 0.089 m

S = Storage Number
CN = Curve Number
(Chen et al., 2016)

Based on the CN-derived storage depth, urban parks in fair condition (0.068m) and good condition (0.089m) absorb approximately 48.6% and 63.6% of direct rainfall respectively for the study site. These values are below the 75.5% absorption suggested by Son & Kwon (2022) based on assessment on their case study. However, Son & Kwon measured their values across eight Korean urban parks without specifying soil type, and Korean soils may differ significantly from Rotterdam's clay-based polder soils. The CN-derived values are therefore considered more appropriate for the Rotterdam context. Both fair and good condition values are provided as reference defaults – designers can adjust the storage depth based on site-specific soil and vegetation conditions.

Bioswale

For bioswales, the storage-depth value is based on the physical storage capacity discussed by Kondratenko et al., (2024), who refer to Dutch guidelines for bioswales, or wadis, by Boogaard et al. (2006). In the investigated full-scale bioswales, Bioswales 1–6 have storage depths of up to 30–50 cm, while Bioswales 7–8 have depths of up to 45 cm. Based on this range, this research adopts **0.40 m** as a representative bioswale storage-depth value. In the workflow, this value represents the maximum water depth that a bioswale patch can temporarily store per unit area before it is treated as saturated. However, because Kondratenko et al. also note that overflow levels may be lower than the total swale depth, this value should be understood as an indicative geometric storage parameter and adjusted when site-specific bioswale dimensions, overflow levels, or hydraulic design data are available.

Permeable Pavement

For permeable pavements, the storage-depth value is related to the temporary storage provided by the pavement structure. Permeable pavement systems allow runoff to pass through the permeable surface and aggregate layers, where water can be filtered, temporarily stored, and infiltrated into the subgrade structure. This means that the rainwater capacity is not only located on the surface, but also within the underlying pavement layers (Kuruppu et al., 2019).

In this research, the storage depth is adopted from Chen et al. (2016), who define a maximum retention depth of **0.075** m for permeable pavement systems. In the workflow, this value represents the amount of rainwater that a permeable pavement patch can temporarily retain or store per unit area before it is treated as saturated. The value can be adjusted if more specific pavement design data, such as sub-base depth, material composition, drainage condition, or maintenance condition, is available.

Cost Assessment

In addition to rainwater-storage performance and building-level resilience improvement, BGI adaptation also has cost implications. Comparing implementation cost is relevant because a scenario with higher performance may also require substantially larger investment. Therefore, the cost comparison is used to support interpretation of the trade-off between adaptation performance and the estimated cost of applying different BGI types across the case study area

The implementation cost values are adopted from the Deltares Wiki database (Brolsma, 2024). These values are used as comparative cost inputs rather than detailed construction-cost estimates. For urban parks, two cost values are assigned to reflect the two vegetation-cover conditions used in the storage-depth calculation: **€40/m² for the 50–75% vegetation-cover condition**, based on the mean value, and €**100/m² for the >75% vegetation-cover condition**, based on the maximum value. **Bioswales are assigned a mean implementation cost of €75/m²**, w**hile permeable pavements are assigned €100/m²**. These cost values allow the adaptation scenarios to be compared not only by rainwater-storage performance, but also by the estimated cost of applying each BGI type across the case study area.

Key Characteristics Summary

Based on the qualitative discussion, storage-depth parameterisation, and cost values explained above, the three selected BGI adaptations represent different approaches to flood adaptation. Urban parks provide larger multifunctional green spaces, bioswales function as linear vegetated runoff systems, and permeable pavements integrate rainwater regulation into hardscape surfaces. Table 7 summarises their key characteristics, including spatial function, rainwater-performance representation, implementation cost, and main design constraints.

	Urban Park	Bioswale	Permeable Pavement
	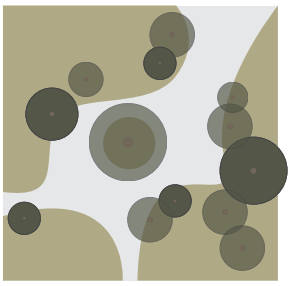	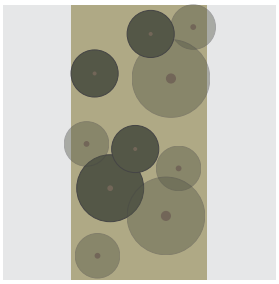	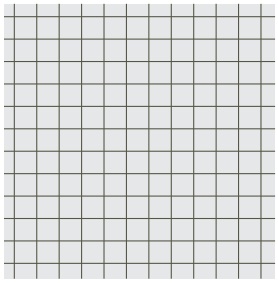
Spatial Aspect			
function	recreation + cooling + ecology + runoff reduction	runoff interception + filtration + streetscape greening	circulation + runoff reduction + temporary storage
spatial application	parks, courtyards, neighbourhood green spaces	street edges, parking lanes, sidewalks, low points	sidewalks, plazas, parking areas, low-traffic streets
constraint	needs larger open space; performance depends on soil/vegetation	needs planted strip; saturation and maintenance matter	lower storage; clogging, load, and sub-base matter
Quantitative Aspect			
storage depth	0.068 m for 50 - 75% grasscover 0.09 m for > 75% grasscover	0.3 - 0.5 m (0.4 m as mean value)	0.075 m
cost	€40/m² for 50 - 75% grasscover €100/m² for > 75% grasscover	€75/m²	€100/m²

Table 7. BGI characteristics summary

2.3 | Computational Workflow

Workflow Overview

Figure 31 shows the overall computational workflow developed in this research. The workflow consists of several connected stages, including spatial and building data input, BGI adaptation input, simulation and processing, and output generation. These stages are used to evaluate the consequences of different BGI design options in relation to runoff absorption, flood-depth formation, and building-level resilience. The purpose of the workflow is to connect spatial design inputs with flood-resilience assessment, so that different BGI adaptation scenarios can be tested under the same rainfall, terrain, and building conditions.

Grasshopper, a visual scripting environment within Rhinoceros 3D, is selected as the main development platform because it is already widely used in architectural and urban design for parametric modelling and design exploration. Its component-based structure allows geometry, parameters, and calculations to be connected within one interactive environment, making it suitable for early-stage design-support workflows. This selection also follows Jia et al. (2022; 2024), who demonstrate the potential of Grasshopper-based stormwater analysis tools to support urban designers in evaluating green stormwater management strategies.

The following sections explain how the computational workflow is constructed and the methodological logic behind its main components. They discuss how spatial and building data are prepared and structured as inputs, how rainfall is represented through particle-based simulation, how BGI adaptation areas modify runoff through absorption logic, how particle results are translated into site flood-depth and building-inundation values, and how these outputs are connected to resilience scoring and visualisation. Beyond producing numerical results, the workflow outputs can later be used to support design interpretation by comparing movement paths, absorbed volume, flood-depth changes, resilience-score differences, and indicative implementation cost across adaptation scenarios.

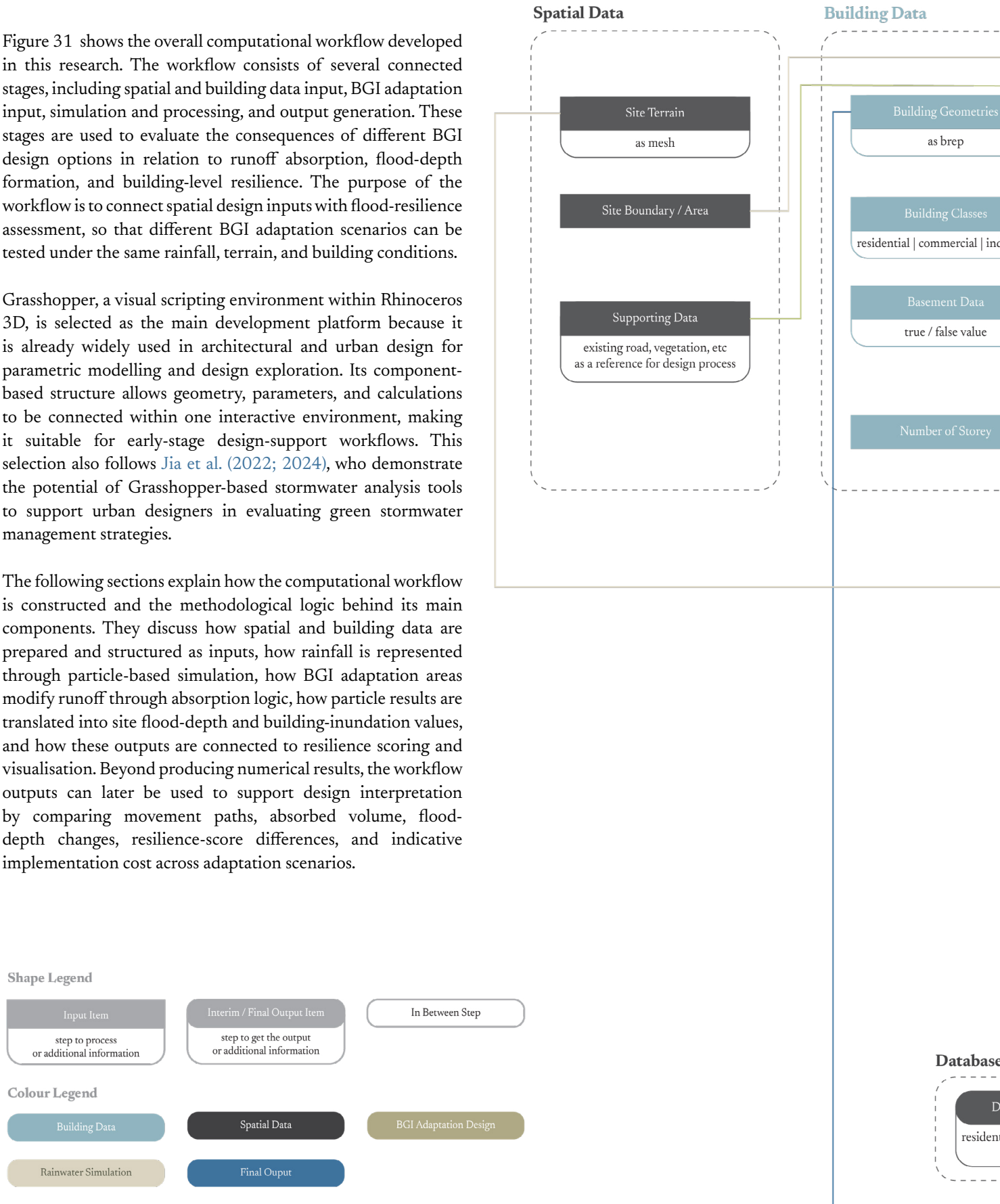

Figure 31. Computational workflow overview

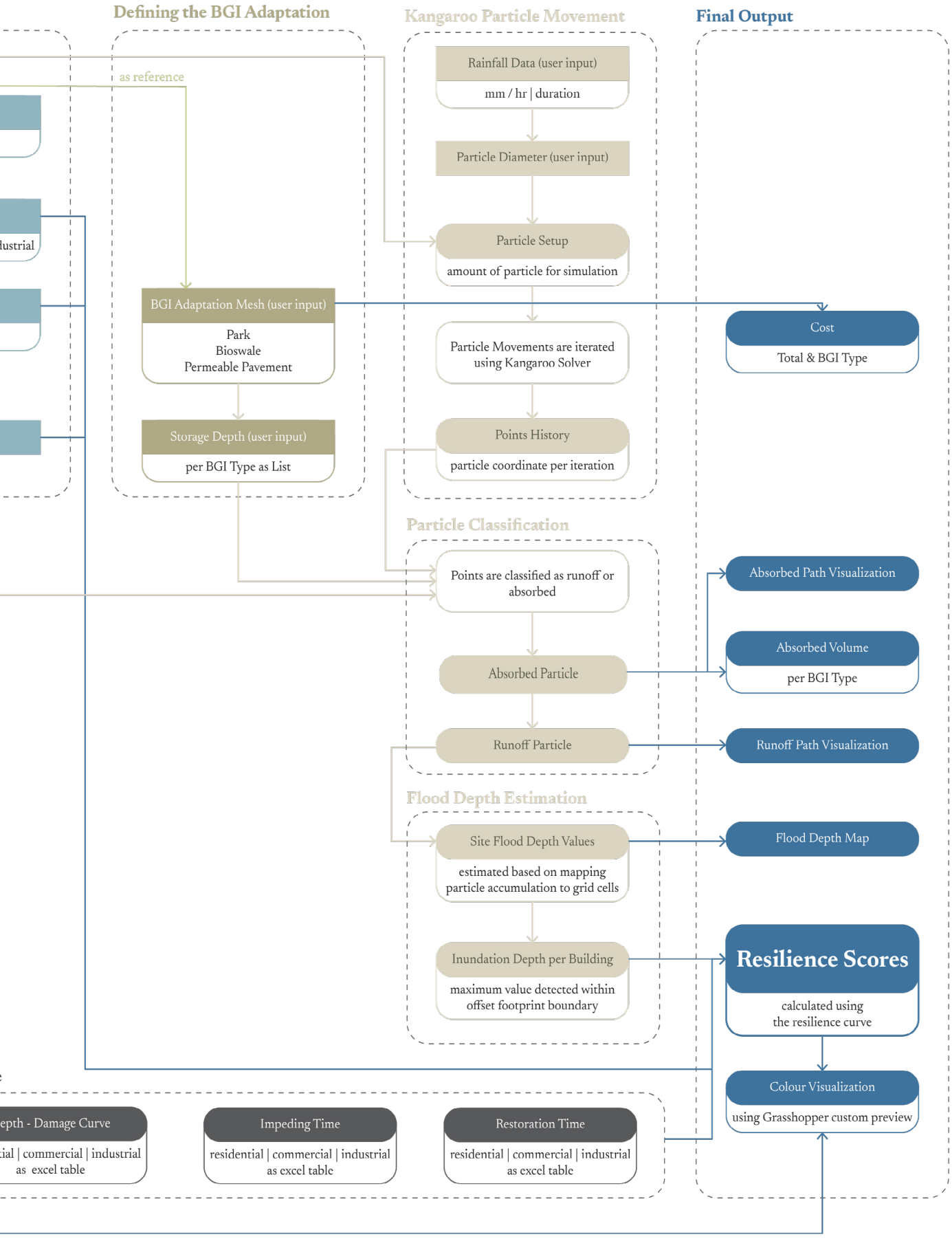
Defining the BGI Adaptation
Kangaroo Particle Movement
Final Output
as reference
Rainfall Data (user input)
mm / hr | duration
Particle Diameter (user input)
Particle Setup
amount of particle for simulation
BGI Adaptation Mesh (user input)
Park
Bioswale
Permeable Pavement
Particle Movements are iterated using Kangaroo Solver
Cost
Total & BGI Type
Storage Depth (user input)
per BGI Type as List
Points History
particle coordinate per iteration
Particle Classification
Points are classified as runoff or absorbed
Absorbed Path Visualization
Absorbed Volume
per BGI Type
Absorbed Particle
Runoff Particle
Runoff Path Visualization
Flood Depth Estimation
Site Flood Depth Values
estimated based on mapping particle accumulation to grid cells
Flood Depth Map
Inundation Depth per Building
maximum value detected within offset footprint boundary
Resilience Scores
calculated using the resilience curve
Colour Visualization
using Grasshopper custom preview
Impeding Time
residential | commercial | industrial
as excel table
Restoration Time
residential | commercial | industrial
as excel table

Spatial Data Input Structure

The terrain model is the main spatial input in the workflow because the rainwater simulation requires a surface where particles can move, spread, and accumulate. In Grasshopper, this terrain needs to be represented as a mesh. The mesh functions as the simulation surface, where slope, surface form, and local depressions influence runoff movement and accumulation.

The level of detail of the terrain mesh affects both simulation accuracy and computational performance. A more detailed mesh can represent surface variation more precisely, but it also increases the number of mesh faces processed during the particle simulation. Therefore, the terrain mesh needs to balance spatial accuracy and simulation efficiency.

Building geometries also affect how the terrain is prepared. In a particle-based simulation, building footprint areas can be removed from the terrain mesh to prevent particles from accumulating within building areas, as applied by Morschek et al. (2019). Alternatively, building geometries can be merged with the terrain to create a continuous simulation mesh, as applied by Jia et al. (2022). While the second approach can provide a continuous surface for particle movement, it can also make the mesh more complex and computationally heavier. If the building geometries are represented with flat surfaces instead of detailed roof geometry, particles may also accumulate on building roofs or remain stuck on flat building surfaces. These two approaches are illustrated in Figure 32.

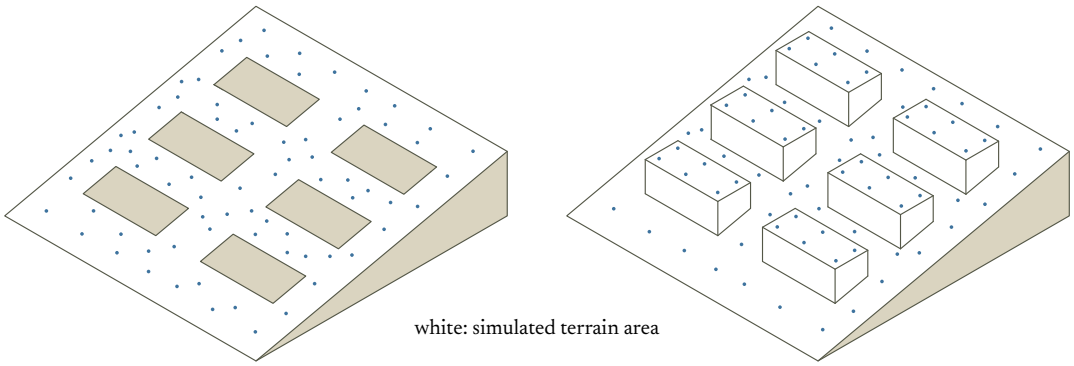

Figure 32. Illustration of terrain mesh preparation approaches for particle-based simulation: terrain with building footprints removed (left) and terrain merged with building geometry (right)

A simulation boundary is also needed to define the area where rainfall volume is calculated. This boundary can be defined separately or derived from the terrain area. Other spatial layers, such as streets or existing green areas, can also be included as reference layers for interpretation and adaptation placement. However, they do not necessarily need to be part of the simulation mesh, because additional geometry can increase mesh complexity and slow down the simulation.

Building Data Input Structure

Following the preparation of spatial geometry, the workflow also requires building attribute inputs for the resilience assessment. These include building class, basement presence, and number of storeys. As defined in Section 2.1, the resilience score depends on the relationship between inundation depth, building class, and vulnerability-related parameters. Therefore, each building Brep needs to remain associated with the correct attribute values throughout the workflow. The building geometries act as the spatial building objects, while the attributes provide the information needed for inundation assessment and resilience scoring. Later, the same geometries are also used to visualise the final building-level results.

In the custom Grasshopper components for resilience calculation, these building attribute inputs are provided separately rather than combined into one building-data object. For example, the resilience-score component receives building class, inundation depth, basement presence, and other resilience parameters as separate input lists, as shown in Figure 33. This structure makes the required parameters visible and adjustable on the Grasshopper canvas, which is useful for testing different assumptions or scenarios.

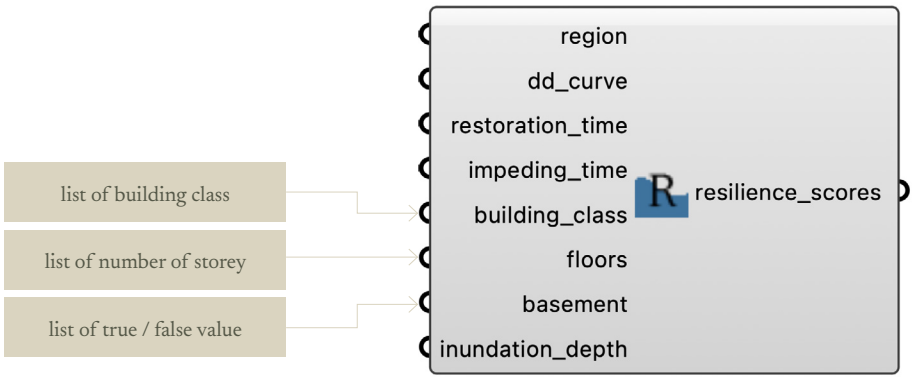

Figure 33. Separate building attribute inputs for the resilience-score component

Because the inputs are provided separately, their order needs to remain consistent. The first item in each input list must refer to the same building, the second item must refer to the next building, and so on. If one list is filtered, shifted, or reordered differently, the component may calculate the result using attributes from the wrong building. Therefore, data matching and order preservation are essential before the inputs enter the component, so that outputs such as damage ratio and resilience score can be assigned to the correct building geometries.

Alternatively, the building geometries and attributes could first be organised within a combined DataTree structure, where each branch contains the information related to one building. The relevant attributes could then be retrieved from each branch and connected to the individual component inputs when needed. This approach is also possible, but it requires careful control of branch structure and item retrieval. In this workflow, separate inputs are used to keep the component structure more transparent and directly editable during scenario testing.

Kangaroo-Based Particle Movement

After the spatial and building data inputs are prepared, the next stage is to model rainfall movement using a particle-based simulation approach. The resulting particle positions are then used to support later calculations related to BGI interaction, infiltration, and flood-depth estimation. In this method, rainfall is represented as discrete particles released over the site surface, allowing runoff movement, accumulation, and flood spread to be visualized spatially. This approach is selected because it provides an intuitive and design-oriented way to observe how water interacts with terrain, buildings, and BGI elements during a rainfall event.

Particle-based approaches have previously been explored in flood simulation for their ability to represent water movement as discrete particles and support real-time visualization of runoff paths and flood spread. Hadimlioglu et al. (2020) for example, developed FloodSim, a flood simulation and visualization framework using position-based fluids for real-time flood spread visualization and particle tracking. Although FloodSim uses a different particle-based fluid method from the Kangaroo setup used in this workflow, both approaches share a similar principle: water movement is represented through discrete particles whose positions can be tracked and interpreted spatially. Similarly, the predecessors of this workflow (Jia et al., 2022, 2024) used a Grasshopper-based workflow with Kangaroo to simulate rainwater movement through particle behaviour.

Although several Grasshopper-based plugins have been developed for rainwater and rainwater simulation, such as Groundhog, this research uses Kangaroo as the primary particle simulation environment. This decision was made because the workflow aims to modify and extend the simulation logic by integrating BGI selection and infiltration behaviour through storage depth capacity. By starting from a more basic and flexible particle-based setup, the workflow allows greater control over how water particles are processed and transferred into the additional assessment components developed in this research.

Rainfall Input

Before the simulation setup is developed, it is necessary to define the rainfall input required to model a rain event. Rainfall data can be presented in different but related formats, either as a total precipitation depth over a given duration or as an hourly precipitation rate, as illustrated in Figure 34. This distinction is relevant because sources such as (Rotterdams WeerWoord, 2023) and historical rainfall guidance often describe rainfall events using total depth and duration, while datasets such as the Klimaateffectatlas provide hourly precipitation-rate values for the Netherlands.

Figure 34. How to Represent 140 mm for 2 hours under different ways

In this workflow, the rainfall event is treated as a predetermined scenario, meaning the simulation follows a deterministic approach. This differs from a probabilistic approach, which considers a range of possible rainfall events and their likelihood of occurrence. Liu et al. (2023) for example, use Monte Carlo simulations to generate multiple possible daily precipitation events to quantify probabilistic urban flood risk and uncertainty under climate change scenarios. In contrast, the purpose of this workflow is to assess and compare flood resilience performance under a fixed rainfall condition. A deterministic scenario-based approach is therefore suitable because it allows different BGI configurations to be evaluated consistently, without aiming to predict the exact probability of flooding.

This study adopts a simplified particle-based runoff accumulation framework similar to Jia et al. (2022, 2024), where rainfall depth is translated into runoff particles for conceptual surface-flow simulation. The framework intentionally simplifies several hydrological processes, including the role of manmade drainage systems. As a result, runoff is interpreted primarily through cumulative surface-water accumulation rather than detailed hydraulic behaviour. Under this assumption, rainfall scenarios with the same total precipitation are treated as producing similar runoff accumulation patterns within the no-drainage framework. For example, 50 mm/hr over 2 hours and 100 mm over 1 hour are both interpreted based on their accumulated rainfall depth. Although the particle simulation shows runoff movement and accumulation during the simulated event, it does not fully capture detailed hydraulic processes such as drainage response, flow timing, or changes in infiltration caused by rainfall intensity. This reflects the conceptual and comparative nature of the workflow, which is intended to support rapid evaluation of BGI performance and building-level flood resilience during early-stage urban design assessment, rather than detailed hydraulic flood prediction.

Particle Movement Iteration

Kangaroo Physics is used as the base engine for modelling rainwater particle movement within Grasshopper. In this workflow, Kangaroo is specifically used for the particle-movement stage of the rainwater simulation, while BGI behaviour, flood-depth calculation, and building-level assessment are handled through separate components developed within the workflow.

The component used to run this particle movement is the Kangaroo Solver. The Solver receives the initial rainwater particles, together with the forces and constraints that define how they move across the surface. It then iteratively updates the particle positions, producing a simplified representation of rainwater movement across the site. In this context, iterations refer to the repeated solver updates used to move particles toward a stable position under the defined forces and constraints. The process is illustrated as follows.

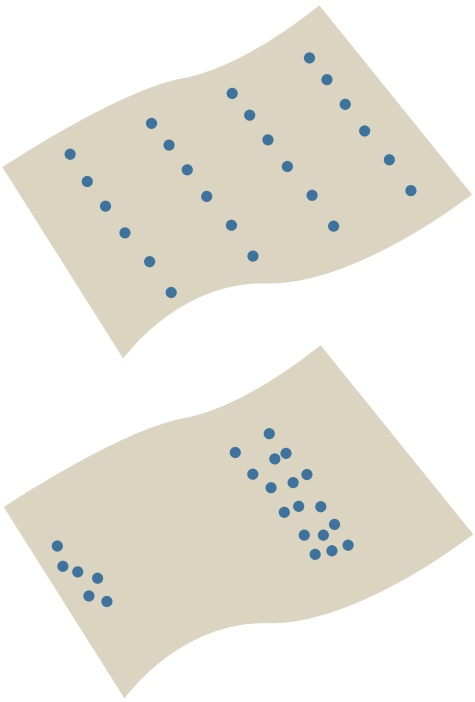

1 The terrain is first populated with rainwater particles based on the number defined by the user.

2 When the iteration mode is activated, the Kangaroo Solver updates the particle positions through repeated iterations until their movement stabilizes. Once a stable condition is reached, the status showed under the component changes from “Running” to “Converged.” The result is then recorded using Grasshopper Data Recorder so that both the final particle positions and movement records can be used in the next stages of the workflow.

After the rainfall scenario is defined, the next step is to determine the number of particles required for the simulation. Following Jia et al. (2022), each particle represents a defined volume of water. The total rainwater volume is calculated from the selected rainfall depth and the terrain area, then divided by the volume of one particle to obtain the required particle count. Since particle volume depends on particle diameter, increasing the particle diameter reduces the total number of particles, while decreasing the diameter increases the number of particles. This relationship introduces a trade-off: smaller particle diameters provide a more detailed representation of runoff movement but increase computational demand, while larger diameters reduce computation but may simplify the flow pattern. The diagram below illustrates the logic of this trade-off.

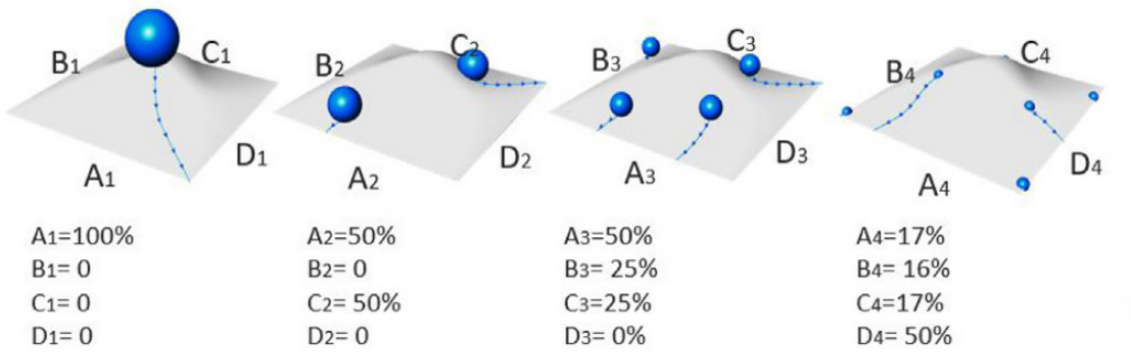

Figure 35. Particle size logic trade off (Jia et all, 2022)

Based on this relationship, the required number of particles is calculated by first deriving the total rainfall volume from the selected rainfall depth and terrain area. This volume is then divided by the volume represented by one particle. As shown in the diagram below, the particle count therefore depends on three main inputs: rainfall depth, terrain area, and particle diameter.

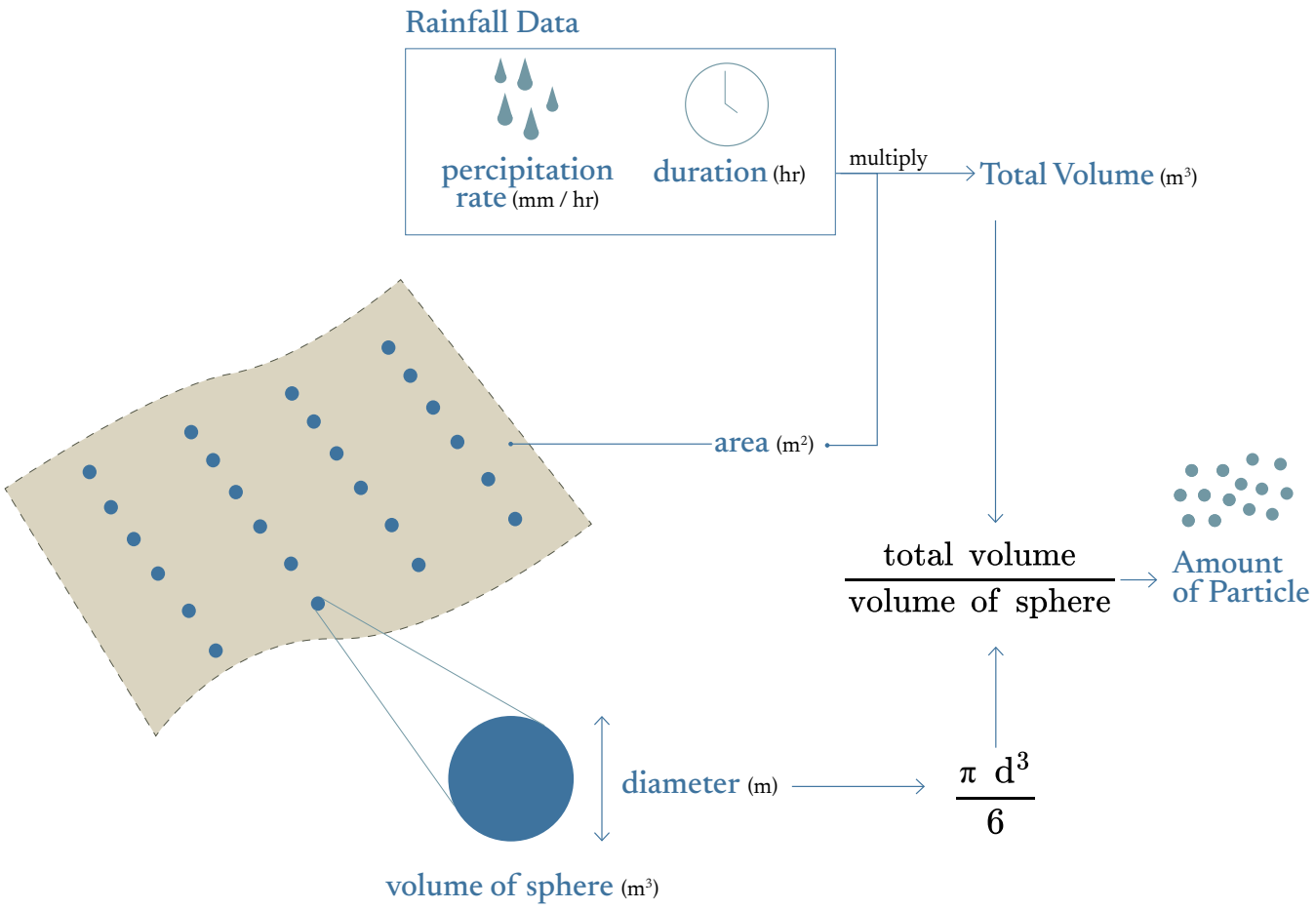

Figure 36. Particle count logic

The calculated particle inputs are then connected to the Kangaroo Solver, together with the required forces and constraints, such as gravity and surface interaction settings. These inputs define how the particles move in response to the terrain mesh. In the Kangaroo Solver, iterations refer to the repeated solver updates used to move the particles toward a stable position under the defined forces and constraints. A higher number of iterations allows the particles more time to respond to the terrain surface and settle into a more stable distribution, but it also increases computation time. The Solver outputs the particle coordinates (x,y,z) at each iteration, allowing the movement of particles across the terrain to be recorded over time. In this workflow, these coordinate outputs are stored using a Data Recorder, so that the particle positions can be used in later processing steps, including runoff-path visualisation, BGI interaction, and flood-depth estimation. The component setup is illustrated in Figure 37.

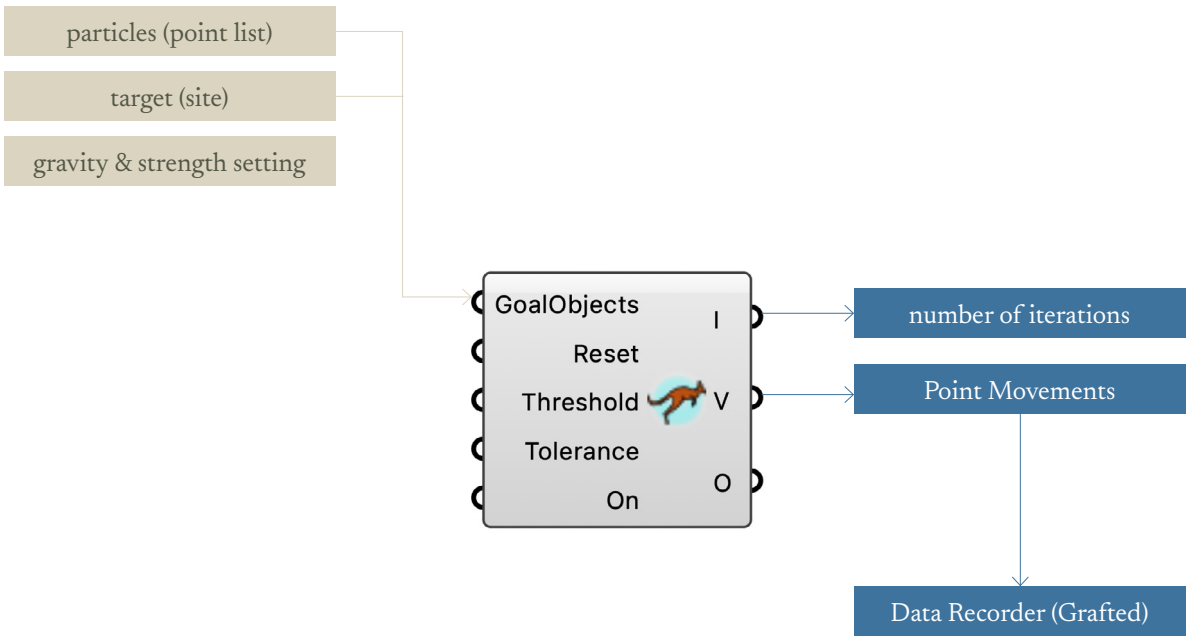

Figure 37. Kangaroo Solver input and output

BGI Adaptation Input and Particle Classification

After the particle movement simulation is conducted using Kangaroo, the next step is to classify the particles based on their end fate: runoff or absorbed. In this stage, two possible site conditions are considered. The first condition occurs when no BGI land-use area is defined, meaning the particles remain classified as runoff. The second condition occurs when BGI land-use areas are defined within the site. In this case, particles that pass through the BGI areas can be classified as absorbed, depending on the storage depth value assigned to each BGI type. To implement this process within the simulation environment, a custom Grasshopper component is developed to translate particle movement results into runoff and absorption values.

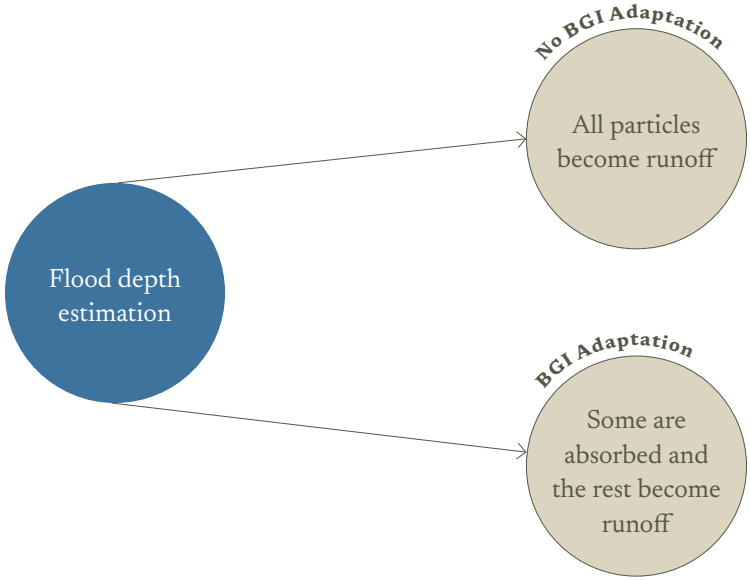

Figure 38. Two possible scenario of flood depth estimation

Defining the Terrain Land Use

When BGI is applied, the simulation environment is designed to make the assignment of BGI areas as straightforward as possible for the user. The process begins with a terrain mesh as the main input in Grasshopper. As illustrated in the figure below, the terrain is then divided into separate mesh regions according to the designated BGI types. These defined BGI meshes are later connected along with their corresponding storage depth sizes to the custom Particle Fate component, which classifies each particle as either runoff or absorbed.

1 Prepare the terrain, either created in Grasshopper or imported from Rhino.

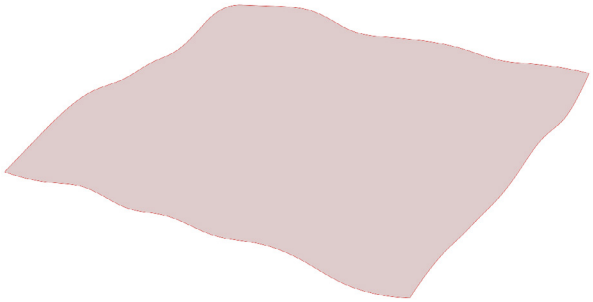

Figure 39. Generated terrain geomety

---

2 Set up layer names in Rhino, then draw polygons representing BGI areas and assign them to the correct layers (easiest in Top View by simply sketching the polygons).

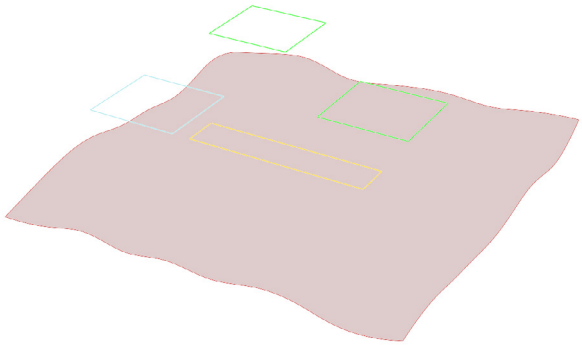

Figure 40. Define the Blue Green Infrastructure

---

3 In Grasshopper, use the preconfigured Geometry Pipeline to detect geometries from each layer; Drappe each polygons onto the terrain and generate corresponding BGI surface areas, and assign unique colors to each mesh for visualization.

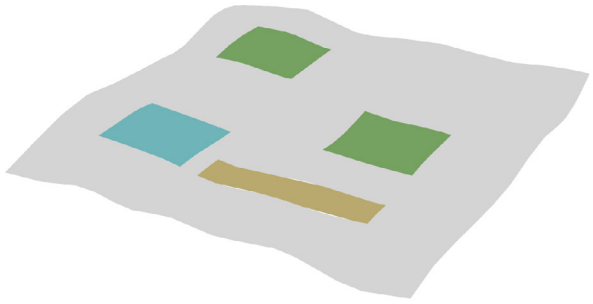

Figure 41. The clustered layers

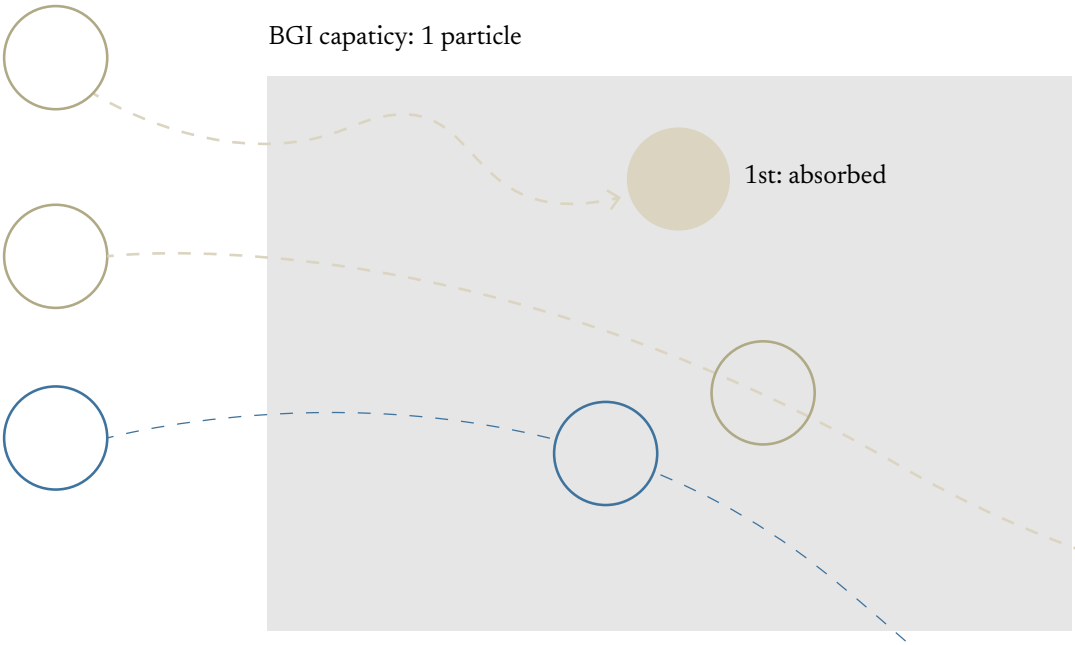

Classifying the Particle Fate

After the particle movement simulation is conducted, the workflow proceeds to particle classification, where each particle is assigned a final condition: absorbed or runoff. This process builds on the particle classification method developed by Jia et al. (2022, 2024), where particles are categorized according to whether they stop within or pass through Urban Green Space (UGS). In their framework, land cover is simplified into UGS and artificial surfaces, with UGS assumed to retain rainwater and artificial surfaces assumed to remain impervious. In this research, the classification logic is further developed to support multiple BGI types rather than a single generic UGS category. Each BGI type is assigned its own storage depth, allowing particles to be classified as absorbed only when they interact with a defined BGI area and when the absorption capacity has not yet been exceeded. Once this limit is reached, the remaining particles are classified as runoff. This extension allows the workflow to compare different BGI strategies and connect their absorption performance to subsequent flood-depth and building-level resilience assessment. The logic of this classification process is illustrated in this diagram.

Capacity of BGI
The maximum particle capacity is derived by dividing the total BGI storage volume (storage depth × area) by the volume of a single particle (calculated from particle diameter).

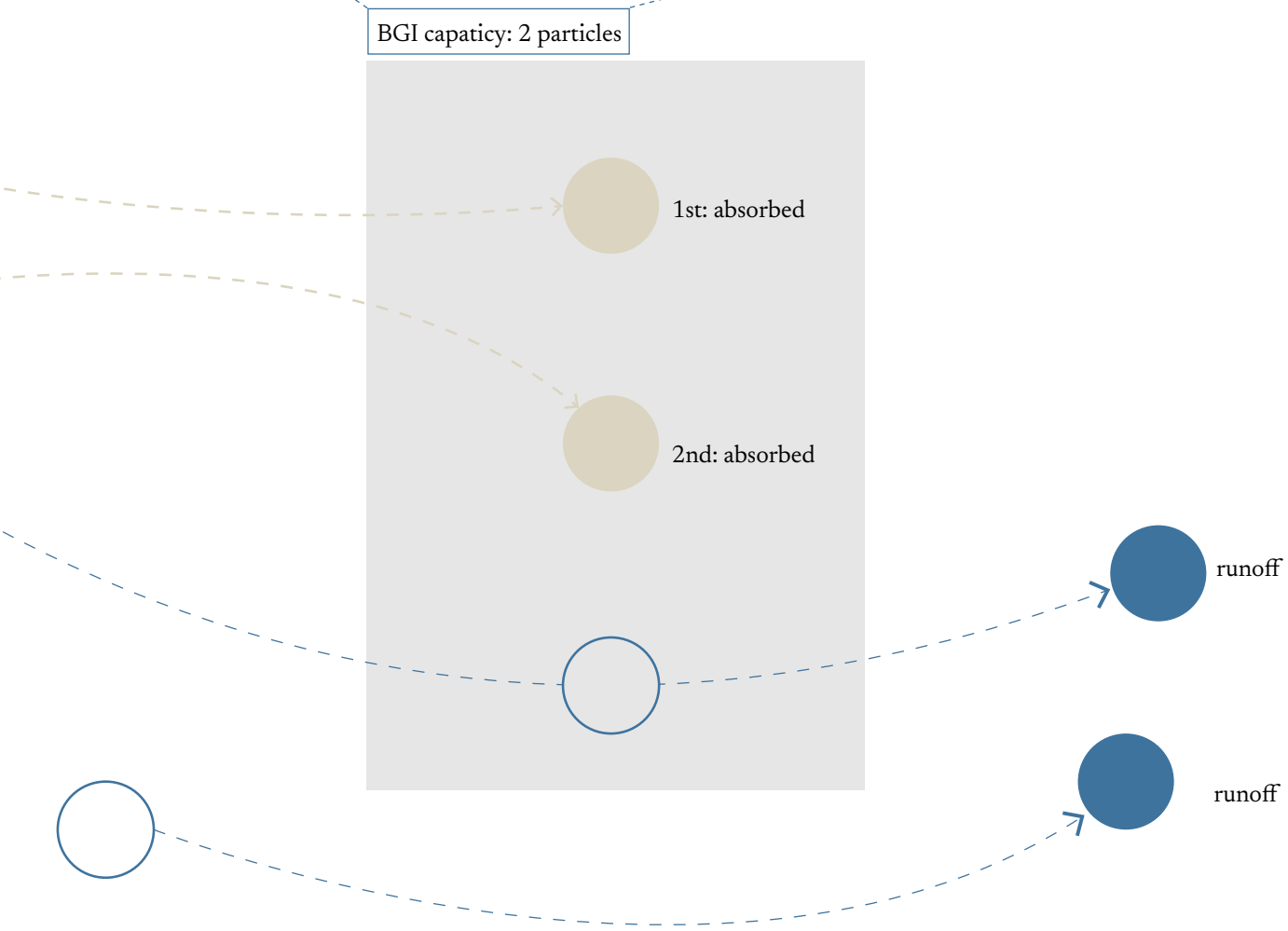

Figure 42 illustrates the custom Particle Fate component, which classifies particles as absorbed or runoff based on BGI interaction and remaining storage capacity. The component also generates supporting outputs, including visualisation attributes for Rhino and a summary of absorbed water volume.

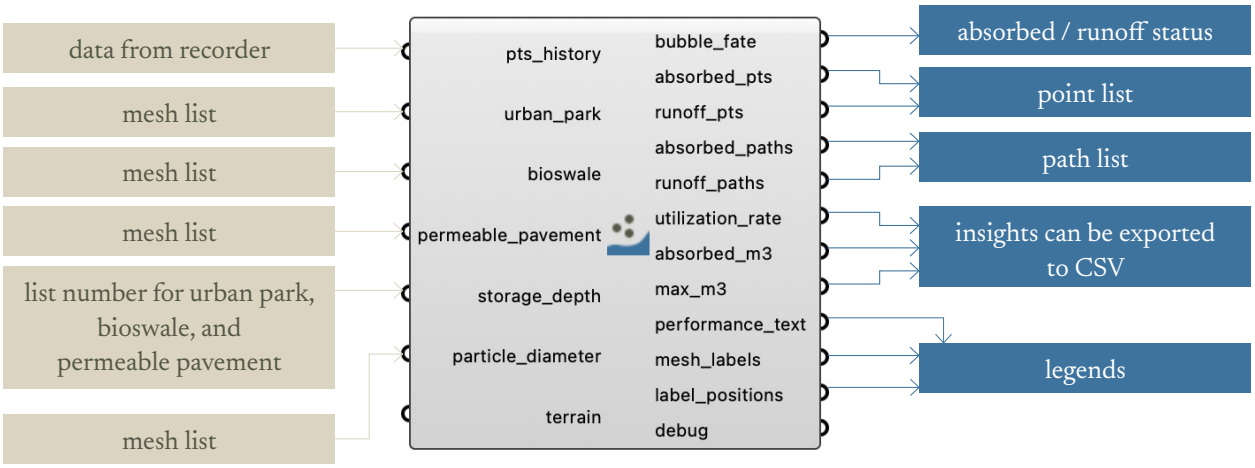

Figure 42. Runoff calculation component

Particle Movement Visualisation

In addition to classifying particles as absorbed or runoff, the Particle Fate component also produces outputs for movement-path visualisation. The outputs are separated into points and paths because they describe different aspects of particle behaviour. The absorbed and runoff points indicate the final classified particle locations, while the absorbed and runoff paths show the movement trajectories leading to those locations. By separating these outputs, the workflow can visualise not only where particles are absorbed or remain as runoff, but also how they move across the terrain before reaching that condition.

These point and path outputs can be connected to Grasshopper's Custom Preview component to display absorbed and runoff movement separately in Rhino. This visualisation helps interpret the behaviour of water in relation to the BGI adaptation areas. It shows where runoff reaches BGI areas, which particles are absorbed, and where remaining runoff continues across the site. This is useful because BGI performance depends not only on storage capacity, but also on whether runoff actually reaches the adaptation area. Figure 43 shows an example of runoff movement-path visualisation generated from the Particle Fate component outputs. The same visualisation can also be generated for absorbed particles.

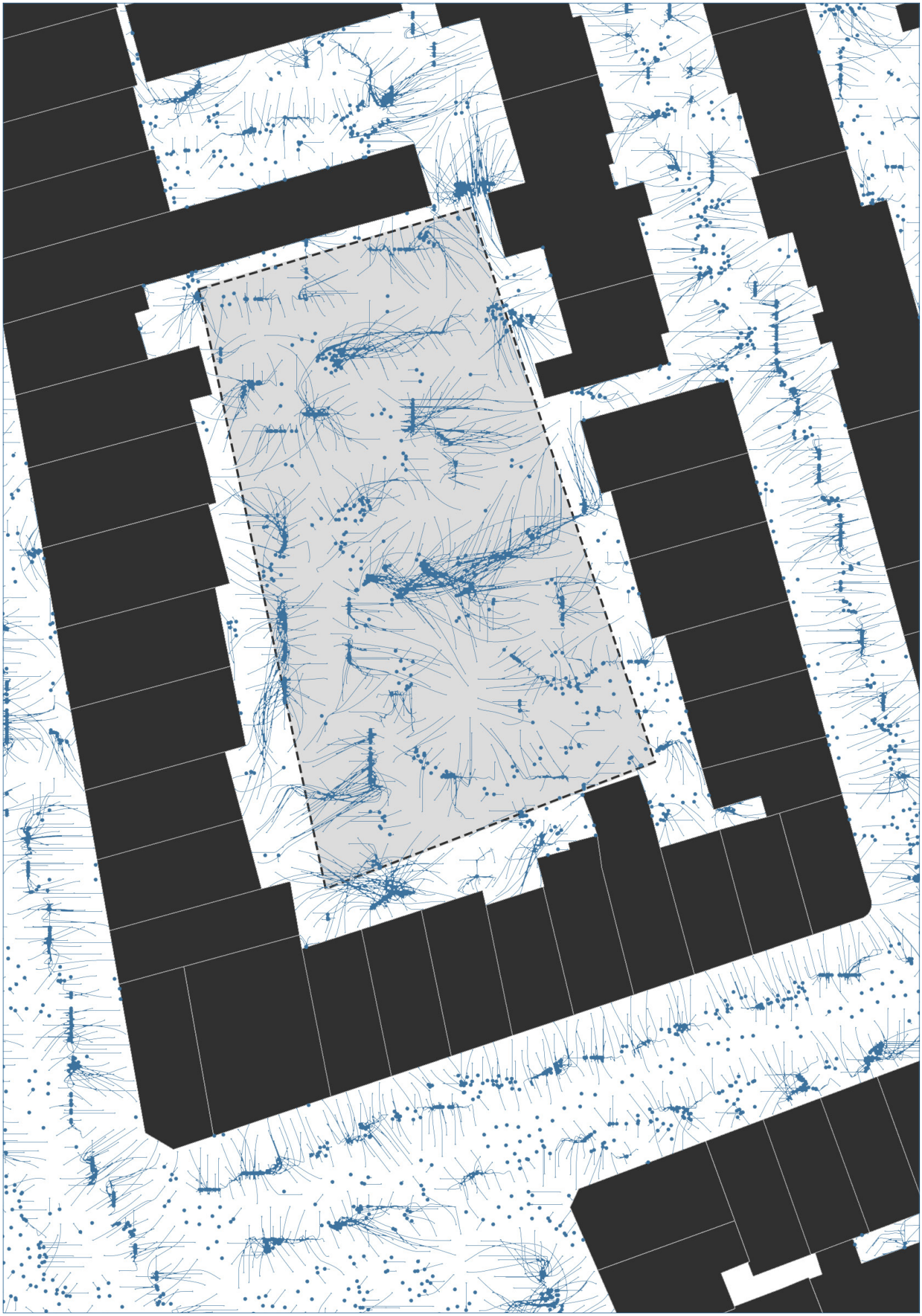

Figure 43. Example of runoff particle movement path visualization

Flood Depth Estimation

Flood Depth Values

To connect building resilience to the simulation, flood depth needs to be retrieved as part of the building depth-damage relationship. This requires translating the runoff particles from the Kangaroo iterations into quantitative flood depth values for the site. To develop this approach, the flood simulation software FloodSim (Hadimlioglu et al., 2020; Hadimlioglu & King, 2019) was reviewed as a reference. FloodSim translates particle simulation results into a grid-based depth map by grouping particles into grid cells and computing a volume-based depth value per cell. This principle is adapted within the Grasshopper environment, where the remaining runoff particles are grouped into a 2D grid and their accumulated volume is converted into estimated flood depth values, as illustrated in this diagram. Each particle represents a sphere of water with volume derived from its radius following Jia et al. (2022).

$$d_c = \frac{N_c \ \frac{4}{3}\pi r_p^3}{A_c}$$

dc = flood depth at cell (m)
Nc = number of particles accumulated in cell
rp = particle radius (m)
Ac = cell area (m²)

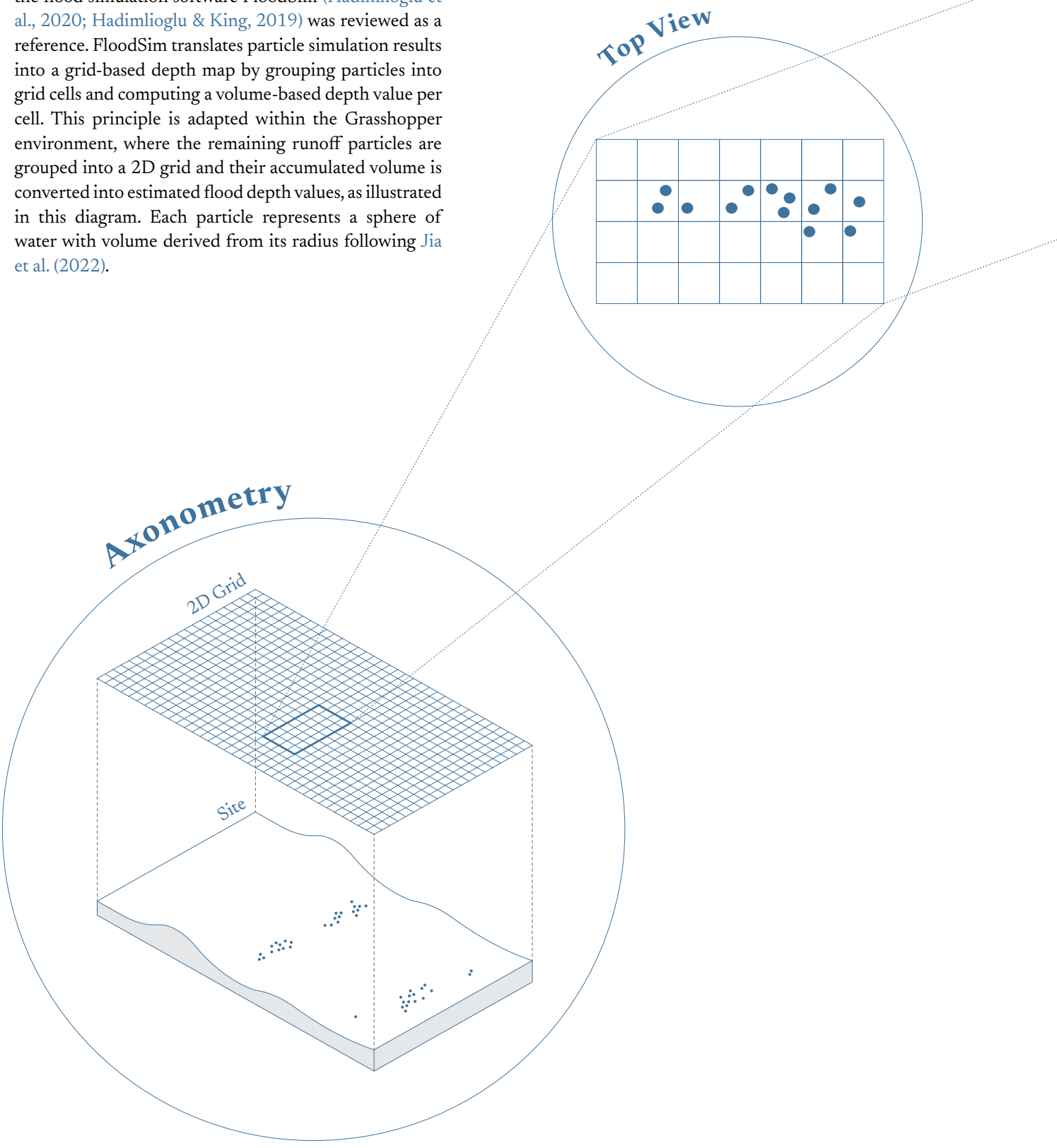

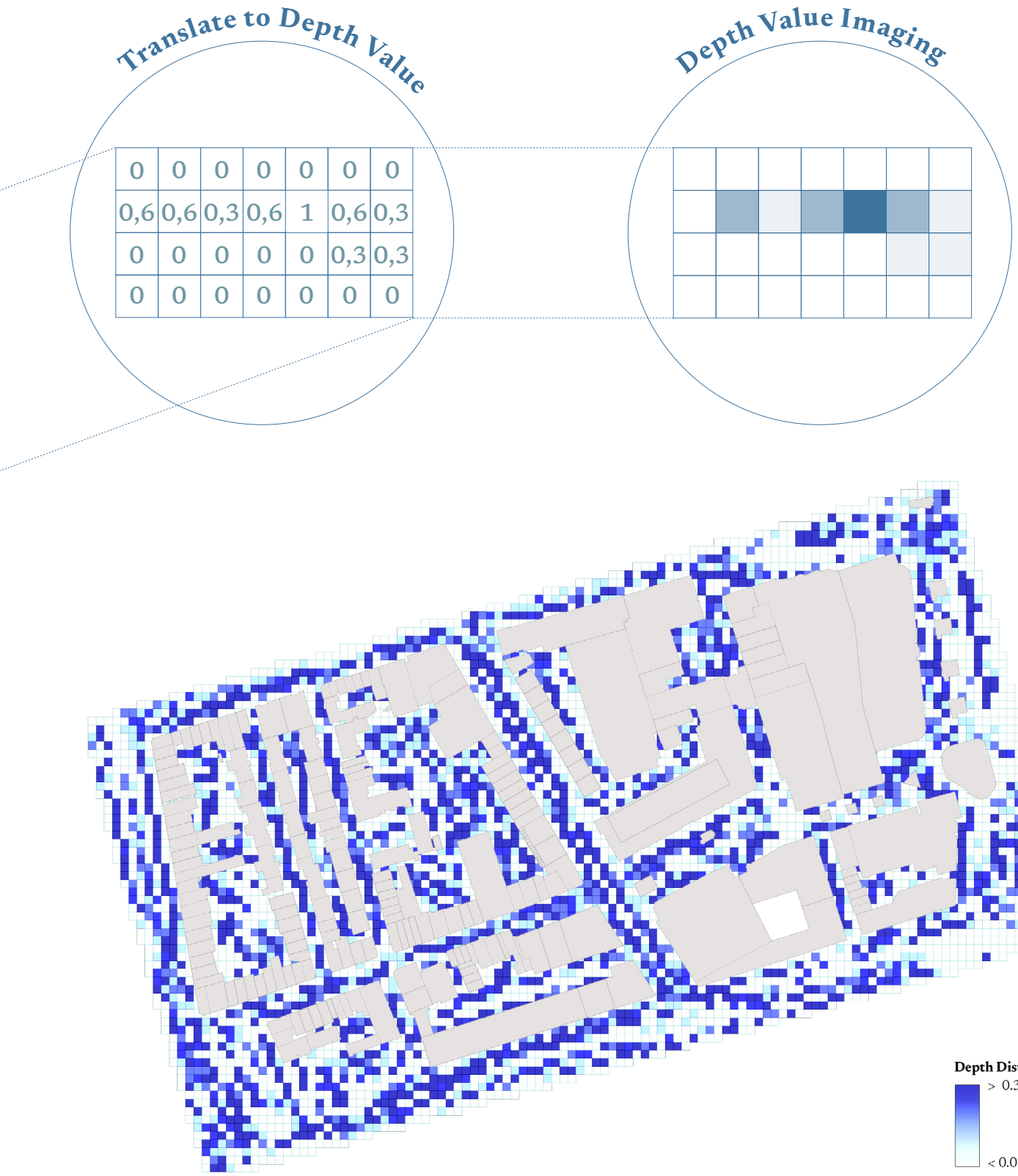

Figure 44. Discrete flood depth value

One consequence of this grid-based representation is that the resulting flood-depth map remains discrete. Each grid cell contains one calculated depth value, meaning that neighbouring cells can have hard boundaries between them even when the actual inundation surface would be more continuous. This can create a stepped or fragmented visual output, as illustrated in the example shown in Figure 44. Therefore, the grid-based depth estimation is complemented with a smoothing step to reduce cell-discretisation artefacts and create a more continuous flood-depth surface before the result is interpreted spatially and used for building-level inundation assessment.

Spatial Smoothing Method

Spatial smoothing is a filtering technique that reduces sharp transitions between neighbouring cells by replacing each cell's value with a weighted function of its surrounding neighbourhood (Gonzalez & Woods, 2018). When applied to the discrete depth grid, this process helps smooth the depth values between neighbouring cells to create a more continuous flood-depth surface. The total water volume across the grid is kept the same, meaning the smoothing only redistributes the depth values rather than adding or removing water. A Gaussian kernel was selected as the smoothing method as it weights neighbouring cells by their distance from the center cell. This means closer neighbours contribute more strongly to the smoothed output than further ones, as illustrated in Figure 45. This is more physically intuitive than a uniform mean filter, where all neighbours are weighted equally regardless of distance. Following Gonzalez & Woods, the smoothed depth value at each cell is computed as a normalised weighted average:

$$d_{smooth}(x,y) = \frac{\sum_{s=-a}^{a}\sum_{t=-b}^{b} e^{-\frac{s^2+t^2}{2\sigma^2}} \cdot d(x+s,y+t)}{\sum_{s=-a}^{a}\sum_{t=-b}^{b} e^{-\frac{s^2+t^2}{2\sigma^2}}}$$

Gaussian Weight
closer neighbours weighted higher

Depth of Neighbouring Cell
at offset (s,t) from center

Sigma
controls smoothing radius

Numerator
weight sum of neighbour depth

Denominator
normalises - preserve volume

s, t = offset distance from center cell in row and column direction

a, b = kernel boundary, defined as kernel radius = 3σ

σ = controls smoothing radius (σ = 1.5 cells = 7.5m)

d(x+s, y+t) = flood depth of neighbouring cell at offset (s,t) from center

dsmooth(x,y) = smoothed flood depth at center cell

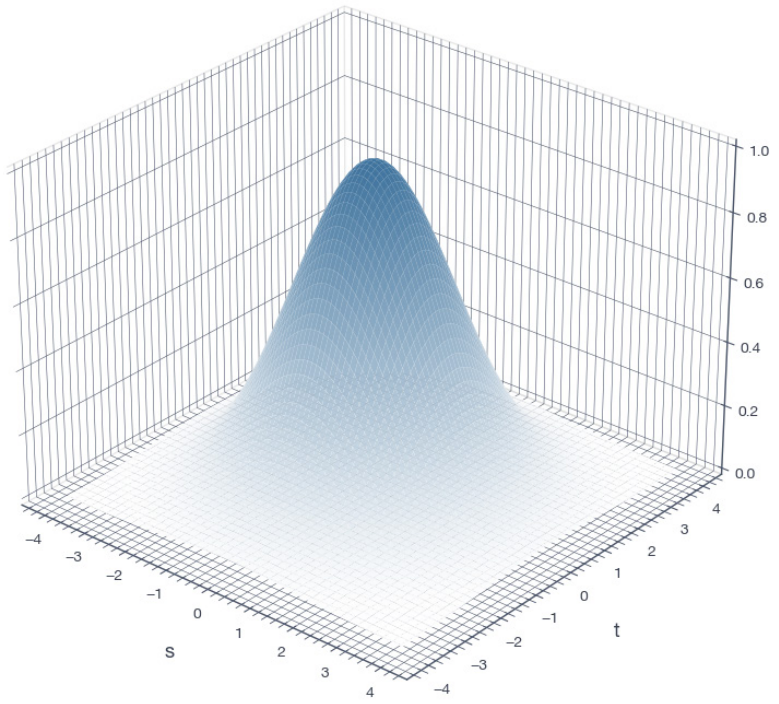

Figure 45. Gaussian kernel shape showing distance-based weighting. The peak represents the center cell receiving weight 1.0, with weights decreasing toward zero at the kernel boundary

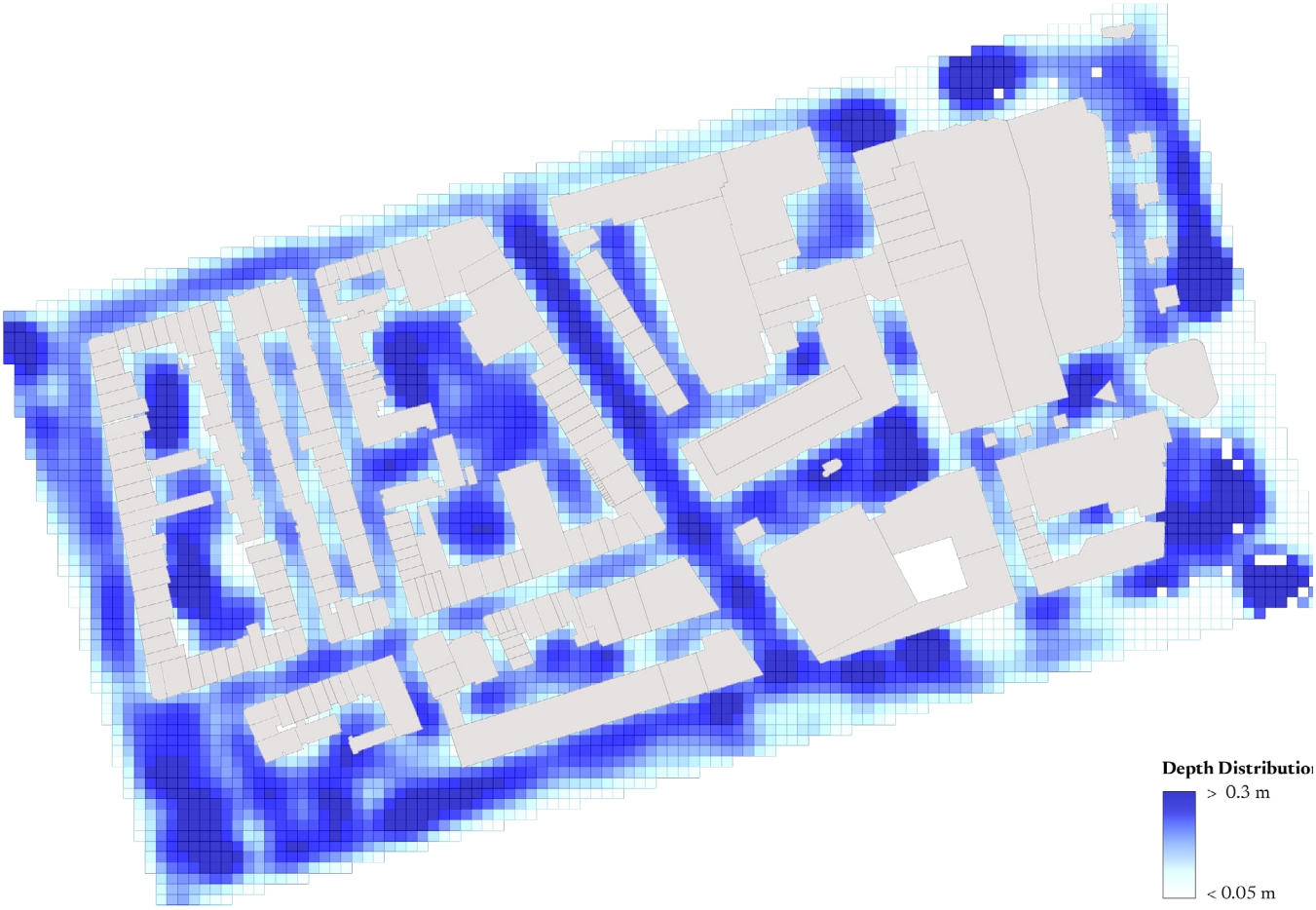

Figure 46. Previous Map Result After Smoothing (Cell Cize 5x5m)

Figure 46 shows the effect of Gaussian smoothing on the grid-based flood-depth values, compared with the previous discrete output. In this workflow, the main spatial distribution of runoff is already determined by the Kangaroo particle simulation, while Gaussian smoothing is applied to the resulting depth grid to reduce its discretised appearance and create a more continuous flood-depth surface.

The resulting Flood-Depth Estimation component is shown in Figure 47.

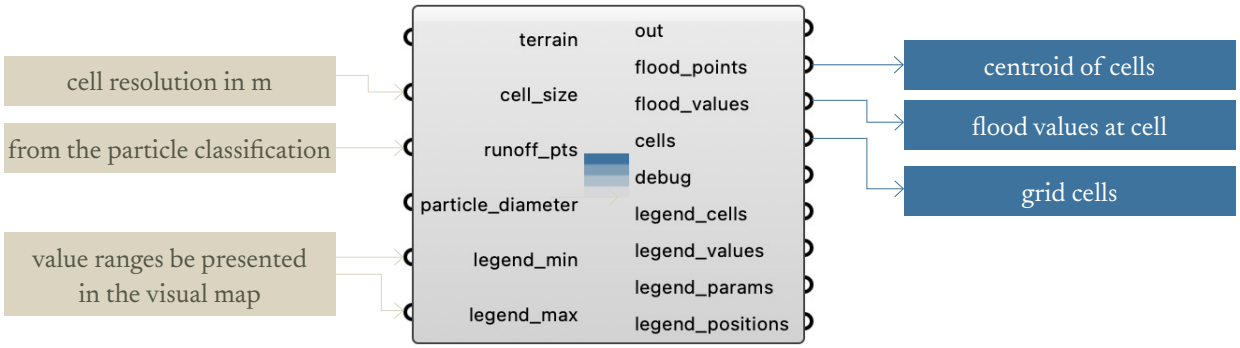

Figure 47. Flood Depth Values estimation

Building Inundation Depth

To connect the flood-depth map with the building-level resilience assessment, the grid-based flood-depth values need to be translated into a representative inundation depth for each building. Building Inundation depth refers to the water depth affecting or surrounding a building under the simulated flood condition. This value is required because the depth–damage relationship defined in Section 2.1 is applied at the building scale, while the flood-depth output is first generated as a spatial grid across the site.

The retrieval logic is adapted from Morschek's Urban Flooding Analysis open course, published on Bauhaus-Universität Weimar's OTP platform, which demonstrates rain-runoff simulation and evaluation in Rhino3D/Grasshopper using Kangaroo (Morschek, 2019). In this workflow, each building footprint is offset to create a surrounding assessment boundary. This boundary defines the area around the building from which nearby flood-depth values are retrieved. The retrieval logic is illustrated in Figure 48.

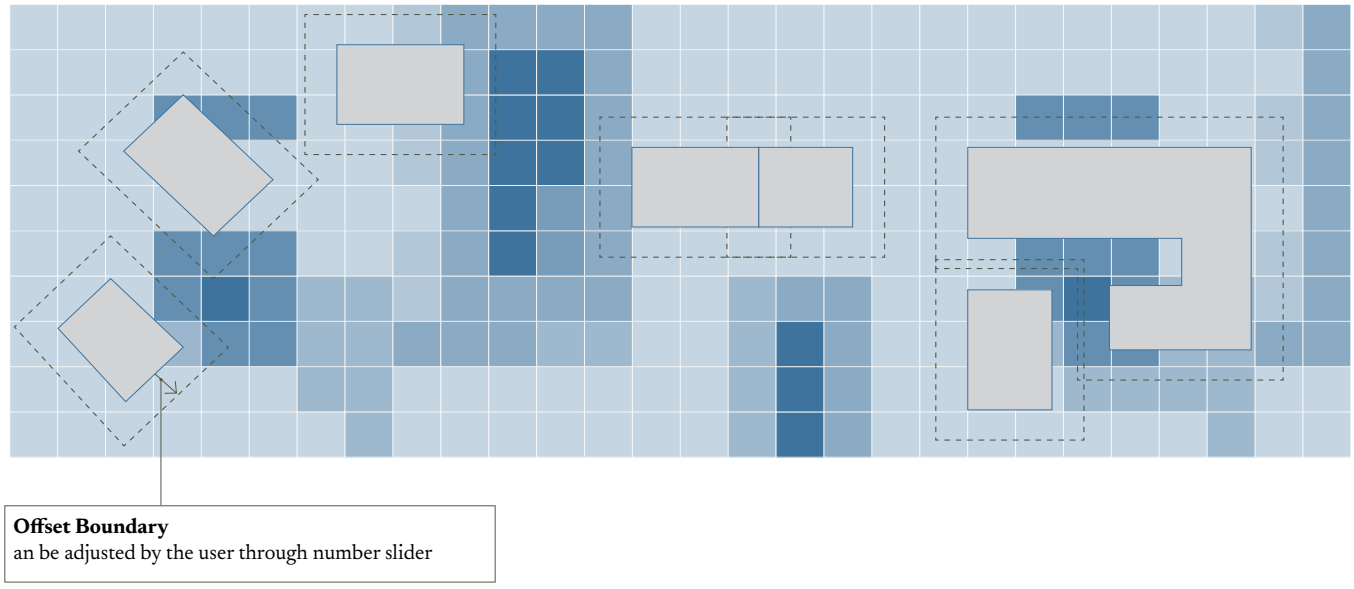

Figure 48. Offset boundary logic for building inundation depth estimation

To implement this process, a custom component is developed to identify the flood-depth grid cell centroids located within the assessment boundary and extract the maximum flood-depth value. The maximum value is used instead of the mean as a conservative representation of building inundation, because it captures the highest potential water depth affecting the building surroundings. This value is then assigned as the representative inundation depth for the building and connected to the depth–damage assessment. The offset distance can be adjusted by the user depending on the site condition and the intended assessment boundary. The component setup is shown in Figure 49.

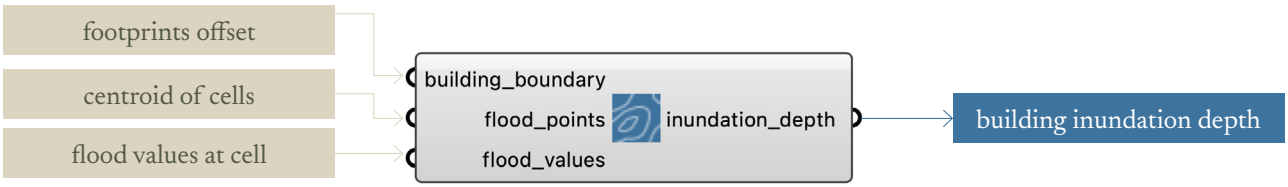

Figure 49. Building Inundation Depth component

Building Resilience Scoring

After the representative inundation depth is retrieved for each building, it is used as the flood-impact input for the building-level resilience assessment. The scoring method follows the resilience definition and depth–damage relationship introduced in Section 2.1. In the workflow, this inundation depth is connected with the required building attribute inputs, such as building class and basement presence, to calculate the building-level resilience score.

The scoring process also relies on external parameter tables stored as Excel files. These include the depth–damage curves, impeding-time values, and restoration-time values defined in the resilience-scoring framework. Storing these parameters externally allows the values to be reviewed, adjusted, or replaced without changing the component structure. This makes the workflow more flexible when testing different damage curves, recovery assumptions, or local parameter values.

The resulting scores are then assigned back to the corresponding building geometries for spatial visualisation and scenario comparison. They can also be exported as CSV files for further post-processing and result communication. Figure 50 shows the full resilience-score component, including the building attribute inputs, inundation-depth input, Excel-based parameter inputs, and generated resilience outputs.

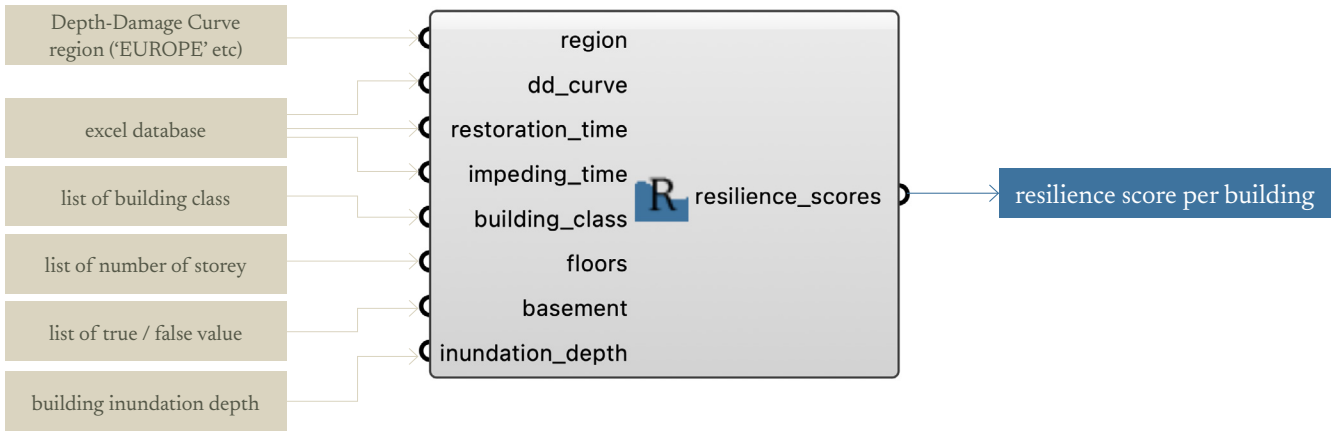

Figure 50. Resilience score component

Indicative BGI Cost Calculation

In addition to hydrological and resilience-related outputs, the workflow also includes an indicative implementation-cost calculation for each BGI adaptation scenario. This cost calculation is not part of the flood-depth or resilience-score computation, but is included as a supporting output for scenario comparison. The cost is calculated by multiplying the area of each BGI adaptation mesh by the assigned implementation cost per square metre for the corresponding BGI type:

$$C_{BGI} = A_{BGI} \times C_{m2}$$

where C_{BGI} is the estimated implementation cost, A_{BGI} is the area of the BGI mesh, and c_{m2} is the cost per square metre assigned to the selected BGI type. The unit cost values are based on the BGI cost parameters introduced in the previous sub chapter. The resulting cost values can then be aggregated by BGI type or by scenario, allowing adaptation scenarios to be compared not only by absorbed volume, flood-depth reduction, and resilience improvement, but also by indicative implementation cost.

03
Case Study

Site Context

Case Study Setup

Rainwater Simulation

Existing Condition

Adapted Design Scenario

3.1 | Site Context

The workflow is tested through a case study in the Lijnbaan area in Rotterdam, the Netherlands. This location was selected because it provides a dense urban context for testing the proposed flood-simulation and building-resilience assessment workflow. The selection is also supported by the Climate Impact Atlas, which indicates that South Holland is expected to experience relatively high extreme hourly precipitation compared with several other Dutch regions. As shown in Figure 51, the projected 1-in-100-year hourly precipitation in South Holland reaches approximately 70–80 mm/hour by 2100 under the highest climate scenario

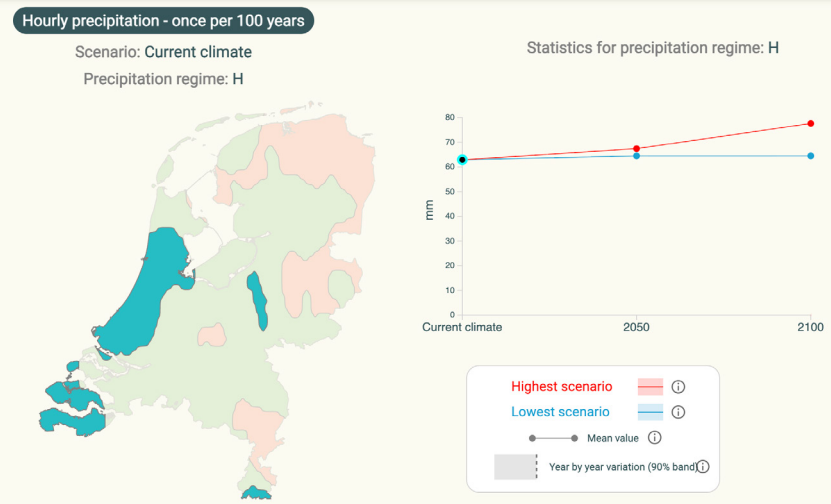

Figure 51. Hourly percipitation statisctics for South Holand (www.klimaeffectatlas.com)

The Lijnbaan area is also suitable because it contains a dense urban fabric with a mix of building functions, including residential, commercial, and other urban uses. As shown in Figure 53, the area is highly built-up, with limited open space between buildings. Although vegetation is present, it is mostly found in small-scale elements such as street trees and planters rather than larger continuous green land-use areas. This makes the site relevant for exploring the potential role of BGI adaptation in dense inner-city environments, where space for large-scale green infrastructure is constrained.

The functional diversity of the area also allows the workflow to test how different building classes respond to the same simulated flood condition. In addition, the Netherlands provides a strong data context for this research. Detailed spatial datasets, such as 3DBAG, terrain data, and building-related information, are relatively accessible and can be combined with existing Dutch and international flood-damage assessment methods. Established depth–damage relationships and flood-damage assessment approaches are also available for the Dutch context, making the case study suitable for testing the workflow in a data-supported urban environment.

> “Rotterdam is built in low-lying polders, which act like a bathtub. Precipitation must be pumped out or, preferably, retained locally through infiltration and water storage.”
>
> –Rotterdam Weatherwise (2023)

Figure 52. Rotterdam City Map

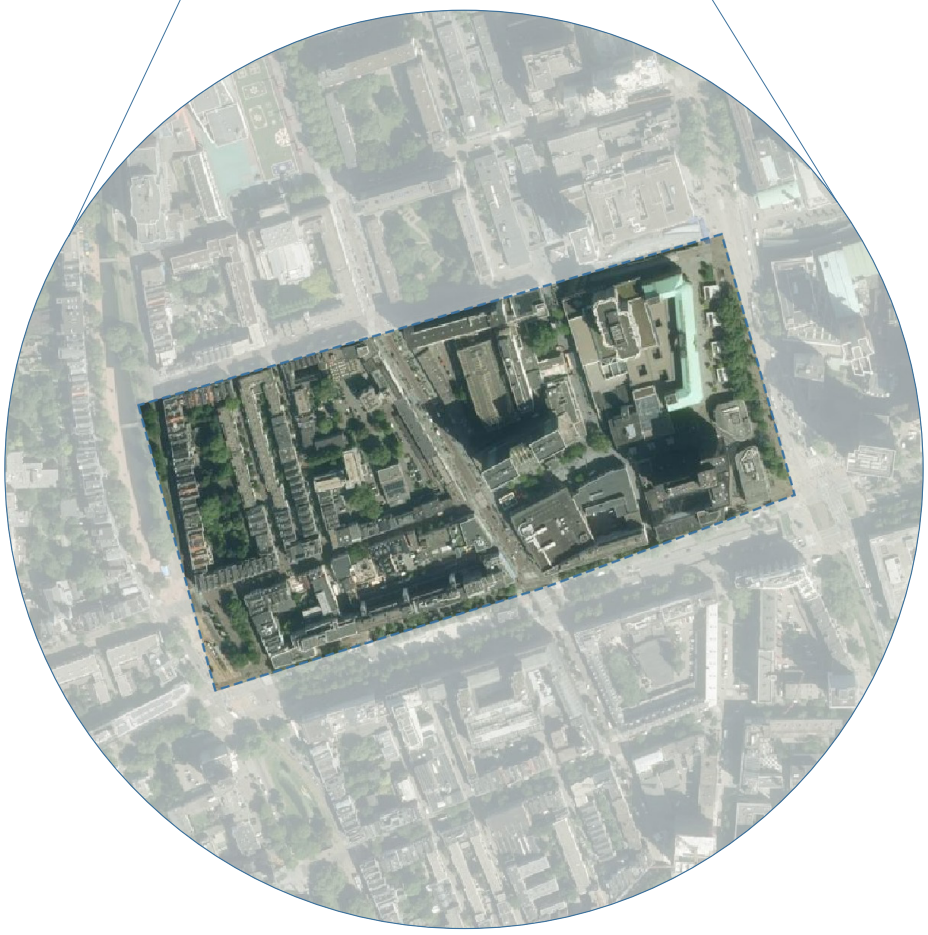

Figure 53. Lijnbaan Aerial Map (Google Earth, 2026)

3.2 | Case Study Setup

Data Input Overview

The general computational workflow has been introduced in Chapter 2. This section revisits the workflow from the perspective of the Lijnbaan case study by showing how it is populated with site-specific input data. Figure 54 provides an overview of these case-specific inputs, including terrain data, building geometry and attributes, and rainfall-simulation input.

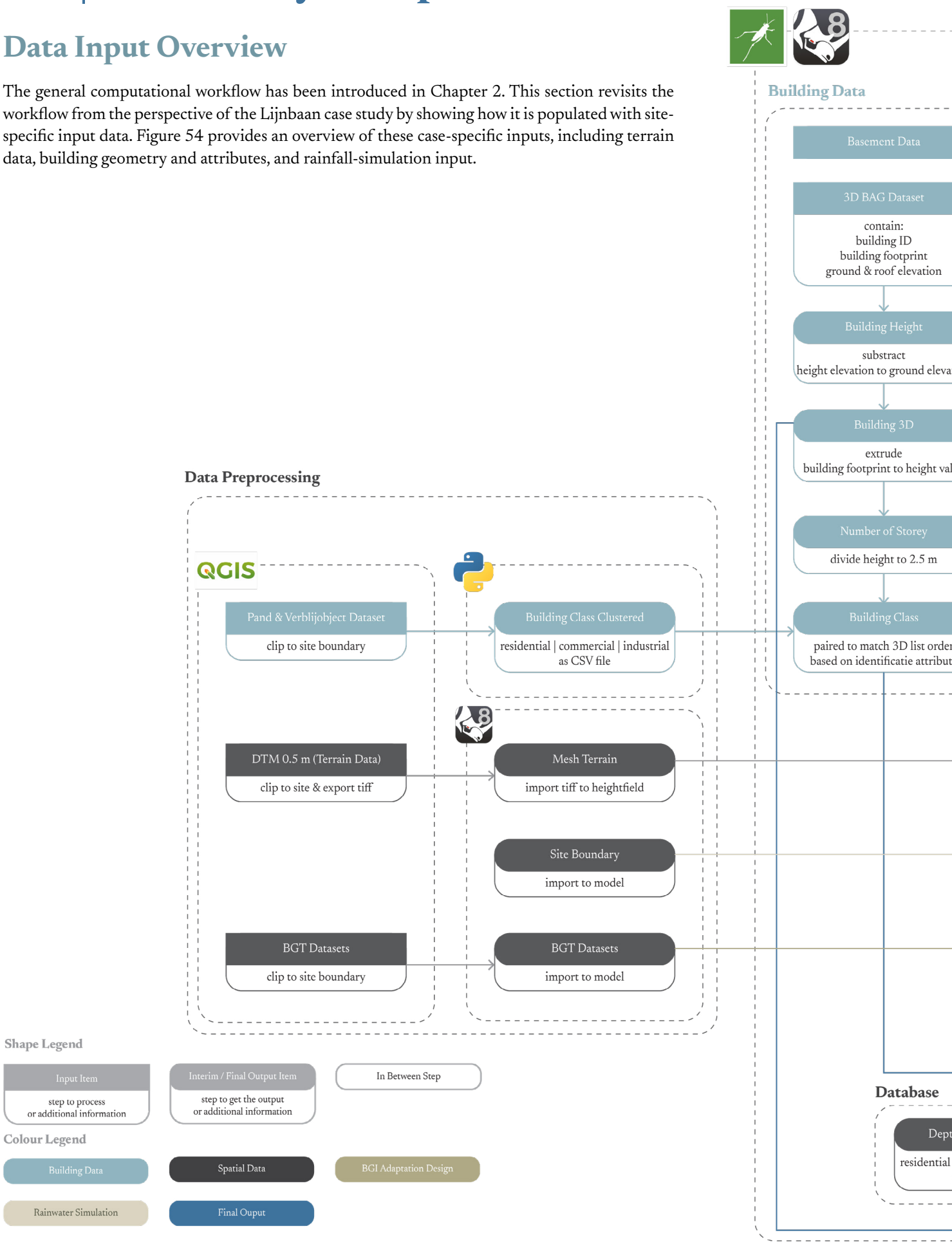

Figure 54. Computational workflow with site Lijnbaan data input

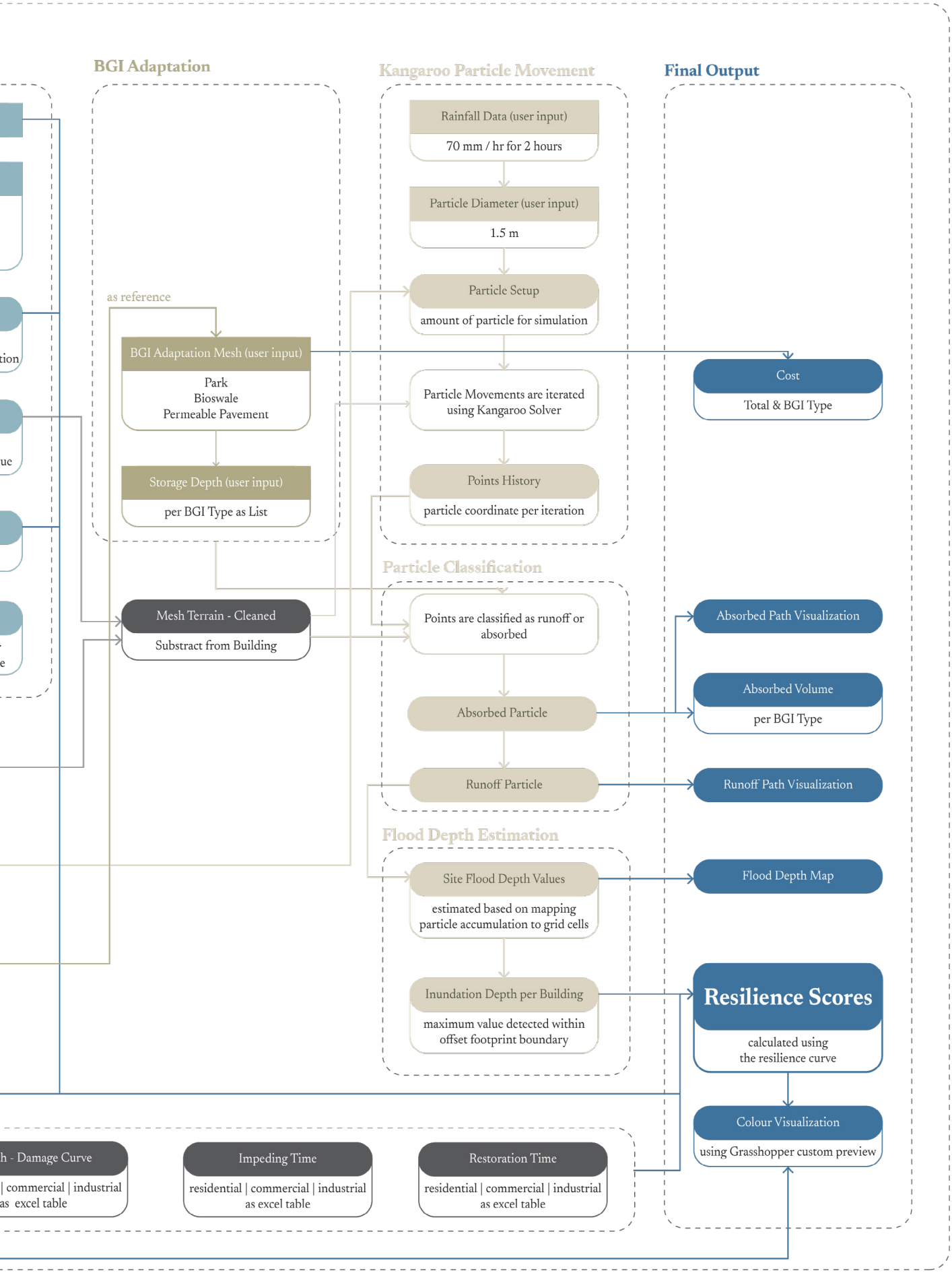
BGI Adaptation
Kangaroo Particle Movement
Final Output
Rainfall Data (user input)
70 mm / hr for 2 hours
Particle Diameter (user input)
1.5 m
Particle Setup
amount of particle for simulation
as reference
BGI Adaptation Mesh (user input)
Park
Bioswale
Permeable Pavement
Particle Movements are iterated using Kangaroo Solver
Cost
Total & BGI Type
Storage Depth (user input)
per BGI Type as List
Points History
particle coordinate per iteration
Particle Classification
Mesh Terrain - Cleaned
Substract from Building
Points are classified as runoff or absorbed
Absorbed Path Visualization
Absorbed Volume
per BGI Type
Absorbed Particle
Runoff Particle
Runoff Path Visualization
Flood Depth Estimation
Site Flood Depth Values
estimated based on mapping particle accumulation to grid cells
Flood Depth Map
Inundation Depth per Building
maximum value detected within offset footprint boundary
Resilience Scores
calculated using the resilience curve
Colour Visualization
using Grasshopper custom preview
Impeding Time
residential | commercial | industrial
as excel table
Restoration Time
residential | commercial | industrial
as excel table

Building Data

Figure 56 provides an overview of the building-related datasets used in the workflow and how they are connected. The main building geometry is obtained from 3DBAG, while additional building class information is derived from the *Verblijfsobject* and PAND datasets accessed through PDOK in QGIS. These datasets are combined to create the building class dataset used later in the workflow.

From 3DBAG, the main attributes used are the building identification attribute (*identificatie*), the LOD 0.0 building footprint, the ground elevation (*h_maaiveld*), and the representative roof elevation (*h_dak_70p*). The identificatie attribute is used to match the 3DBAG geometry with the building class dataset. The LOD 0.0 geometry provides the building footprint, while the height-related attributes are used to generate simplified 3D building geometry. The building height is calculated by subtracting *h_maaiveld* from *h_dak_70p*, and this height is later used to estimate the number of storeys.

The *Verblijfsobject* dataset provides the building class (function) and building-related identification, while the PAND dataset is used as a geometric reference to double-check the building ID and footprint. These attributes are merged using the building ID as the linking key. Since one building can contain multiple records in the source dataset, each building ID is assigned a single building class before being matched with the 3DBAG geometry.

After the building attributes are prepared, they are structured in Grasshopper as parallel lists, as shown in Figure 55. Each list stores one type of information, such as geometry, building ID, roof elevation, ground elevation, basement presence, and building class. The index position links the attributes together, meaning that all values at the same index refer to the same building. This structure allows the workflow to retrieve and calculate building-specific information during the resilience assessment.

The available datasets do not contain building-specific information on basement presence. Therefore, basement presence is treated as a scenario-based assumption rather than a verified attribute. Commercial and industrial buildings are assigned True, assuming the possible presence of basement or below-grade storage and service spaces, while residential buildings are assigned based on a simplified floor-area threshold. Dwellings above 75 m² are assigned True, while smaller dwellings are assigned False.

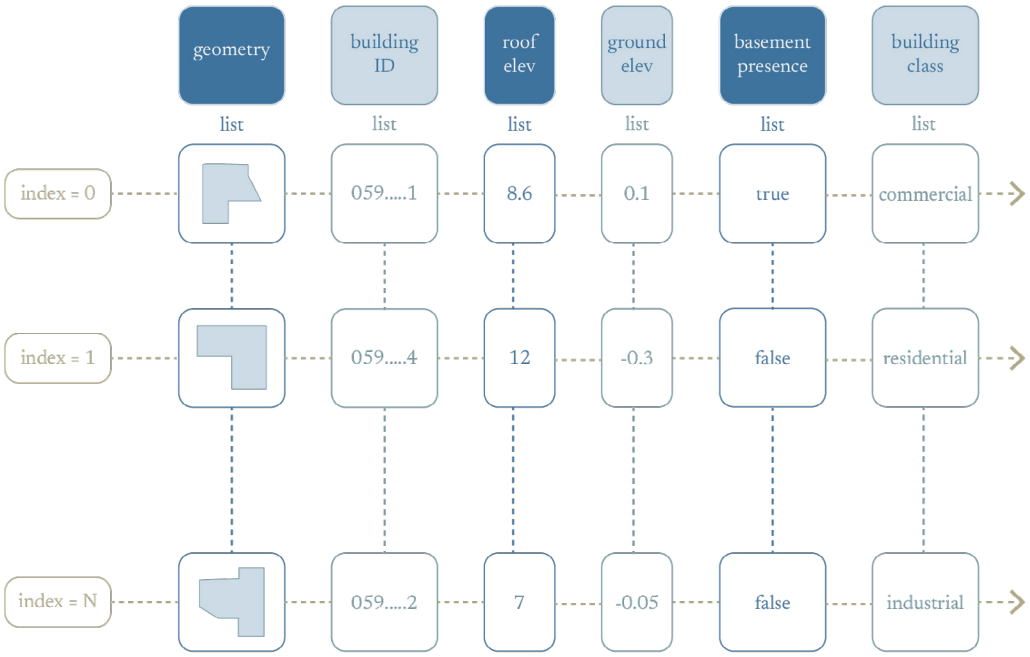

Figure 55. Parallel-list structure of building data in Grasshopper

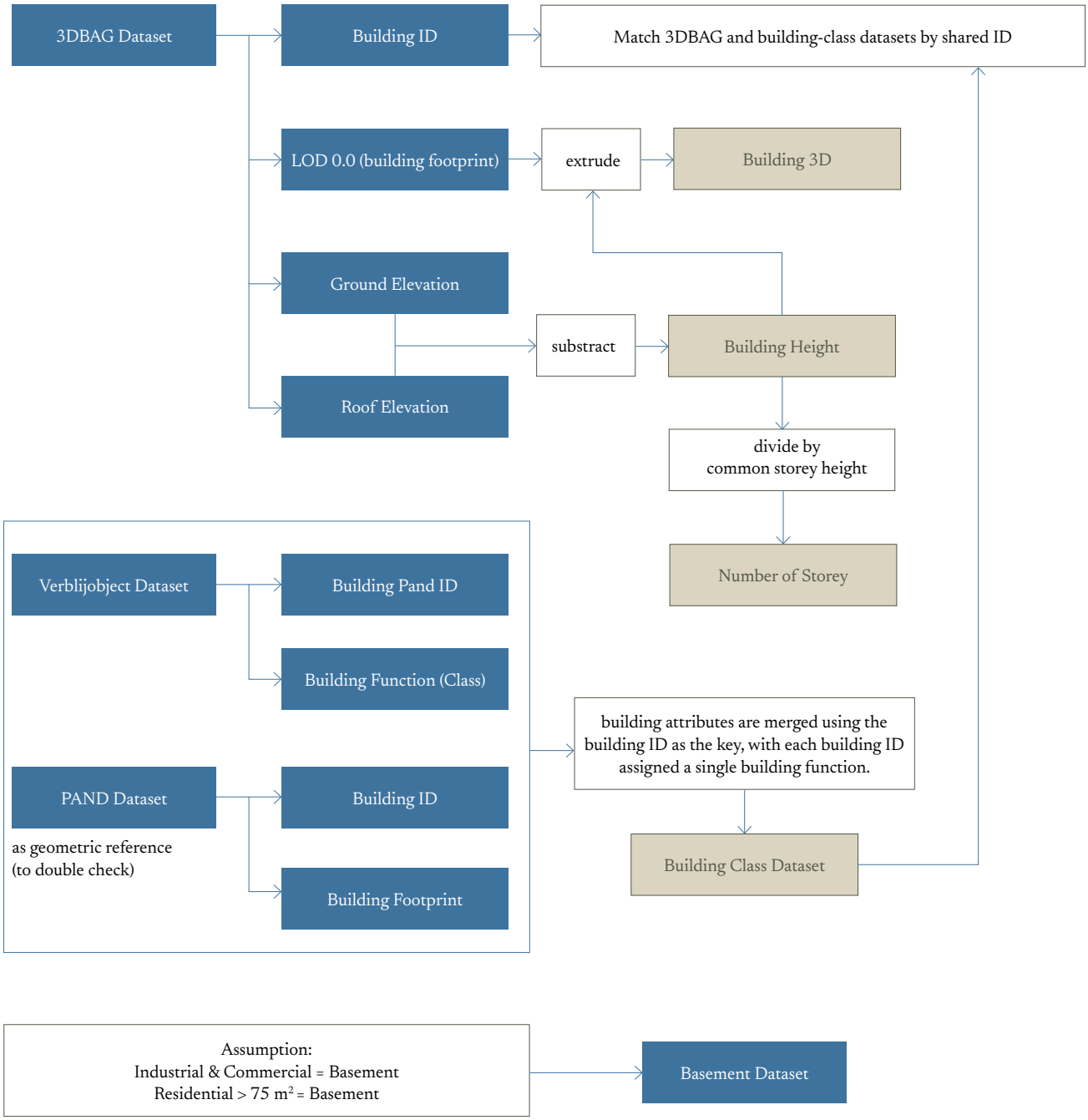

Figure 56. Building data sources and attribute-matching process used in the workflow.

3D BAG Dataset

3DBAG is selected as the primary building-geometry dataset. It is an open and regularly updated dataset containing detailed 3D building models of the Netherlands, generated by combining building information from the BAG with height data from the AHN. The dataset provides building models at multiple levels of detail and is available in several formats, including CityJSON, GeoPackage, OBJ, WMS, and WFS.

For this research, 3DBAG is suitable because it can be imported into Grasshopper as polygonal building geometry while retaining associated building attributes. This is enabled through the CityJSON plugin, which allows both geometry and attribute data to be accessed within the Grasshopper environment. Relevant attributes include the building identification number, ground elevation, building height, and other geometry-related information.

Level of Detal (LOD)

3DBAG provides multiple Levels of Detail (LOD), allowing flexibility depending on the required level of analysis. LOD 0.0 represents building footprints, LOD 1.2 and 1.3 provide extruded geometries with varying degrees of detail, and LOD 2.2 includes more complex representations incorporating roof structures. The data can be The visualization of each LOD can be seen in Figure 57 until 59.

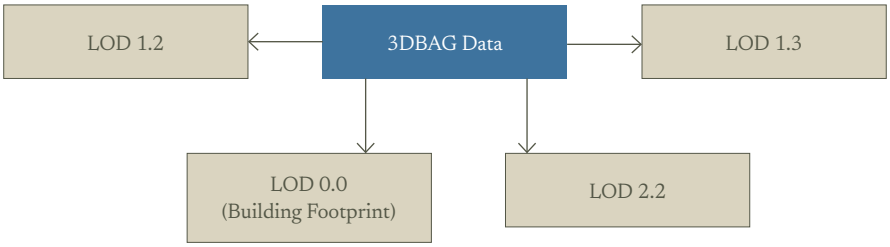

Figure 57. LOD 1.2 Data (www.3dbag.nl)

Figure 58. LOD 1.3 Data (www.3dbag.nl)

Figure 59. LOD 2.2 Data (www.3dbag.nl)

A limitation of using higher Levels of Detail (LOD 1.2–2.2) is that each building may be represented by multiple geometries treated as separate entities. This increases data complexity and reduces efficiency for simulation and colour visualisation, where a single geometry per building is preferred. Therefore, this workflow uses LOD 0.0 footprints and generates 3D geometry through extrusion, with the Z-axis height derived from the native height attributes in the 3DBAG dataset.

LOD 0.0 is selected because it provides simplified building footprints that are lighter to process in Grasshopper. This is suitable for the simulation workflow, where each building needs to be treated as a single object with consistent attributes. However, because LOD 0.0 is a simplified representation, some building geometries may be missing or less detailed. Resolving these missing geometries is outside the scope of this research, so the workflow continues using the available LOD 0.0 data.

When importing 3DBAG data into Grasshopper, the geometry can either be imported in its georeferenced position or moved directly to a local origin. In this workflow, the 3DBAG geometry is first kept in its georeferenced position to maintain spatial alignment with the terrain data prepared in QGIS. This alignment step is important because the terrain and building datasets are prepared separately but need to correspond spatially in the Grasshopper model.

After the building geometry and terrain mesh are aligned, both datasets are moved together to the local origin point (0,0,0) in Grasshopper. This preserves their relative position while making the model easier to view, manage, and process within the Grasshopper environment. Figure 60 illustrates how the 3DBAG data is imported through the CityJSON plugin using the georeferenced import option.

Georeference Option
Set to True to import the 3DBAG geometry in its original georeferenced position. Set to False to import the geometry near the local origin point (0,0,0).

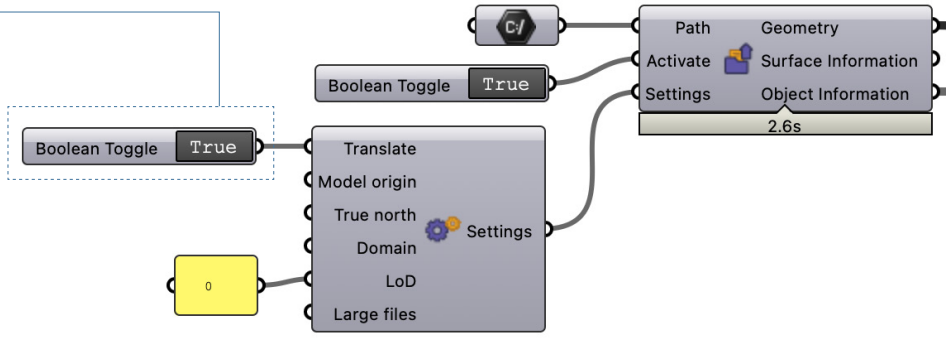

Figure 60. Importing 3DBAG Data using CityJSON

Building Class

Building Class data is obtained from the PAND and Verblijfsobject datasets provided by the PDOK database of the Netherlands. The PAND dataset contains 2D building geometries, comparable to LOD 0.0 in 3DBAG, while Verblijfsobject provides building class information. Both datasets share the identificatie attribute as a common key. Figure 62 illustrates this relationship, where PAND is represented by blue geometries and Verblijfsobject by grey points.

All preprocessing is carried out in Python. The workflow begins by merging PAND and Verblijfsobject, using PAND as the geometric reference to ensure alignment with building footprints. Each PAND identificatie is then assigned a single class. Since one identificatie in Verblijfsobject may correspond to multiple classes, a priority hierarchy is established to select only one typology per building. After this consolidation, the resulting typologies are further classified into one of the categories used in the depth-damage curve. Although filtering could theoretically be performed directly using the identificatie attribute, data mismatches were encountered. Therefore, using PAND as the reference dataset improves geometric consistency with 3DBAG and minimizes synchronization errors.

common key

bag_pnd
599100000689828
599100000670930
599100000671529

PAND Attribute Table

pandidentificatie	gebruiksdoel
599100000689828	woonfunctie
599100000689828	woonfunctie
599100000689828	woonfunctie
599100000670930	kantoorfunctioe
599100000670930	woonfunctie
599100000670930	bijeenkomstfunctie
599100000671529	woonfunctie
599100000671529	industriefunctie

Verblijobjects Attribute Table

each BAG_PND identificatie is assigned a single typology from the gebruiksdoel column based on a predefined typology hierarchy

Merged Attribute

clustering of building classes into residential, industrial, and commercial classes

identificatie	gebruiksdoel
599100000689828	residential
599100000670930	commercial
599100000671529	industrial

CSV Class List

Figure 61. Building class data preprocessing

Building Class Matchmaking

As discussed in Chapter 2, the workflow uses a parallel-list data structure to manage geometry and attributes in Grasshopper. In this case study, this structure is implemented by keeping the geometry and attribute lists in the same order throughout the workflow, so that each list index refers to the same building. This guarantees that building geometry remains correctly linked to its corresponding ID, height, basement assumption, and later flood, damage, and resilience values.

The main exception occurs during the building class assignment process, because the building class data is imported separately as a CSV file. In this file, the data is structured as a lookup table, where each building identification number (identificatie) is linked to a corresponding building class. A custom Grasshopper component is therefore developed using Python 3 to perform a lookup for each identificatie in the 3DBAG attribute list and retrieve the matching building class from the CSV file.

After the lookup process, the output building class list is arranged according to the original order of the 3DBAG dataset. This is important because the geometry and attributes in the main workflow are still managed as parallel lists. Preserving the original 3DBAG order ensures that each building geometry remains aligned with the correct building class and can be used consistently in the following steps, including extrusion, flood-depth assignment, damage calculation, and resilience scoring.

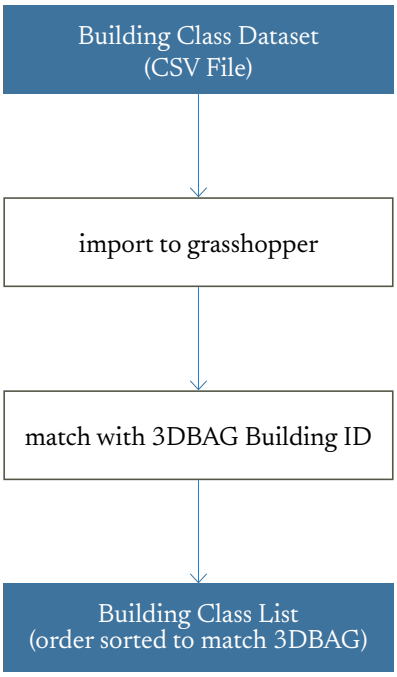

Figure 62. Building class matchmaking in Grasshopper

Building Class Patching

During the building class matching process, 144 out of 239 buildings were initially unidentified because they could not be matched with a corresponding record in the Verblijfsobject dataset. Before patching, the directly matched dataset consisted of 58 residential buildings, 34 commercial buildings, and 3 industrial buildings. To reduce missing values in the resilience assessment, a data-patching step was applied to the unidentified buildings using a proximity-based approach. In this step, each unidentified building is assigned a building class based on the closest nearby building with an identified class.

Figure 63 shows the building classes before patching, while Figure 64 shows the result after patching. After this step, the dataset consists of 142 residential buildings, 87 commercial buildings, and 10 industrial buildings.

This approach allows the simulation to include buildings that would otherwise be excluded from the damage and resilience calculation. Proximity-based patching is used because nearby buildings often share similar planning context or dominant area function, especially in dense urban blocks where related uses tend to be clustered. However, since the classification is inferred from surrounding buildings, there is still a possibility of mismatch with the actual building use. This is especially relevant in dense urban areas, where neighbouring buildings may have different functions despite being spatially close.

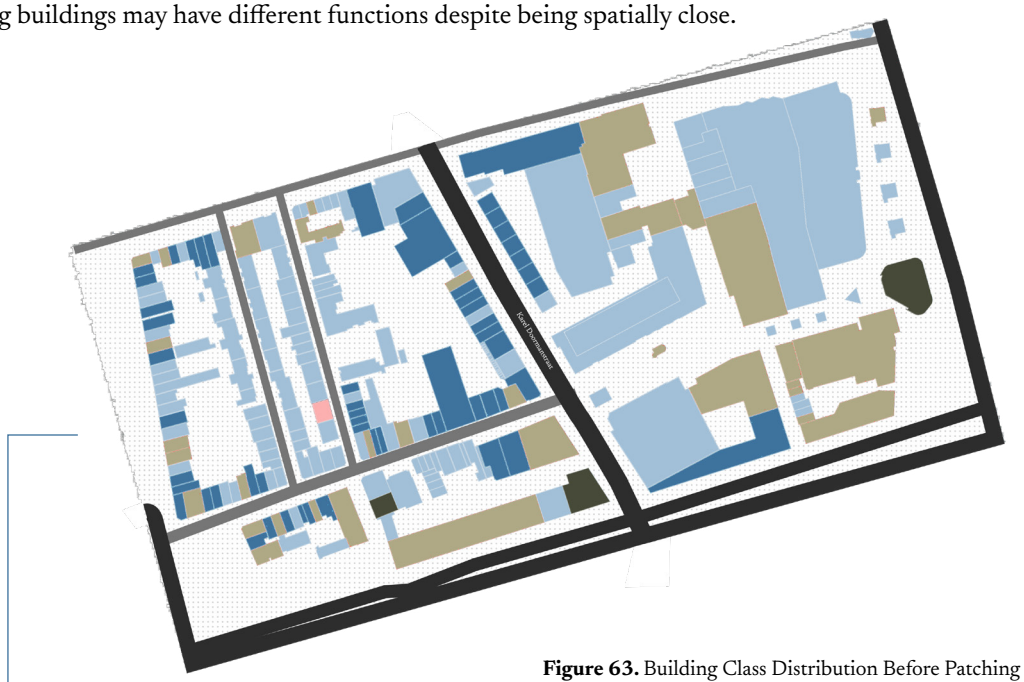

Figure 63. Building Class Distribution Before Patching

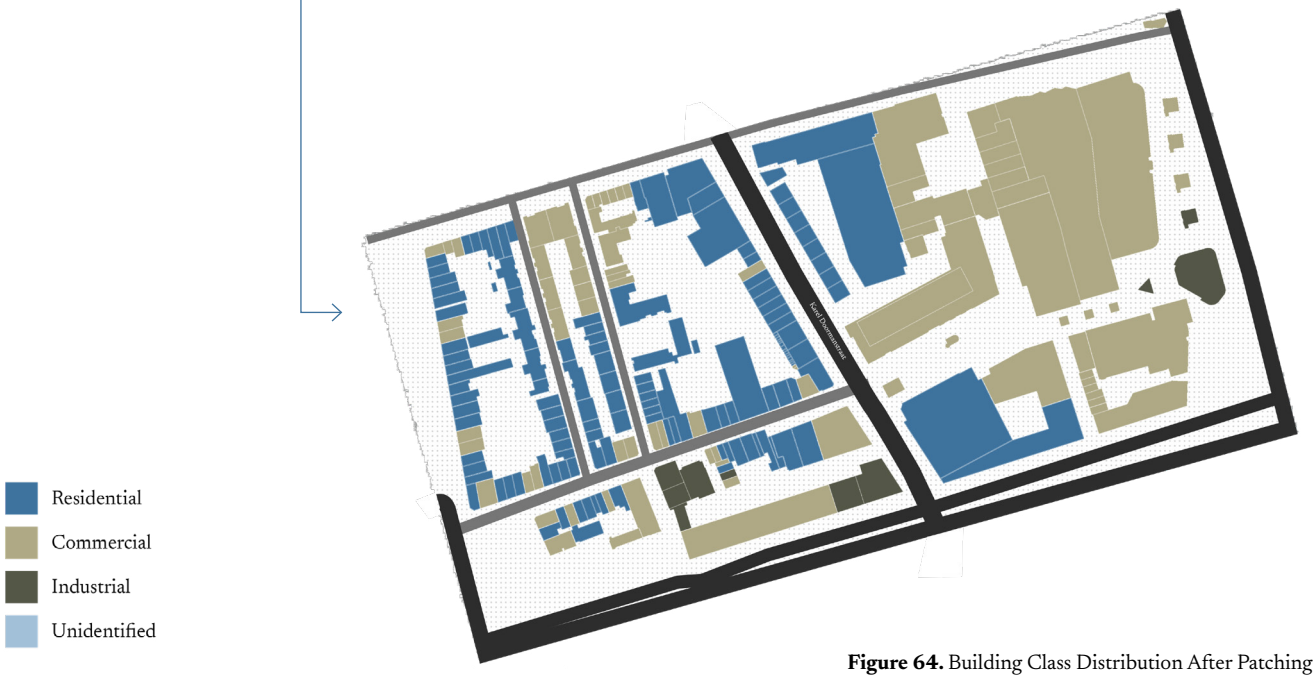

Figure 64. Building Class Distribution After Patching

Basement Data Assumption

Because comparable building-specific basement data could not be obtained, basement presence is treated as an assumed parameter in the workflow. Each building is assigned a Boolean value, where TRUE indicates assumed basement presence and FALSE indicates no assumed basement presence. The figure below visualises this assumption, with buildings shown in blue representing those assigned with basement presence (TRUE).

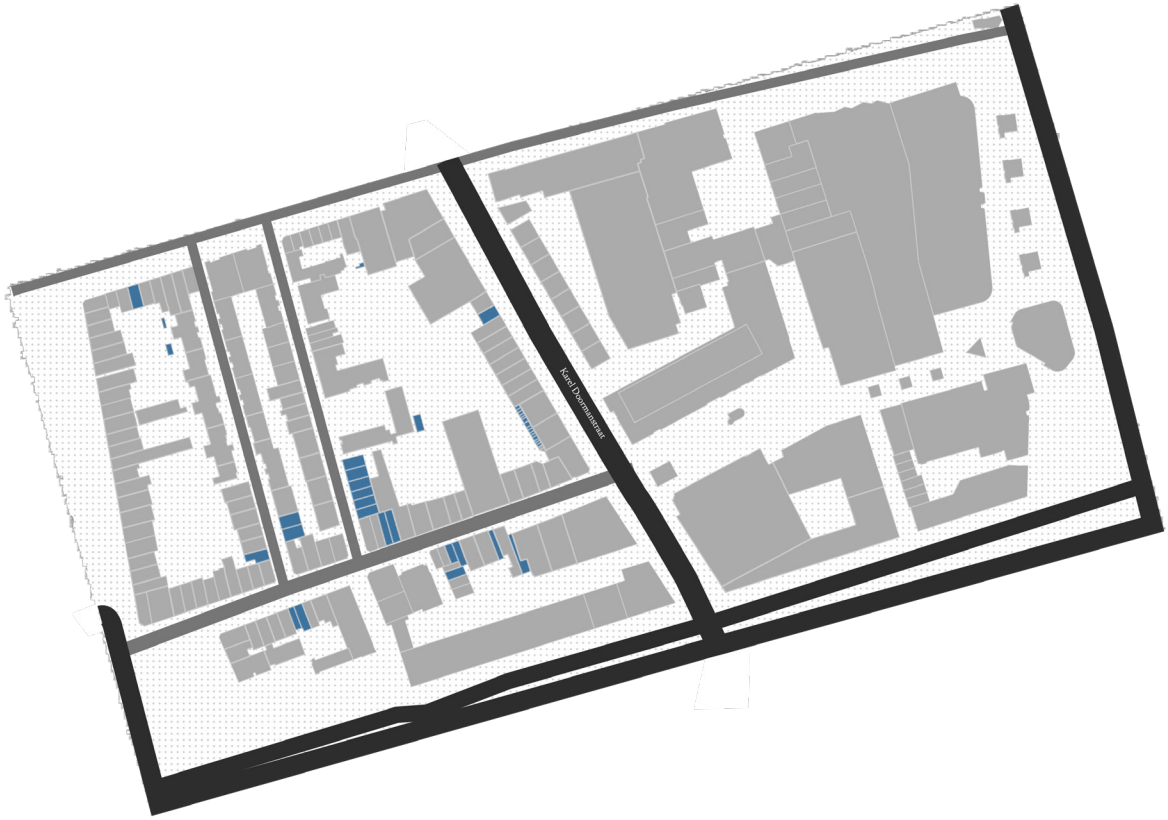

Figure 65. Map of assumed basement presence in the building dataset. Blue indicates buildings assigned with basement presence

Terrain Data

The terrain model is obtained from the DTM 0.5 m dataset accessed through PDOK. This dataset provides the ground elevation information used as the base surface for the rainwater simulation. Before being used in Grasshopper, the terrain data is processed through QGIS and Rhino. The figure on the right illustrates the terrain preparation workflow, from raster preprocessing in QGIS to mesh generation and alignment in Grasshopper.

The terrain preparation process consists of the following steps:

1 **Clip the DTM raster to the case study boundary**
The DTM raster is clipped in QGIS to reduce the terrain data to the selected study area.

2 **Fill NoData cells**
Missing raster cells are filled using the Fill NoData tool to create a continuous terrain surface.

3 **Export the processed terrain as TIFF**
The clipped and filled raster is exported as a TIFF file for import into Rhino.

4 **Export the site boundary as DXF**
The case study boundary is also exported as a DXF file. Since the DXF retains its georeferenced position, it is used as a spatial reference during the Rhino import process.

5 **Import the TIFF as a heightfield in Rhino**
The TIFF file is imported into Rhino as a heightfield and converted into a terrain mesh. The DXF boundary is used to check that the terrain remains aligned with the case study area.

6 **Detect the terrain mesh in Grasshopper**
The generated terrain mesh is referenced into Grasshopper for further processing.

7 **Align terrain and building geometry**
The terrain mesh is aligned with the georeferenced 3DBAG building geometry. After alignment, both datasets are moved together to the local origin point (0,0,0) to improve model readability and computational handling.

8 **Cut the terrain mesh using building geometry**
The terrain mesh is cut using the building footprints so that the remaining mesh represents the open terrain surface used for the rainwater simulation.

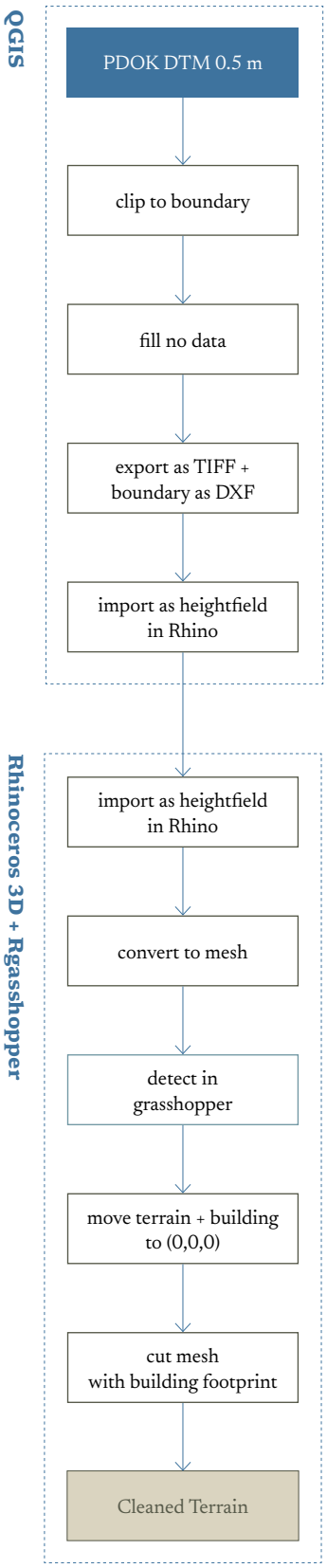

Figure 66. Terrain preprocessing steps

Supporting Spatial Data

BGT data is used to provide additional spatial reference for the case study, including existing vegetation, road surfaces, and other public-space elements. The data is retrieved from the Dutch national geospatial data portal and processed in QGIS. Since BGT contains historical registration information, objects with an end registration date are removed during preprocessing to avoid including outdated elements. The cleaned layers are clipped to the case study boundary and exported as DXF files. These DXF layers retain their georeferenced position, allowing them to align with the terrain and 3DBAG building geometry before all datasets are moved together to (0,0,0) in Grasshopper. The BGT layers are used mainly as top-view reference layers and are not draped onto the terrain mesh. Figure 65 shows the combined view of terrain, buildings, streets, and existing vegetation used as spatial reference for the workflow.

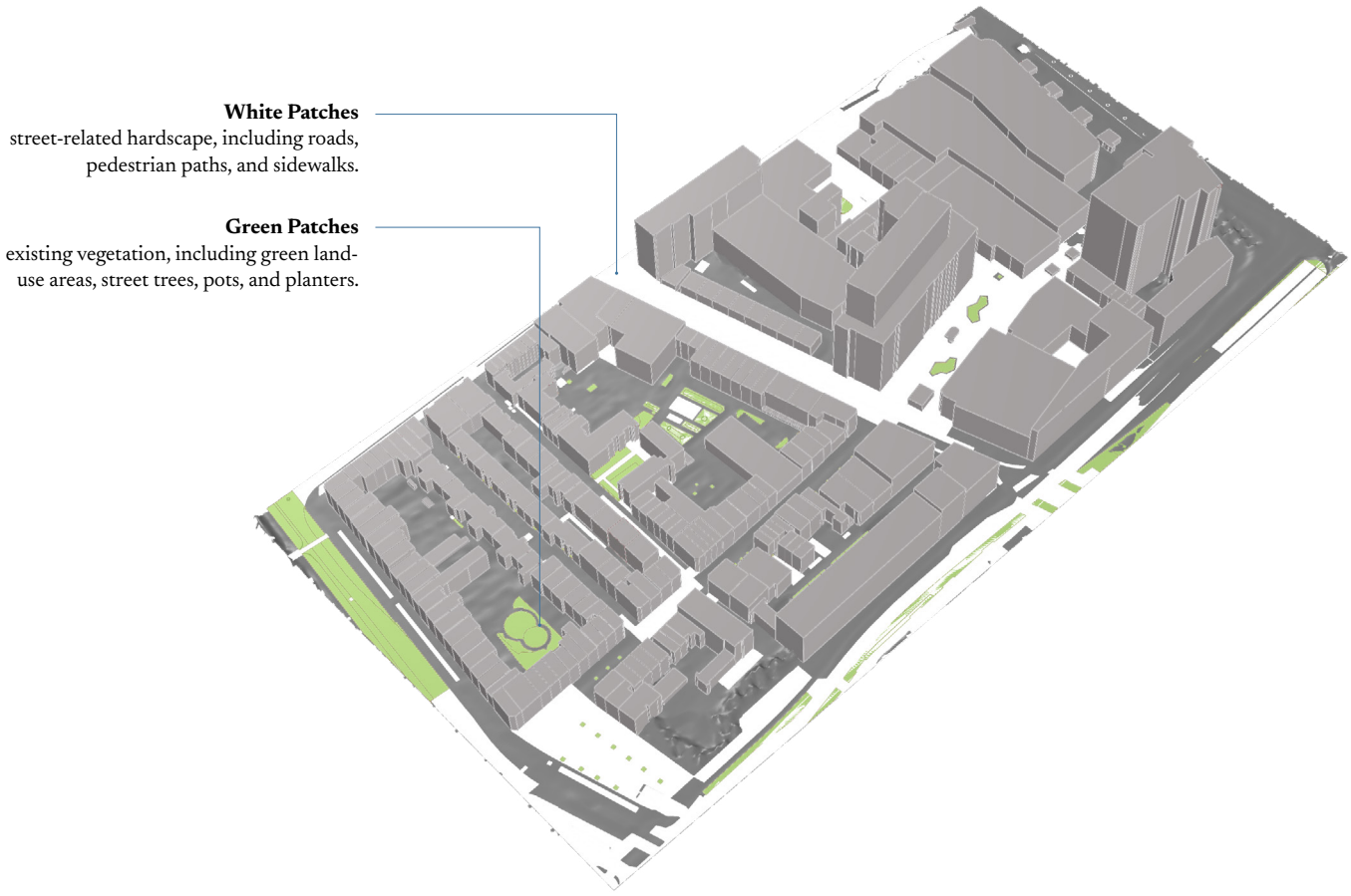

Figure 67. Rhino 3D Perspective View of Building, Terrain, and BGT Data

Rainfall Data

To obtain the rainfall input for the simulation, several rainfall references were first reviewed. Rotterdam Weatherwise identifies 100 mm of rainfall in 2 hours as an extreme rainfall condition and uses it as one of the design references for climate-adaptive urban development in Rotterdam (Rotterdams WeerWoord, 2023). However, the Climate Impact Atlas provides flood-depth datasets for more severe short-duration rainfall scenarios, including 140 mm in 2 hours, equivalent to an average intensity of 70 mm/hour. This scenario is therefore selected as the rainfall input for the workflow, because it represents a severe pluvial flood condition and also provides a corresponding flood-depth reference map that can be used to compare the initial inundation result without adaptation.

3.3 | Rainwater Simulation

Kangaroo Configuration Test

To translate the selected rainfall scenario into the particle-based simulation, the particle setting is adjusted to represent the rainfall volume applied to the Lijnbaan case study. The study area covers approximately 18,6 ha, resulting in a total rainfall volume of approximately 26,053 m³ for the selected 140 mm rainfall event. Compared with Jia et al. (2024), which used a 1-hour rainfall depth of 17.3 mm represented by approximately 12,000 particles with a diameter of 0.5 m, this research applies a substantially larger rainfall volume.

Before selecting the particle size used for the design-comparison stage, several preliminary simulation tests were conducted to compare different particle configurations and hardware conditions, as summarised in Table 8. The tests were run on two devices: a MacBook Pro M3 with 16 GB RAM and a higher-performance desktop computer with an AMD Ryzen 9 7900X 12-Core Processor, NVIDIA GeForce RTX 4080 GPU, and 64 GB RAM. In Table 8, the iteration number indicates the number of Kangaroo solver updates used to reach a stable particle distribution for each tested configuration. The purpose was to identify a setting that remained workable for a neighbourhood-scale case study while still representing the selected rainfall volume with sufficient spatial resolution.

No	Computer	Total Percipitaton (mm)	Particle Diameter (m)	Number of Particles	Number of Iterations	Converged Time
1	Laptop	100	2	4420	> 15920	Stopped before Converged (more than 2 Hours)
2	Laptop	280	2	12439	2260	Under 2 Hours
3	Laptop	300	2	13328	2260	Under 2 Hours
4	High performing	140	2	6219	> 13000	Stopped before Converged (more than 2 Hours)
5	High performing	100	1,5	10530	600	15 to 30 minutes
6	High performing	300	2	13328	2740	Around 1 Hour
7	High performing	140	1,5	14743	610	15 to 30 minutes
8	High performing	140	1	49757	2720	Under 2 Hours

Table 8. Rhino 3D Perspective View of Building, Terrain, and BGT Data

The result shows that particle diameter has a strong effect on the number of particles required to represent the same rainfall volume. Since each particle represents a spherical volume of water, reducing the particle diameter reduces the volume represented by each particle and increases the number of particles needed. For the selected 140 mm rainfall event, reducing the particle diameter from 2 m to 1.5 m increases the particle count from approximately 6,219 to 14,743 particles, while reducing it further to 1 m increases the count to approximately 49,757 particles.

However, convergence is not determined only by particle count. Some simulations with larger particle diameters and fewer particles still required a high number of iterations or stopped before convergence, suggesting that sparse particle distribution may lead to less stable movement across the terrain. At the same time, smaller particles increase computational load because more particles need to be processed.

Therefore, the particle diameter needs to balance several factors. While particle-number selection is commonly related to the stability of runoff-accumulation results, this workflow also uses particles for BGI absorption logic. Since each particle carries a defined water volume, particle size affects how much water is classified as absorbed or runoff when particles interact with BGI areas. For this reason, the selected particle diameter must balance rainfall-volume representation, movement stability, computational demand, and the level of detail required for BGI absorption assessment.

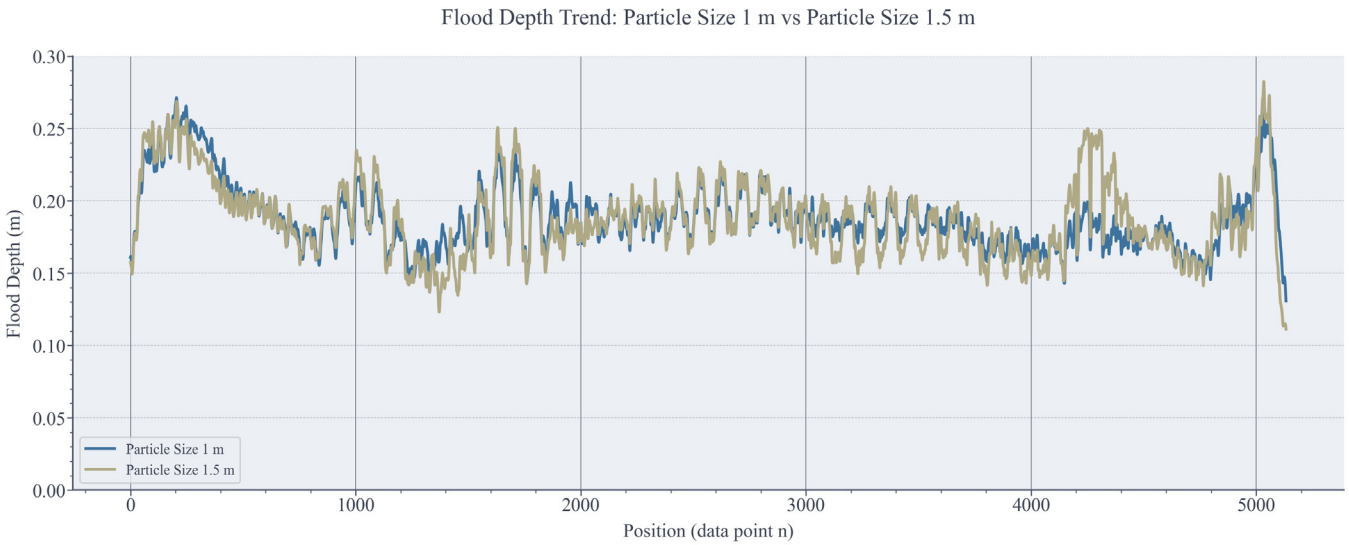

Figure 68. Comparison of flood depth trends for different particle sizes

Figure 68 compares the flood-depth trend produced by the 140 mm rainfall simulation using particle diameters of 1 m and 1.5 m. Overall, both settings generate a very similar depth pattern across the sampled positions. The main peaks, depressions, and general fluctuations occur in approximately the same locations, indicating that the overall spatial trend of flood-depth distribution remains consistent despite the change in particle size. However, the 1.5 m particle setting shows slightly more irregular local fluctuation, while the 1 m particle setting appears somewhat smoother and more stable. This suggests that reducing particle size refines the representation of flood-depth variation, but does not fundamentally change the overall depth pattern. In this sense, the comparison indicates that the 1.5 m setting is still able to reproduce the general flood-depth trend, while the 1 m setting offers a more detailed representation at the cost of substantially higher particle count and computation time.

Based on this comparison, the 1 m particle diameter was selected for the design-comparison stage. Although the 1.5 m setting produces a similar overall flood-depth trend, the 1 m setting provides finer particle resolution. This is important because particles are used not only to estimate runoff accumulation, but also to classify BGI absorption. Since each particle represents a defined volume of water, a larger particle diameter would classify a larger amount of water at once as either absorbed or runoff. The 1 m particle setting therefore allows the absorption logic to respond more gradually while remaining computationally manageable.

Retrieving Flood Depth

Comparison with Real Data

To convert the remaining runoff particles into flood-depth values, the particles are aggregated into grid cells and translated into depth based on the water volume within each cell. The resulting flood-depth resolution is therefore influenced by both the particle diameter and the selected grid-cell size. Since the selected particle diameter is relatively large, a grid cell that is too small may cause a single particle or small particle cluster to produce an unrealistically high local depth value. For this reason, two grid-cell sizes, 2.5 × 2.5 m and 5 × 5 m, were tested under the no-adaptation condition and compared with the Klimaateffectatlas reference map for the same percipitation rate. This comparison is used as a validation check to assess which grid size produces a more suitable flood-depth representation for the case study, considering spatial consistency with the reference map and computational manageability for later building-inundation retrieval. Overall, both grid sizes produce a similar flood-depth trend, but differences are observed in the spatial smoothness and local depth variation. These differences are further examined through the map comparison and percentile distribution shown in Figure 69.

Figure 69. Comparison between simulation result with cell 5 x 5 m, cell 2.5 x 2.5 m, and Climate Impact Atlas Map

Trend Consistency vs Real Map
The 5m map produces a smoother depth gradient more consistent with the real map, with deeper flooding concentrated along the main streets and lighter values toward building edges. The 2.5m map loses this gradient quality (appearing more fragmented)

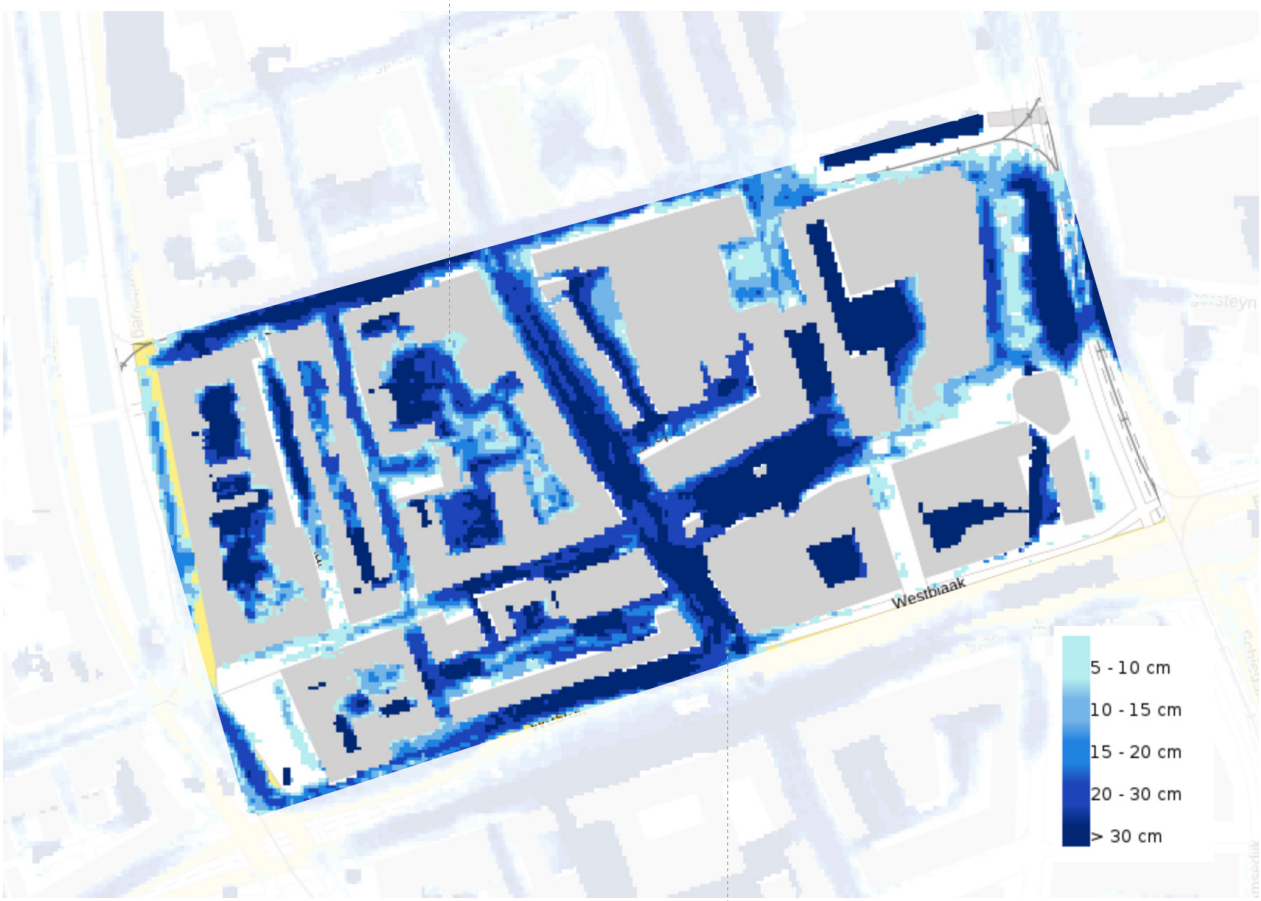

Climate Impact Atlas Map

Boundary Limitation
Inconsistencies are observed more at the boundary of the site between the generated map and the KlimaEffektAtlas. This is because the simulation only considers rainfall within the defined site boundary, whereas in reality runoff from surrounding areas also contributes to flooding at the site edges. This is acknowledged as the limitation of the simulation.

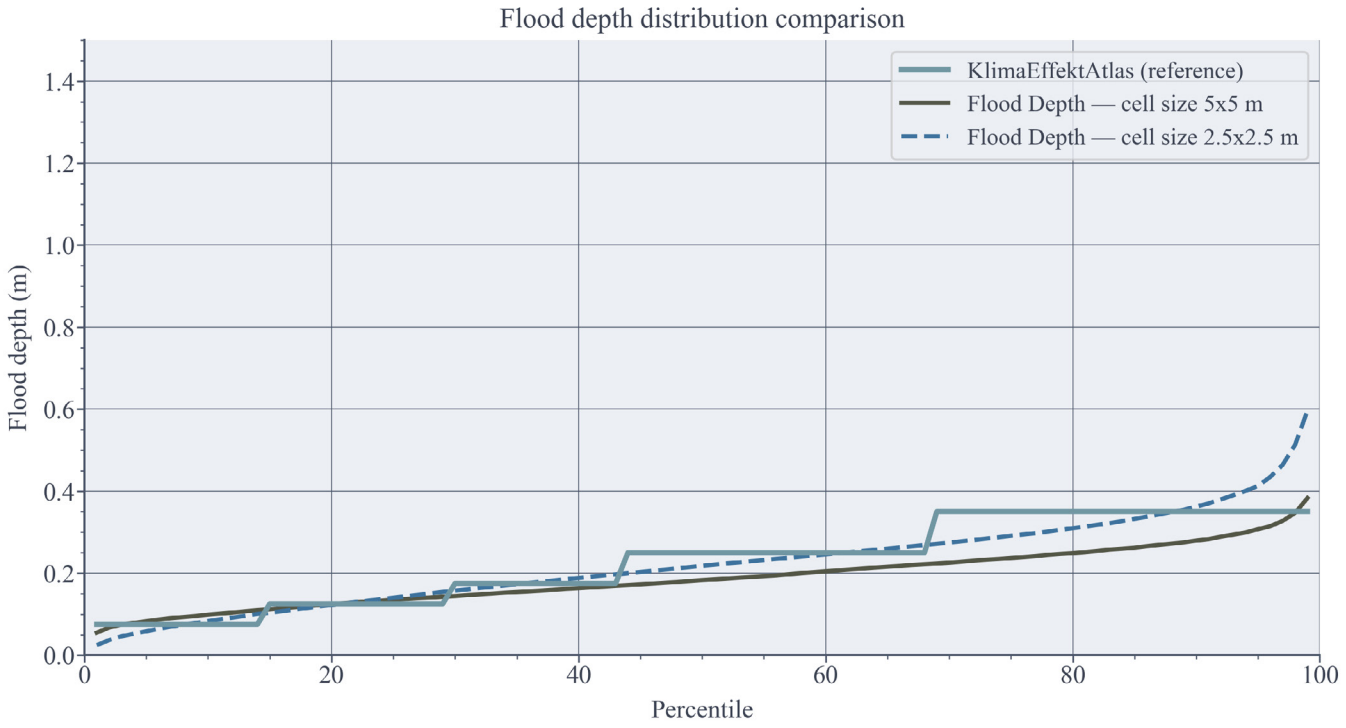

Figure 70. Percentile value comparison between simulation result with cell 5 x 5 m, cell 2.5 x 2.5 m, and Climate Impact Atlas Map

To evaluate the influence of grid-cell size on flood-depth estimation, the 5 × 5 m and 2.5 × 2.5 m grid results were compared against the Klimaateffectatlas reference map using both spatial map comparison and percentile statistics. A direct cell-by-cell comparison is not possible because the reference data uses a different spatial resolution and alignment. In addition, the Klimaateffectatlas flood-depth map is stored as categorical depth ranges rather than exact continuous values. Therefore, the comparison is used to evaluate general spatial and distributional consistency rather than exact depth agreement.

The map comparison shows that the 5 × 5 m grid produces a smoother flood-depth gradient that is more consistent with the reference map, with deeper flooding concentrated along the main streets and lower values toward building edges. In contrast, the 2.5 × 2.5 m grid captures more local variation, but the result appears more fragmented and more sensitive to local particle clustering. This is also reflected in the percentile comparison, where the 2.5 × 2.5 m grid shows stronger high-depth values at the upper percentiles because particle accumulation is calculated over a smaller cell area.

For this reason, the 5 × 5 m grid-cell size is selected for the final design-comparison stage. This resolution provides a more stable and generalised flood-depth surface for neighbourhood-scale building inundation retrieval. It also reduces the number of grid centroids that need to be checked against each building assessment boundary, which is important because inundation depth retrieval is repeated across the adaptation scenarios. Using the estimated reference mean based on the midpoint of the Klimaateffectatlas depth classes, the simulated mean depth remains lower, with a mean-depth ratio of approximately 1.2 between the reference and simulation values (0.22 m compared with 0.188 m). The remaining difference is partly attributed to the simplified simulation boundary, which does not include potential inflow from surrounding areas, and partly to the categorical nature of the reference data.

Final Configuration Setup

Based on the preliminary particle-configuration tests and flood-depth grid comparison, the final simulation configuration used for the design-comparison stage is summarised in Figure 71. The selected setup uses a 140 mm rainfall event, represented by 49,757 particles with a 1 m particle diameter. The remaining runoff particles are then converted into flood-depth values using a 5 × 5 m grid-cell resolution. For building-inundation retrieval, an 8 m offset boundary is applied around each building footprint. This offset is used to ensure that nearby grid centroids are captured, especially because the grid is not always perfectly aligned with the building geometry and site orientation. The retrieved flood-depth values within this boundary are then used to estimate the representative inundation depth for each building.

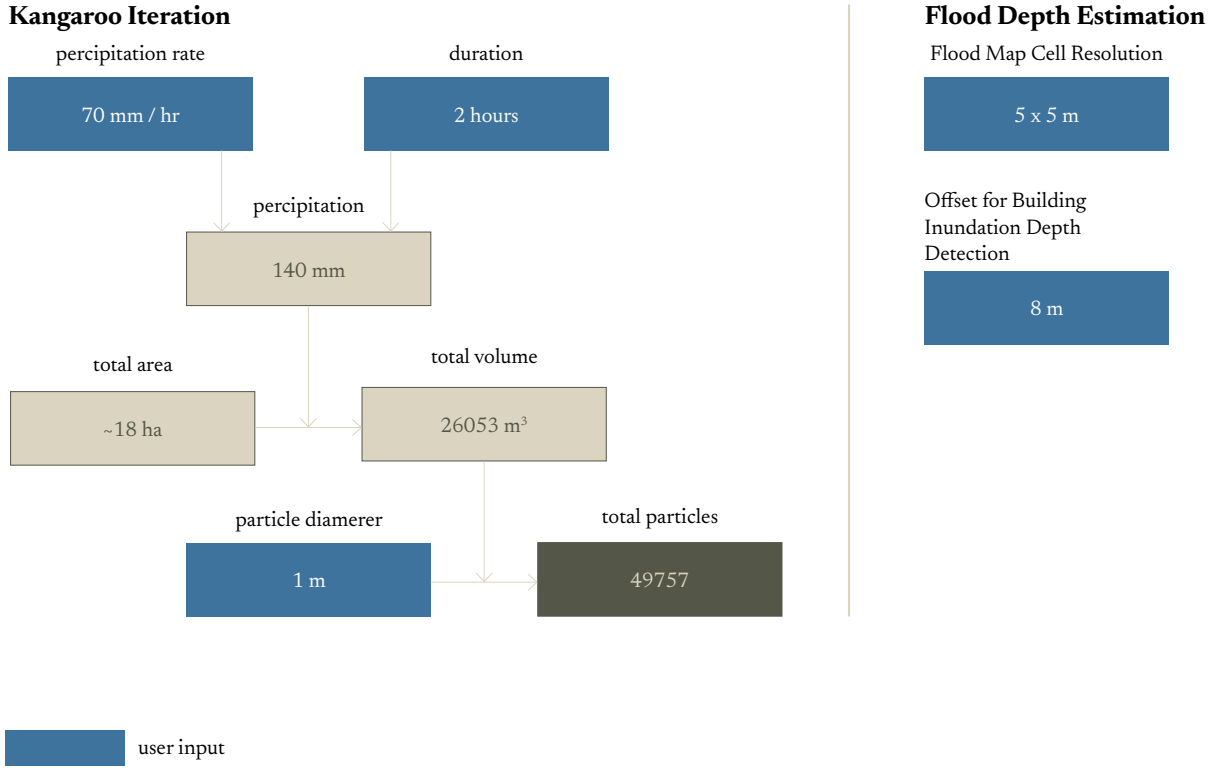

Figure 71. Rainfall & Flood Setting Summary

Since the terrain condition remains unchanged across the adaptation scenarios, the Kangaroo particle-movement simulation does not need to be repeated for each design scenario. Instead, the recorded particle coordinates are reused, and only the later processing stages, including BGI absorption classification and flood-depth estimation, are repeated for each adaptation scenario.

3.4 | Existing Condition

Without Existing Green Space

The site is first simulated under the No BGI scenario to establish the baseline flood condition and identify the maximum flood depth occurring within the study area. The tested rainfall event represents a short and severe precipitation scenario in the Dutch context, with 140 mm of rainfall over 2 hours. Under this scenario, the simulated flood depths remain below 1 m. This is consistent with Klimaeffectatlas map and the general characteristic of urban pluvial flooding , which is often shallow, localised, and strongly influenced by surface runoff accumulation.

Figure 72 shows the spatial distribution of building resilience scores under the No BGI scenario, where each point represents the centroid of a building footprint. The full building resilience map used for the assessment is provided in Appendix RS-01. Figure 73 shows the relationship between inundation depth and resilience score for each building.

Overall, buildings exposed to higher maximum flood depths tend to receive lower resilience scores. However, buildings with similar flood depths can still have different resilience scores because the calculation also includes building-specific parameters, such as building class, basement assumption, depth–damage relationship, and building-class-dependent impeding and restoration time.

This variation is visible, for example, in grid zone B2 and C3, where several buildings show relatively high resilience scores compared with nearby buildings under similar local flood conditions. These buildings correspond to those without an assumed basement, suggesting that basement presence has a noticeable influence on the final resilience score.

The baseline resilience scores remain mostly within the range of approximately 0.8–0.95, which is expected because the assessed flood depths remain below 1 m, where the selected depth–damage curves generally produce relatively low damage ratios. Therefore, the assessment focuses mainly on the relative change between scenarios, where even small changes in resilience score can indicate how different BGI adaptation scenarios influence flood exposure, damage reduction, and building resilience across the site.

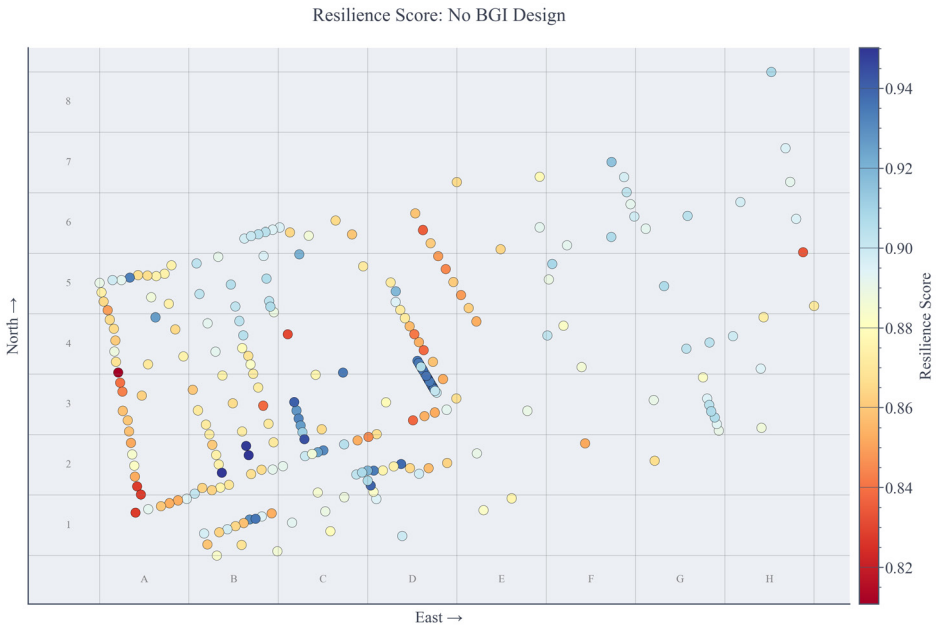

Figure 72. Spatial graph of resilience score without BGI adaptation

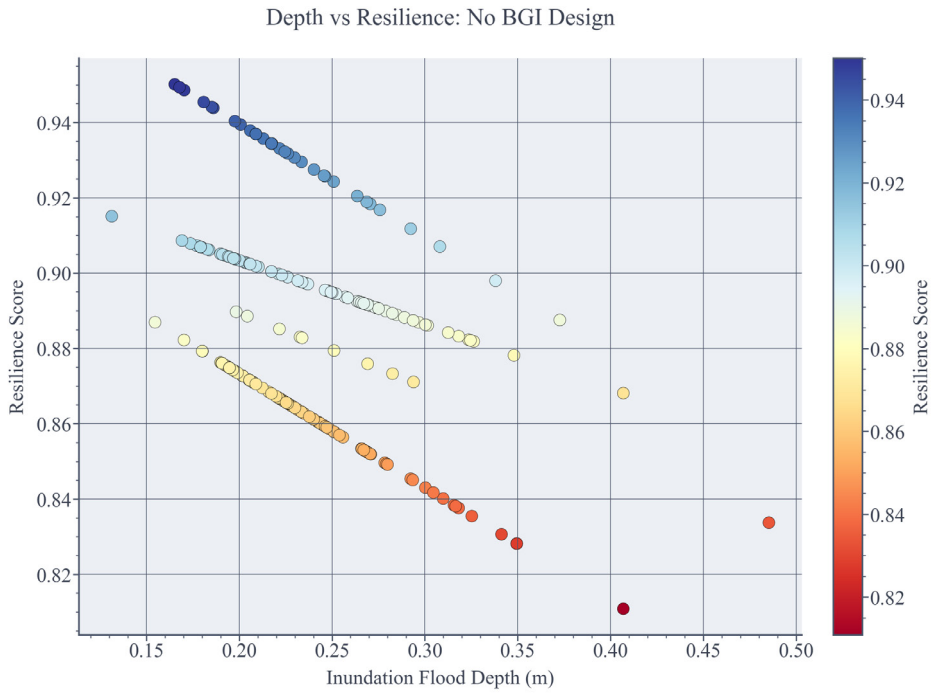

Figure 73. Scatter graph of resilience score - without BGI adaptation

With Existing Green Space

After the baseline condition is established, existing green surfaces are added as the Existing BGI scenario (Figure 74). The spatial data is extracted from the BGT dataset, mainly from the *begroeid terreindeel* layer, which represents vegetated land-cover areas. Road-related surfaces from *wegdeel* or *ondersteunend wegdeel* are not included as BGI in this scenario, because pavements are treated as impervious unless specific evidence of permeability is available.

Not all green elements from the dataset are included in the simulation. Only ground-level green surfaces that can reasonably contribute to rainwater absorption or temporary storage are considered. Green elements that are likely to be disconnected from the ground surface, such as raised planters, are excluded. Green areas located on or directly associated with railway infrastructure are also excluded, because their hydrological behaviour and accessibility as BGI are less certain within the scope of this workflow.

In this scenario, all selected existing green surfaces are assigned the storage-depth value of urban parks with 50 – 75 % percentage of grass cover. This is a conservative estimation. Based on visual observation using Google Earth, the existing green areas do not consistently show design characteristics of engineered BGI systems such as bioswales. Therefore, they are treated as general vegetated surfaces rather than as specialised runoff-retention infrastructure. This allows the Existing BGI scenario to represent the likely contribution of current ground-level greenery without overestimating its absorption capacity.

Figure 74. Siteplan with existing BGI configuration

To understand the effect of existing BGI, two comparison graphs are used: a spatial change graph and a resilience-score comparison graph. Figure 75 shows the spatial difference in resilience score between the Existing BGI scenario and the No BGI baseline, while Figure 76 compares the resilience score of each building before and after existing BGI is included.

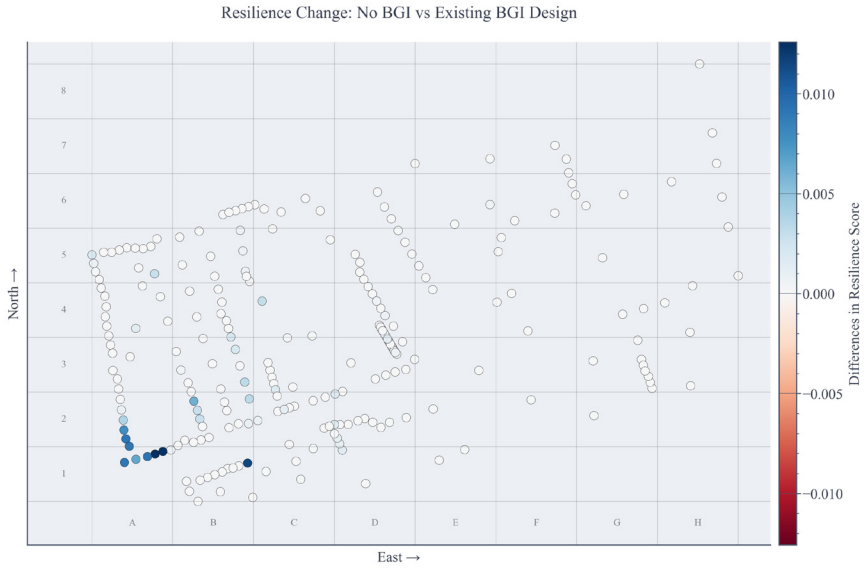

Figure 75. Spatial graph of building resilience score differences between existing design and no green space condition

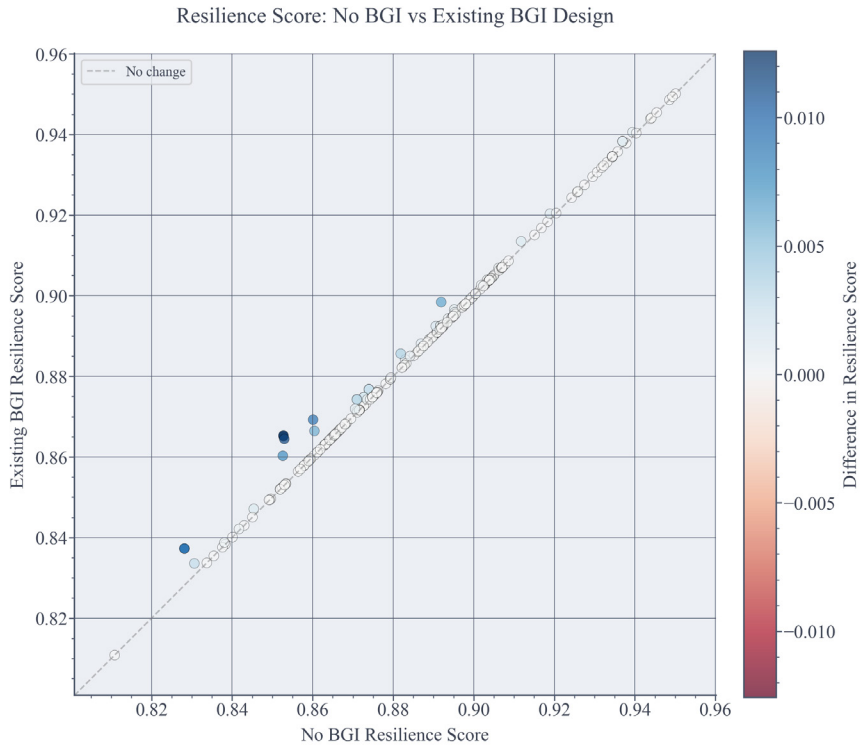

Figure 76. Scatter graph of building resilience score differences between existing design and no green space condition

The results show that most buildings remain close to the no-change line, indicating that the existing BGI produces only a limited change in resilience score across the site. The most visible improvement occurs around grid zone A1–A2, where several buildings show a positive change. This suggests that Urban Park 1 has a local influence on nearby buildings. The existing BGI cluster around grid zone C4 also shows some effect, but the change is more subtle.

The building with the lowest resilience score remains largely unaffected. This is expected because there is no existing BGI located close to this building or along the runoff path contributing to its flood exposure. Therefore, the Existing BGI scenario shows that existing green areas can have local benefits, but their effect depends strongly on their spatial relationship to runoff movement and nearby vulnerable buildings.

3.5 | Adaptated Design Scenario

After the existing condition is understood through the comparison between the No BGI baseline and the Existing BGI scenario, the workflow is continued into the design exploration stage. Two additional design scenarios are developed to test how different BGI adaptation choices may influence building flood resilience.

Scenario 1

Scenario 1 is developed by maintaining the general location of the existing BGI areas while increasing their adaptation capacity. Instead of introducing new BGI locations across the site, this scenario expands and upgrades the existing green areas. The park area is enlarged while keeping the same assumed soil condition, with an infiltration performance of 50–75%. Some existing green surfaces are converted into bioswales, while selected hardscape areas in the southern part of the site are changed into permeable pavement. The permeable pavement area is expanded to include wider pedestrian and sidewalk zones where adaptation is spatially possible.

Figure 78 illustrates the spatial configuration of Scenario 1, including the expanded park area, bioswale locations, and permeable pavement zones.

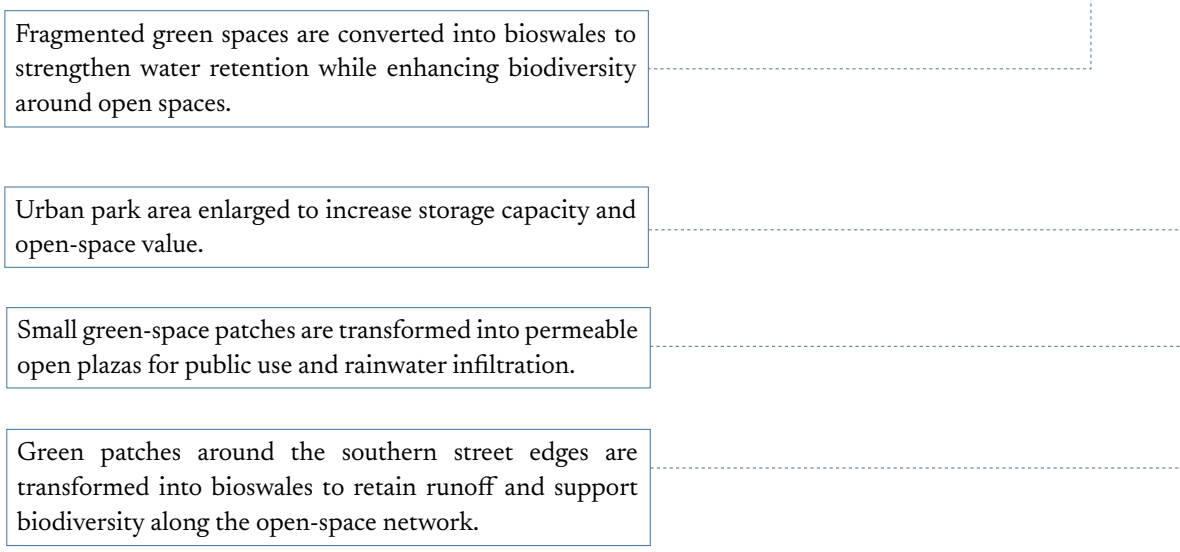

Figure 77. BGI Adaptation Site Plan for Scenario 1

Figure 78. BGI Adaptation Site Plan for Scenario 1

Scenario 2

Scenario 2 is developed to test the effect of increasing BGI adaptation in the eastern part of the site, while also introducing more variation in the western part. In this scenario, the courtyards within the building cluster are converted into permeable pavement, and small bioswales are added in open spaces between buildings. Additional permeable pavement is introduced along Karel Doormanstraat, where runoff from the street is expected to pass through. This adaptation is intended to test whether slowing down or absorbing water along the street can reduce flood impact before it reaches the lower accumulation area.

All urban park adaptations in Scenario 2 are modelled using the urban park >75% vegetation cover coefficient, representing a higher assumed storage depth than the 50–75% vegetation condition. The adaptation strategy in the southern part of the site follows Scenario 1, so that the effect of additional adaptation in the eastern area can be observed more clearly. Figure 79 illustrates the spatial configuration of Scenario 2.

The open space is transformed into permeable pavement to support multifunctional use, including parking, while improving rainwater infiltration.

Small existing green patches are removed to test their effect on the result.

Urban park area is retained from scenario 1, with increased storage depth for >75% vegetation cover.

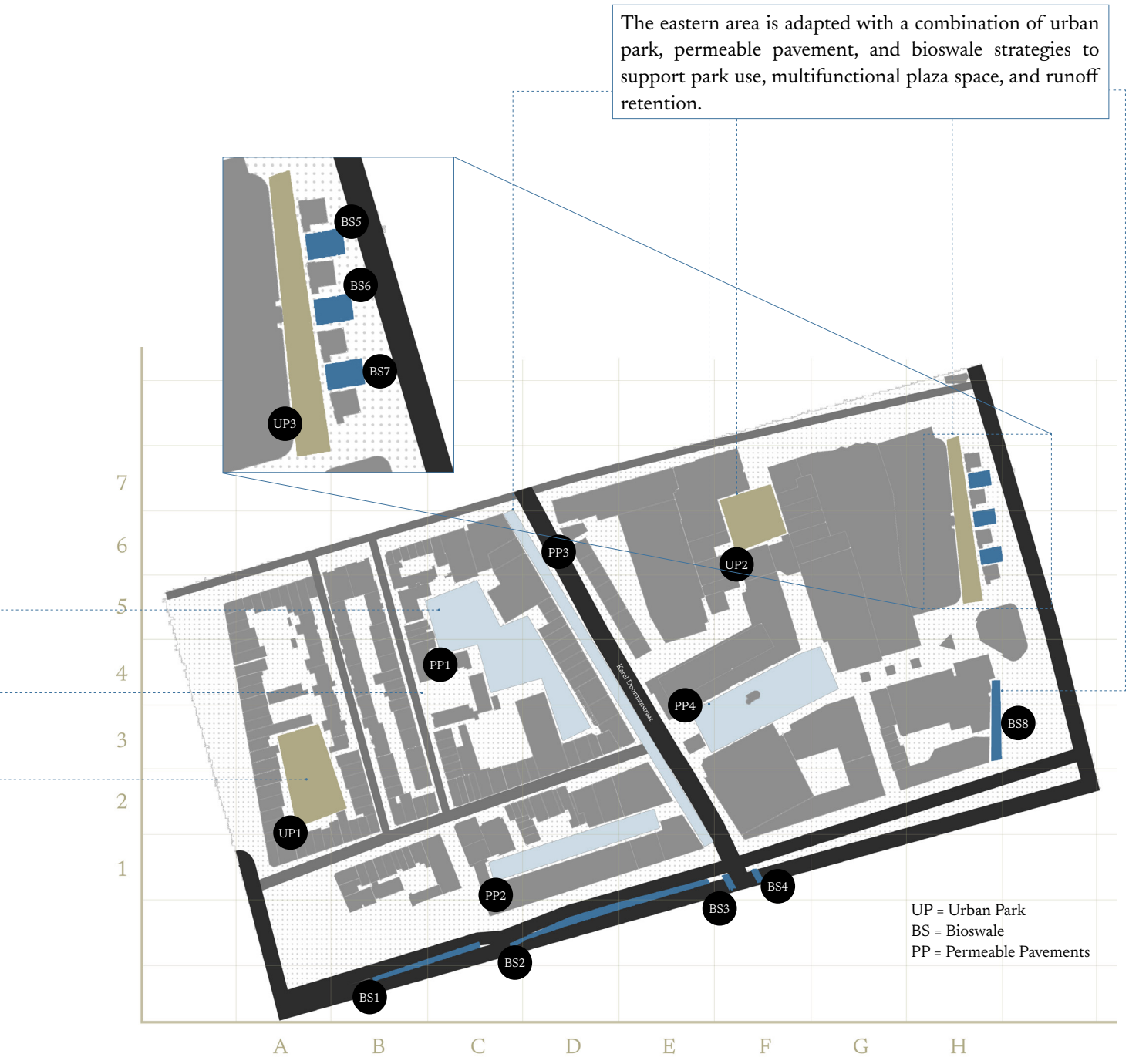

Figure 79. BGI Adaptation Site Plan for Scenario 2

Design Comparison

After the design scenarios are developed, the results of Scenario 1 and Scenario 2 are compared against the Existing BGI condition to evaluate how different design decisions influence the resilience outcome. The comparison focuses on the statistical outputs generated by the workflow, including changes in flood depth, building resilience score, BGI utilisation, and indicative cost. The graphs presented in this section therefore summarise the main quantitative differences between scenarios. The full flood-depth maps and Rhino visualisations are provided in the Appendix (code FM for flood maps and RS for resilience scores) to support the spatial interpretation of the results.

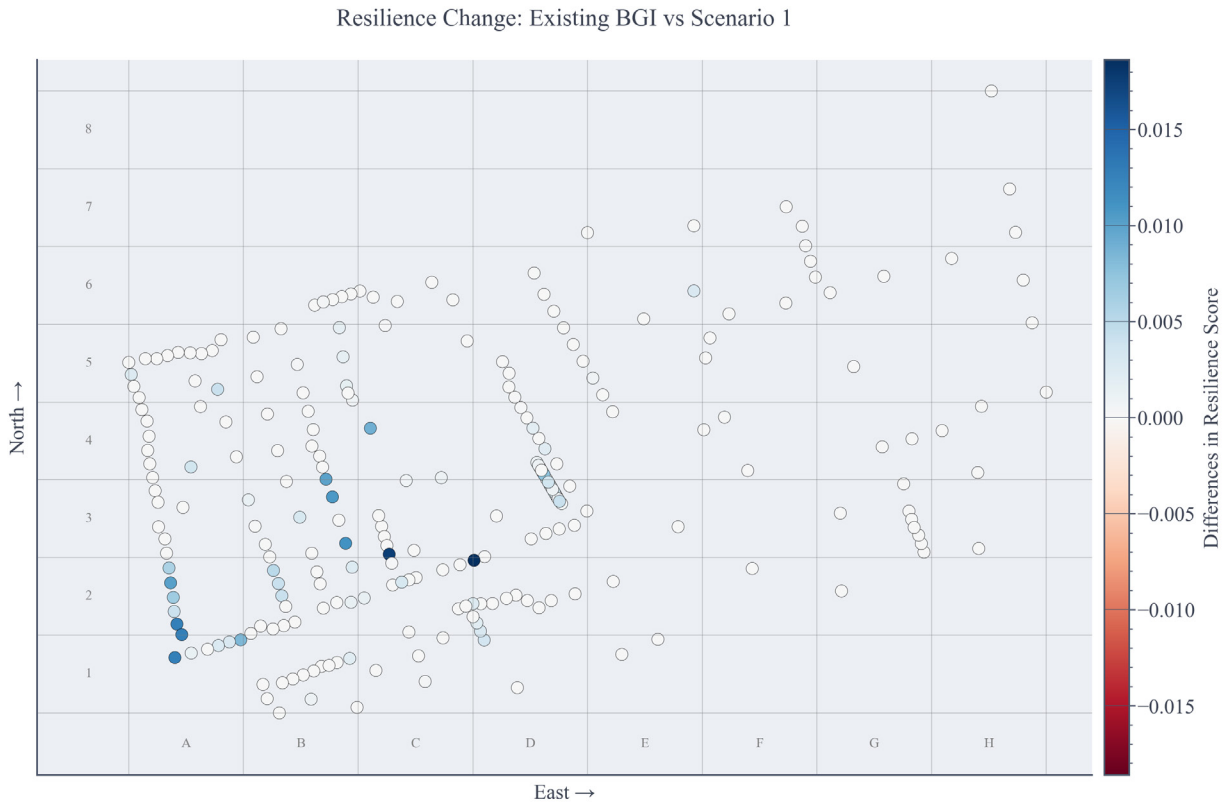

Figure 80. Spatial graph of building resilience score differences between existing design and scenario 1

Figure 80 shows the spatial change in resilience score between the Existing BGI condition and Scenario 1. Since Scenario 1 mainly maintains the existing BGI placement and increases its capacity, the improvement remains mostly local. The eastern part of the site shows almost no visible change. The most visible improvement occurs around UP1, where the expanded urban park further increases the resilience scores of buildings that already improved in the Existing BGI scenario. This suggests that the area still receives enough runoff for the expanded park to absorb additional water. However, converting part of the existing BGI cluster into bioswales does not produce a strong improvement around grid zone C4–D4. PP1 also produces only a slight local improvement around the D1–D2 area, suggesting that its effect remains limited to the immediate surrounding buildings.

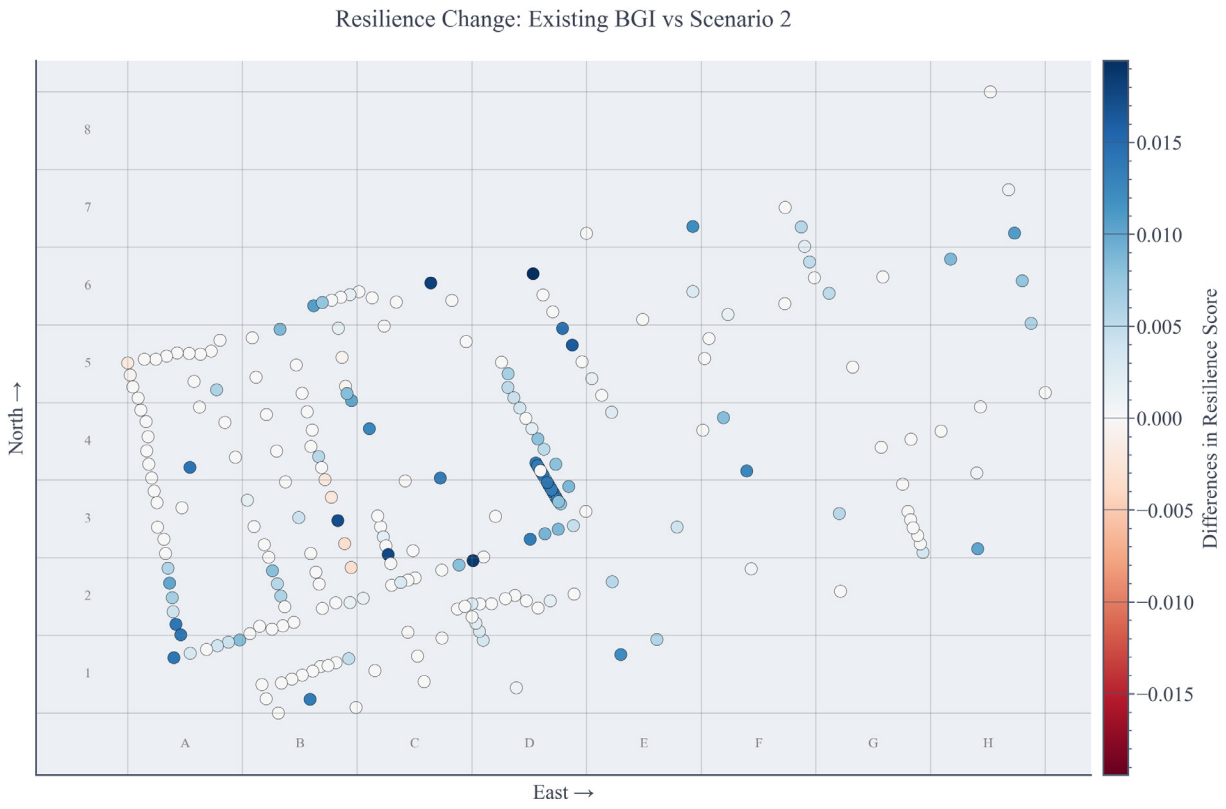

Figure 81. Spatial graph of building resilience score differences between existing design and scenario 2

Figure 81 shows the spatial change in resilience score between the Existing BGI condition and Scenario 2. Compared with Scenario 1, Scenario 2 produces a broader distribution of positive changes. The permeable pavement along Karel Doormanstraat improves the resilience scores of buildings directly facing the street. Although this area is not the main ponding location, it appears to be part of the runoff pathway (see Figure 86 for further discussion), suggesting that intercepting water before it accumulates can still influence nearby building resilience. PP4 also contributes to improvement, although the effect is not as large as expected considering its adapted area. In the eastern part of the site, buildings around grid zone H6–H7 benefit from the combined effect of BS5–BS7 and UP3, while the smaller BS8 also supports improvement for the building around H3.

The comparison also shows the effect of removing existing BGI elements. In Scenario 2, three existing BGI areas from existing, UP3–UP5, are removed. After their removal, several buildings around B3–B4 show a slight negative change in resilience score. This indicates that these existing BGI areas still contributed to local flood reduction.

Overall, Scenario 1 mainly strengthens the effect of existing BGI locations, while Scenario 2 produces a broader spatial response by introducing adaptation along runoff pathways. This suggests that BGI placement in relation to water movement can be as important as the total adapted area or storage depth.

A further investigation of Urban Park 1 (UP1) confirms the observation from the scenario comparison. In Scenario 1, UP1 is modelled using the urban park 50–75% vegetation cover coefficient, while in Scenario 2 it is modelled using the urban park >75% vegetation cover coefficient, which has a higher assumed storage depth. As shown in Figure 82 and 83, the absorbed and runoff path visualisations indicate that water continues to reach the UP1 area in both scenarios. This explains why increasing the size and rainwater performance of UP1 still produces improvement in the surrounding buildings. In this case, UP1 is not only an available green area, but is also located along an active runoff path, making it an effective location for BGI adaptation.

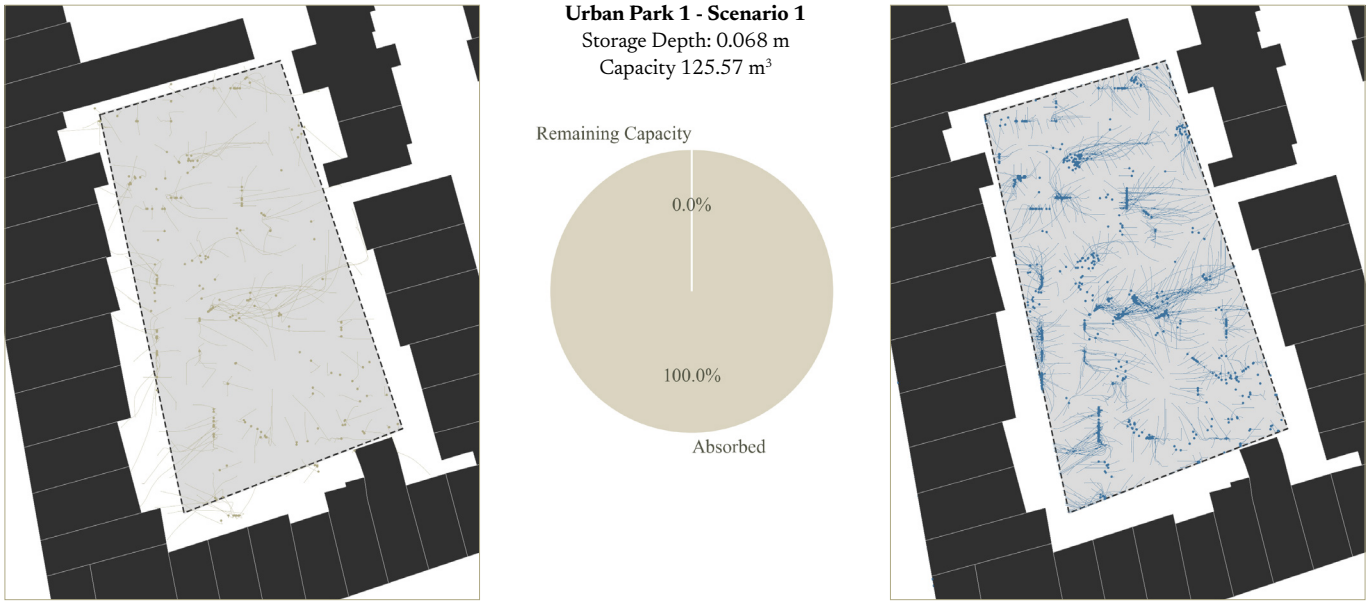

Figure 82. Absorbed Path vs Runoff Path for Scenario 1

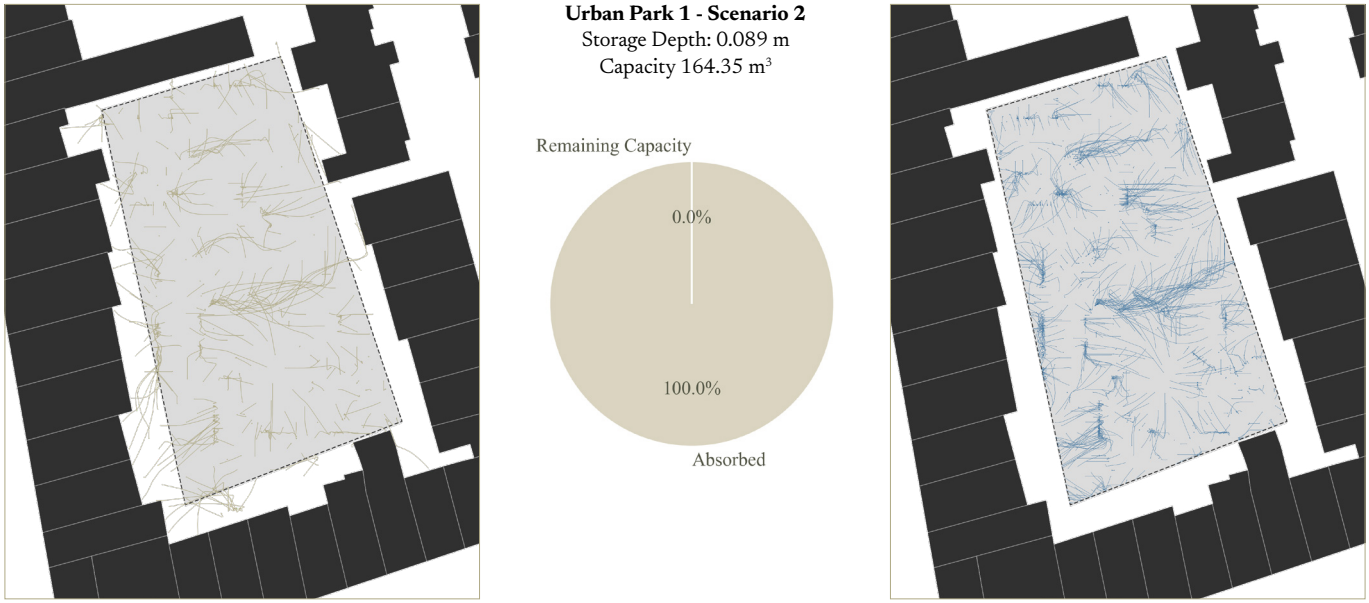

Figure 83. Absorbed Path vs Runoff Path for Scenario 2

The existing green spaces in the southern part of the site are retained in both design scenarios. In Scenario 1, these areas are labelled as B11 and B12, while in Scenario 2 they are labelled as BS3 and BS4. The difference in naming occurs because the Grasshopper labelling process assigns indices automatically, so the same spatial BGI area may receive different labels in different scenarios.

The comparison shows that these areas were already fully utilised when calculated as urban parks with 50–75% vegetation cover and a storage depth of 0.068 m. After being converted into bioswales, which have a higher storage depth, the same areas still retain remaining capacity, with 9.1% and 14.4% capacity left (Figure 84 and 85). This indicates that changing the BGI type from urban park to bioswale increases the rainwater capacity of the same spatial area.

However, the result also suggests that the effectiveness of these areas is not determined by storage capacity alone. Since the original green spaces were already fully utilised, they are likely positioned along active runoff pathways where water is already being received. Nevertheless, the Scenario 1 resilience-score map shows that converting these areas into bioswales does not produce a substantial improvement in nearby building resilience scores. This indicates that increasing BGI capacity is not always sufficient if the absorbed runoff does not significantly reduce flood exposure around affected buildings.

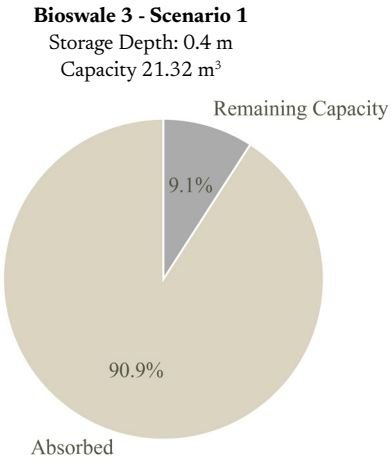

Figure 84. Absorption percentage for Bioswale 3

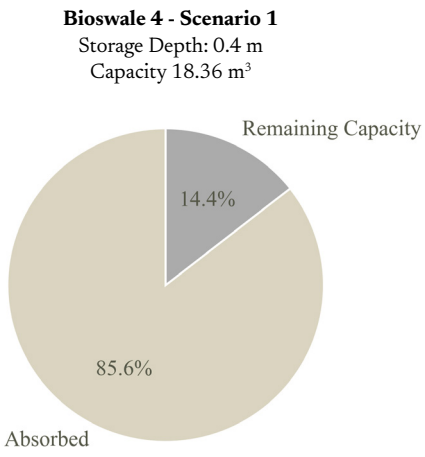

Figure 85. Absorption percentage for Bioswale 4

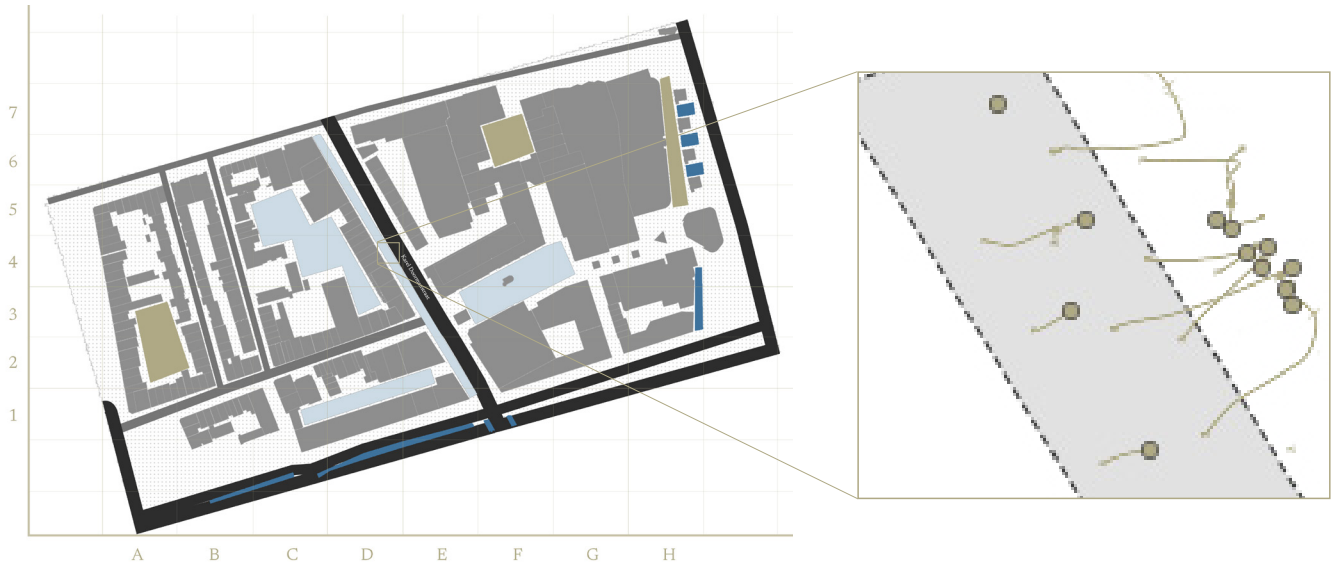

Figure 86. Absorbed Path vs Runoff Path for Scenario 1

Figure 86 shows a detailed view of the absorption path in PP3. The points represent the final particle positions recorded from the movement simulation, while the lines show the movement paths followed by the particles before reaching those positions. The figure shows that several particles are absorbed before reaching their final runoff location, indicating that PP3 is positioned along an active runoff pathway. This demonstrates that BGI performance is not only related to where water finally accumulates, but also to whether the adaptation area can intercept runoff during its movement across the site.

Cost Comparison

Figure 87 and Figure 88 compare the estimated implementation cost and utilisation rate of each BGI element in Scenario 1 and Scenario 2. In both scenarios, most BGI elements show high utilisation rates, indicating that the selected adaptation areas generally receive runoff and are actively used in the simulation. However, utilisation rate alone does not fully explain the effect of each BGI element on building resilience. Therefore, the cost comparison needs to be interpreted together with the spatial resilience-score changes discussed earlier.

In Scenario 1 (Figure 87), most bioswales have relatively low implementation cost because they occupy smaller areas, while still showing high utilisation rates. The largest cost contributors are PP1 and UP1, which also show high utilisation rates. However, their resilience impact differs. UP1 corresponds with a visible improvement in the surrounding buildings (grid cell A1-A2), while PP1 produces only a slight local improvement around the D1–D2 grid zones. This shows that high utilisation and high cost do not automatically result in strong building-level resilience improvement.

In Scenario 2 (Figure 88), the cost range becomes much wider. Several urban park and permeable pavement elements have substantially higher costs, especially PP1, PP4, UP1, and UP2. PP4, for example, corresponds with a clear resilience improvement around one large building in the F4 grid zone. Although the improvement appears to affect only one building, the impact is still visible because the affected building has a large footprint. This suggests that the value of a BGI element should not only be judged by the number of buildings affected, but also by the scale and vulnerability of the buildings receiving the benefit.

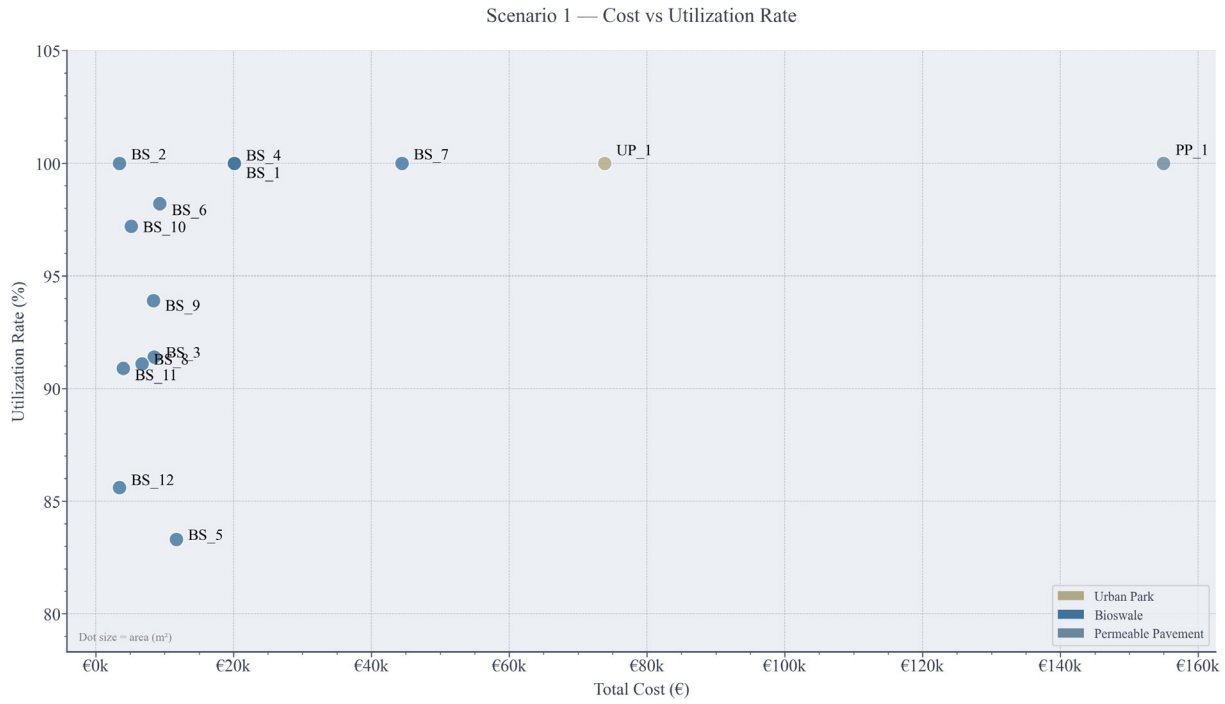

Figure 87. Cost and utilisation-rate comparison of BGI elements in Scenario 1

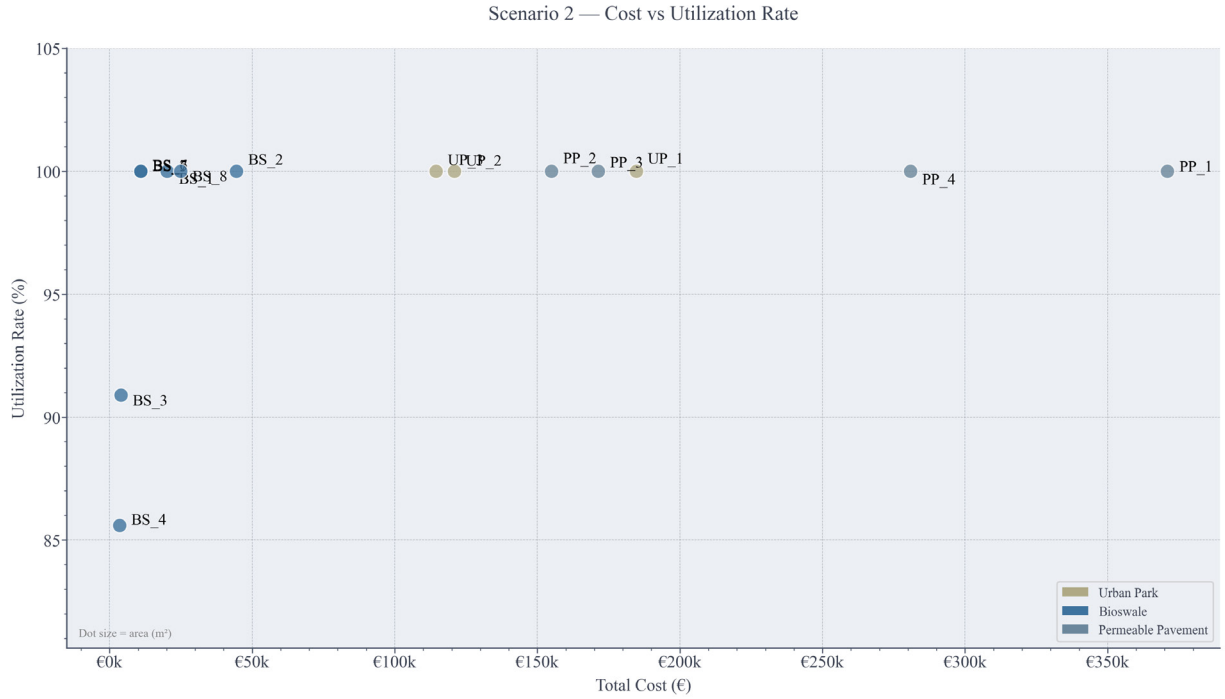

Figure 88. Cost and utilisation-rate comparison of BGI elements in Scenario 2

Overall, the comparison shows that cost, utilisation rate, and resilience-score improvement need to be interpreted together. A high utilisation rate indicates that a BGI element receives runoff and uses its storage capacity, but it does not automatically mean that it produces strong building-level resilience improvement. Similarly, a higher-cost element may be justified when it contributes to meaningful improvement around vulnerable or large buildings, but may be less efficient if the improvement remains very local. This demonstrates that the workflow can support design decisions not only by calculating individual indicators, but by helping compare how cost, runoff absorption, spatial location, and building-level resilience outcomes relate to each other.

04
Discussion

Representing Building Resilience

BGI as a Multidimensional Adaptation

Simulation and Computational Trade Off

Workflow Adaptibility: Case Study and Beyond

From Results to Insights

4.1 | Representing Building Resilience

From Flood Intensity to Building Vulnerability

Building flood resilience is not only determined by the intensity of flooding, but also by the vulnerability and recovery characteristics of the exposed building. In this workflow, flood intensity is represented through inundation depth, which is retrieved from the rainwater simulation and used as the main input for the depth–damage relationship. However, the final resilience score also depends on building-specific parameters, including building class, basement assumption, and class-dependent impeding and restoration time. Therefore, the workflow translates flood exposure into a building-level resilience score by combining both the hazard condition and the characteristics of the affected building.

This distinction is visible in the case study results, especially in the scatter plot comparing inundation depth and resilience score. Buildings with similar inundation depths can still fall within different resilience-score ranges, showing that flood intensity alone does not determine the final outcome. Instead, the score also reflects building-specific vulnerability and recovery parameters, including basement presence, building class, and class-dependent impeding and restoration time. This allows the workflow to differentiate between buildings that experience similar flood exposure but may have different levels of vulnerability and recovery capacity.

Expanding Resilience Representation

While the workflow already moves beyond flood intensity by including building-specific vulnerability and recovery parameters, its current representation of resilience is still mainly based on physical damage. In this implementation, the quality factor Q is represented as 1 – physical damage, meaning that the resilience score is strongly influenced by the selected depth–damage relationship. This provides a clear and measurable structure for comparing scenarios, but it also limits how far the workflow can represent other types of disruption.

This limitation is especially relevant for pluvial flooding. Pluvial flood depths may be relatively shallow, but they can still disrupt building functionality through access disruption, ground-floor use, basement use, technical systems, or short-term business operation. This aligns with UNDRR's framing of resilience as the ability to resist, absorb, adapt to, and recover from hazards while preserving and restoring essential basic structures and functions (UNDRR, 2017). UNDRR also frames exposure and vulnerability as including not only physical assets, but also loss of property or service, health impact, economic impact, environmental impact, and recovery time.

In the current workflow, buildings are grouped into three broad classes: residential, commercial, and industrial. This was necessary for the case study implementation because the available building-function data had to be clustered into consistent categories before it could be used in the resilience calculation. However, this simplification may reduce the variability of vulnerability between different building uses. In reality, urban functions are more diverse, and different buildings may experience different types of disruption even under the same flood depth. For example, healthcare facilities, schools, offices, shops, housing, and technical buildings may have different sensitivity to access disruption, basement flooding, equipment damage, service interruption, and recovery time.

Therefore, future development of the workflow could benefit from a more functionality-oriented representation of Q, rather than relying only on physical damage. More detailed building-use categories and pluvial-specific disruption relationships could allow the workflow to represent not only how much physical damage occurs, but also how different building functions are interrupted and prioritised for recovery.

4.2 | BGI as a Multidimensional Adaptation

Within the Broader Spatial System

As discussed in Chapter 2, BGI can be understood as an adaptation approach that uses, supports, or is inspired by natural processes to address environmental, social, and economic challenges. This reflects a broader role of BGI beyond water regulation alone. In urban environments, BGI can also contribute to spatial quality, ecological value, thermal comfort, public amenity, and everyday urban use.

This multifunctional character is what makes BGI particularly relevant for dense urban areas. In contexts where the urban fabric is compact and open space is limited, adaptation measures need to perform more than one role. A surface may need to support rainwater retention while still functioning as a pedestrian route, courtyard, plaza, green space, or access area. This is important for designers because a space is not defined only by its physical surface, but also by how it is intended to be used. The same area can have different spatial meanings depending on whether it is designed as a park, a bioswale, a sidewalk, a plaza, or a courtyard. Therefore, selecting a BGI adaptation is also a design decision about what role that space should perform in daily urban life. In this sense, BGI adaptation is multidimensional: it operates not only as part of the water system, but also as part of the broader spatial system.

Representation in Early-Stage Design Simulation

Because the resilience assessment is linked to flood depth through the depth–damage relationship, the current BGI representation focuses mainly on how each adaptation affects local rainwater storage and infiltration. In the workflow, this is simplified into storage depth, which refers to the assumed depth of rainwater that a BGI patch can temporarily absorb, retain, or store per unit area. This allows different BGI types to be compared within the same simulation structure and makes the effect of each adaptation readable in relation to flood-depth reduction and building resilience.

However, the challenge of early-stage design simulation is to simplify BGI performance without making it meaningless. A simplified parameter is necessary so that the workflow remains manageable and can be used for scenario comparison, but the parameter still needs to reflect a relevant design difference between BGI types. In this research, storage depth is used because it provides a direct link between BGI adaptation, rainwater volume, flood-depth reduction, and the resulting resilience score.

At the same time, this representation does not capture the full behaviour of BGI systems. Real BGI performance is influenced by temporal processes such as drainage, repeated absorption after emptying, soil saturation, vegetation condition, maintenance, and evapotranspiration. Therefore, the storage-depth values should be understood as simplified performance assumptions for early-stage comparison, rather than exact representations of real BGI behaviour.

Economic Consequences of BGI Selection

In addition to rainwater performance and spatial function, BGI selection also has economic consequences. Different BGI types have different implementation costs, which affects how suitable they are when applied across larger urban areas. In this research, the cost values are derived from a referenced database and used as comparative values within the Dutch context. This allows the adaptation scenarios to be evaluated not only in terms of how much water each BGI type can store, but also in relation to the cost of applying it across the case study area.

This adds another layer to the design decision. A BGI type with higher storage depth is not automatically the most suitable option, and a larger adapted area is not automatically more efficient. For example, bioswales have the highest storage depth among the selected BGI types, ranging from 0.30 to 0.50 m, with an implementation cost of €75/m². In comparison, permeable pavement has a lower storage depth of 0.075 m, but a higher implementation cost of €100/m². However, permeable pavement can maintain hardscape functions such as pedestrian movement, access, courtyard use, or plaza activity, while bioswales require dedicated planted space and cannot replace all urban functions. Therefore, the economic consequence of BGI selection needs to be considered together with rainwater performance and spatial feasibility, especially in dense urban areas where adaptation space is limited.

4.3 | Simulation and Computational Trade-Off

Simplified Simulation for Design Exploration

The simulation workflow developed in this research is intended as an early-stage design-support method, rather than a replacement for detailed hydrodynamic flood modelling. Its purpose is to make rainwater movement, accumulation, and the potential effect of BGI adaptation spatially readable within a computational design environment. This allows different adaptation scenarios to be tested and compared in relation to building flood resilience, while still remaining connected to design decisions such as location, surface type, and adaptation area.

In this workflow, rainwater movement is represented through a particle-based simulation in Grasshopper. Rainfall is translated into particles that move across the terrain surface, allowing runoff direction and accumulation areas to be visualised. For design exploration, this is useful because the output is not only numerical, but also spatial. Designers can observe where water tends to move, where it accumulates, and where adaptation measures may be more effective. This makes the simulation useful not only for calculating flood-depth input, but also for supporting the reasoning behind BGI placement.

However, this approach also requires simplification. The simulation does not aim to represent all hydraulic processes involved in pluvial flooding, such as detailed flow velocity, drainage-network interaction, soil-water dynamics, or temporal water-level changes. Instead, it focuses on producing a comparative and spatially interpretable result that can support scenario-based design exploration.

Particle to Depth Estimation

After the particle simulation is completed, the output still needs to be translated into flood-depth values before it can be used in the building resilience calculation. This is an important step because the resilience score is linked to inundation depth through the depth–damage relationship. Since the simulation produces discrete particle locations rather than a continuous water surface, the accumulated particle volume is first converted into depth values within a grid structure. The resulting depth grid is then smoothed using Gaussian smoothing to create a more continuous inundation surface.

This smoothing process helps reduce the fragmented appearance of the depth output. Without this step, flood depth would only be strongly represented around individual particle locations, making the result less suitable for building-level assessment. By smoothing the calculated depth values across nearby grid cells, the workflow produces a depth surface that can be spatially interpreted and matched with building locations.

At the same time, it should be noted that the Gaussian smoothing operates in the 2D grid domain without accounting for terrain elevation. This means that depth values are redistributed based on spatial proximity alone, rather than following local elevation differences, barriers, or terrain morphology. For the relatively flat terrain of the Rotterdam case study, this has limited impact on the interpretation of the result. Further development would be needed to apply this component to sites with more significant topographic variation, where depth redistribution should respond more directly to elevation change.

Particle Resolution and Computational Performance

Particle resolution is one of the main computational trade-offs in the simulation workflow. As shown in the particle-size comparison in Chapter 3, reducing the particle diameter increases the number of particles needed to represent the same rainfall volume. This can improve the spatial resolution of runoff movement and accumulation, but it also increases the computational demand of the simulation. In the case study, this is relevant because the rainfall event represents a relatively large total water volume across the neighbourhood-scale site.

Computational performance is not only affected by the total number of particles, but also by the terrain mesh resolution and simulation settings. A finer terrain mesh or a higher iteration setting may improve the accuracy of particle movement, but it can also increase simulation time significantly. Therefore, the selected simulation setup reflects a compromise between spatial detail, computational feasibility, and the ability to test multiple adaptation scenarios within Grasshopper.

This trade-off also affects the representation of BGI absorption. Since each particle represents a defined volume of water, particle size determines how much water is classified at once when it interacts with a BGI area. In the current workflow, partial absorption is not yet implemented. This means that when the remaining absorption capacity of a BGI area is smaller than the volume represented by one particle, that particle is classified as runoff rather than being partially absorbed. As a result, the workflow may slightly overestimate remaining runoff in some conditions. This can be understood as a conservative limitation of the current simulation setup, rather than a direct measurement of exact BGI performance.

4.4 | Workflow Adaptibility: Case Study and Beyond

Application to the Case Study

Within the Lijnbaan case study, the workflow shows how different spatial datasets can be combined to support building-scale flood resilience assessment and BGI adaptation testing. The Rotterdam context provides relatively strong open-data availability, including 3DBAG for building geometry, DTM/AHN data for terrain modelling, BGT data for existing surface and vegetation information, and Climate Impact Atlas data for the rainfall and flood-depth reference. These datasets made it possible to construct a simulation environment that connects terrain, building attributes, rainfall input, BGI parameters, and resilience scoring within one workflow.

At the same time, the case study also shows that data availability alone is not enough. The datasets still needed to be cleaned, aligned, converted, and simplified before they could be used in Grasshopper. For example, the terrain data had to be clipped, filled, imported, and converted into a mesh; the 3DBAG building geometry had to be matched with additional building-class information; and the BGT layers had to be filtered and prepared as spatial reference for existing vegetation and hardscape conditions. This means that the workflow is not only a simulation process, but also a data-preparation process.

The case study demonstrates that this structure can support scenario-based comparison. By keeping the same terrain, rainfall event, building data, and resilience calculation constant, different BGI adaptation scenarios could be tested under comparable conditions. This allowed the results to show not only whether a scenario improved resilience scores, but also where the improvement occurred and how it related to BGI placement, runoff pathways, and local building vulnerability. Therefore, within the case study, the workflow was useful for connecting spatial design decisions with building-level resilience outcomes.

However, the application also reveals practical limitations. The workflow depends strongly on the quality and completeness of the input data. Missing or simplified attributes, such as building class or basement presence, need to be estimated or categorised before they can be used in the resilience calculation. In addition, several steps still require manual checking, especially during terrain preparation, spatial alignment, and scenario modelling. This makes the workflow suitable for structured design exploration, but it also means that careful data handling remains essential for producing reliable and interpretable results.

Another important part of the case study application is the data structure used inside Grasshopper. Since the workflow combines building geometry, building ID, elevation values, building class, basement assumption, inundation depth, and resilience score, these values need to remain connected to the correct building object throughout the process. In the case study, this is mainly handled through a parallel-list structure, where each index refers to the same building across different attribute lists. This allows the simulation output and building attributes to be matched consistently, so that the flood-depth result can be translated into building-level resilience scores.

However, this also means that the workflow depends on careful data handling. When data is imported from different sources, such as 3DBAG, building-class tables, terrain data, and simulation outputs, the matching process needs to be controlled. For example, building-class information is imported separately and matched to the 3DBAG building geometry using the building ID. If the list order or ID matching is incorrect, the wrong attribute can be assigned to a building. Therefore, the data structure is not only a technical organisation step, but also an important condition for making the case study application reliable.

Application to Other Location Context

Although the workflow was developed through the Lijnbaan case study, its general structure can potentially be applied to other urban contexts. The depth–damage curve used in the workflow is not based on a single local source only, but includes references from different regional contexts, including Europe, Asia, and America. This makes the damage-assessment component relatively adaptable, because the curve can be reviewed, adjusted, or replaced depending on the available local reference.

At the same time, this also highlights a limitation of the current case study. Even within the Dutch context, some vulnerability and recovery-related parameters, such as impeding time and restoration time, are derived from broader or non-Dutch references, including HAZUS-based assumptions. Therefore, if the workflow is intended to produce a more location-specific assessment, these values would need to be adjusted using local empirical data, local building recovery records, or context-specific expert assumptions.

The main challenge for applying the workflow to another location is therefore not only the resilience formula itself, but also the availability and suitability of input data. The Lijnbaan case study benefits from the Dutch open-data environment, where building geometry, terrain elevation, surface information, and climate-related datasets are relatively accessible. In other regions, comparable datasets may be less complete, less detailed, or not openly available. As a result, applying the workflow elsewhere would require careful review of local data availability, damage references, BGI performance values, and cost data before the results can be interpreted meaningfully.

4.5 | From Results to Insights

Interpreting Scenario Results

The scenario results are useful for comparing the no-BGI condition, Existing BGI condition, and proposed adaptation scenarios, but the resilience score alone does not fully explain the spatial reasons behind the change. Therefore, the score needs to be read together with the inundation-depth maps, runoff movement, BGI location, and BGI utilisation.

This becomes visible in the case study results. Some buildings show only small changes in resilience score, but the spatial maps still reveal where adaptation affects local runoff or reduces nearby accumulation. At the same time, some BGI areas show limited influence not necessarily because their storage value is low, but because they are not positioned where runoff is actively passing through or accumulating. This means that the scenario comparison is not only about measuring improvement, but also about understanding why improvement occurs in certain locations and not in others.

For this reason, additional checks such as runoff-path analysis and BGI utilisation are important. The runoff-path check shows whether water actually reaches a certain adaptation area, while the utilisation check shows whether the storage capacity of that area is being used. These outputs help avoid interpreting the results only from total BGI area or storage depth. A larger adaptation area may still have limited effect if it does not receive much runoff, while a smaller area may be more relevant if it is located along an active runoff path.

Therefore, the main value of the scenario results lies in supporting design interpretation. The outputs help identify which adaptations produce local improvement, which buildings remain vulnerable, and which BGI locations may be less effective under the tested rainfall condition. In this sense, the workflow does not only produce a final score, but also provides spatial evidence to support further reasoning about BGI placement and configuration.

Insights for BGI Configuration

The scenario results also show that BGI effectiveness depends strongly on configuration. In this research, configuration is not only understood as the type of BGI selected, but also its location, size, spatial function, and position in relation to runoff movement. This is important because the same BGI type can perform differently depending on where it is placed within the site.

In the case study, the most meaningful improvements occurred when BGI adaptations were located where runoff was actively passing through or accumulating. For example, the enlargement of Urban Park 1 continued to improve nearby building resilience because the runoff-path check showed that water still reached this area. This suggests that the adaptation was not only larger, but also positioned in a relevant part of the water movement pattern. In contrast, some other BGI areas showed more limited influence even when they covered a larger surface, because they did not receive as much runoff under the tested rainfall condition. This means that BGI configuration should not be evaluated only by total area or storage capacity. A larger adapted area does not automatically create a larger resilience improvement, and a higher-storage BGI type is not automatically the most suitable option. The result needs to be interpreted through the relationship between water movement, available space, storage capacity, and building vulnerability. For example, bioswales can provide higher storage capacity, but they require dedicated planted space. Permeable pavement has lower storage capacity, but it can be applied to surfaces that still need to function as sidewalks, courtyards, access routes, or plazas.

The scenario comparison also shows the importance of placing BGI along runoff pathways, not only at final accumulation areas. In Scenario 2, the permeable pavement along Karel Doormanstraat showed that adaptation can still contribute when it intercepts runoff before water reaches more vulnerable or lower-lying areas. This supports the idea that BGI placement should be based on how water moves through the site, rather than only on where open space is available.

Therefore, the main insight for BGI configuration is that adaptation needs to be spatially strategic. The workflow helps show which BGI areas are actually receiving runoff, whether their storage capacity is being used, and how this affects nearby building resilience. This makes it possible to compare BGI options not only as technical components, but as spatial design decisions that balance rainwater performance, urban function, and implementation cost.

Workflow Usability and Result Communication

The workflow is useful for design exploration because the simulation can be checked spatially while the model is being developed. In Rhino and Grasshopper, the terrain, buildings, runoff movement, BGI adaptations, and resilience results can be viewed together in the same modelling environment. This makes it possible to test different scenarios and directly observe how changes in BGI placement or type affect the surrounding area. For the design process itself, this is useful because the workflow does not only produce numbers, but also gives spatial feedback that can support decision-making.

The difficulty appears more clearly when the results need to be translated into presentation or report figures. Grasshopper and Rhino can show the outputs during the modelling process, but they do not automatically produce clear visual communication elements such as legends, consistent colour scales, labels, figure layout, or scenario comparison diagrams. As a result, the outputs still need to be refined before they can be easily understood by others.

One way to address this is by exporting the simulation results from Grasshopper into CSV files and continuing the post-processing in Python. This allows the numerical outputs, such as building resilience scores, inundation depth, BGI absorption, and scenario comparison values, to be processed more flexibly. Python can then be used to generate clearer graphs, organise comparison tables, and produce more consistent visual outputs than what is easily achievable directly in Grasshopper and Rhino.

This is important because the design insight from the workflow depends strongly on visual interpretation. The resilience score helps compare scenarios, but the maps and diagrams explain where the change happens and why. For example, inundation-depth maps, runoff-path checks, BGI utilisation diagrams, and building resilience maps all need to be visually readable to support the interpretation of the result. Therefore, result communication becomes a separate step after the simulation. This does not limit the workflow as a design-exploration tool, but it shows that clearer export, post-processing, and visualisation procedures are needed to make the results more accessible for evaluation and presentation.

05
Conclusion

Summary of Findings

Recomendation

Future Development

Reflection

5.1 | Summary of Findings

As cities continue to densify, pluvial flooding becomes an increasingly relevant urban hazard. Its impacts vary across different urban receptors, including buildings, whose vulnerability depends on factors such as building function and recovery capacity.

Blue-Green Infrastructure offers a spatial adaptation approach that combines rainwater regulation with other urban functions. This is especially relevant in dense urban areas, where available space is limited and adaptation measures need to provide multiple benefits. Reflecting the idea of **Grounded Resilience**, this research examines how building flood-resilience assessment can ground the spatial design of ground-based BGI adaptation strategies by identifying which configurations improve resilience scores to support more targeted adaptation decisions.

To address this, the research develops a Grasshopper-based rainwater simulation workflow that links ground-based BGI adaptation with building-level flood resilience assessment. By keeping the same rainfall, terrain, and building conditions while changing the BGI configuration, the workflow allows adaptation scenarios to be compared consistently. It also allows runoff behaviour to be observed and used to interpret why certain BGI locations are more effective than others. The comparison shows how different BGI configurations influence runoff absorption, flood-depth reduction, and resilience-score changes across the neighbourhood.

The following section summarises the findings by directly answering the research sub-questions.

Building Resilience

How can pluvial flood resilience be defined and quantified at the building scale?

Building-scale pluvial flood resilience is defined in this research as the ability of a building to maintain or recover its function after exposure to flood depth. In the workflow, this is quantified through a resilience score derived from inundation depth, building class, depth–damage relationship, basement assumption, and restoration-related parameters. The findings show that this scoring structure is useful for comparing relative changes between scenarios, but it remains limited for pluvial flood resilience assessment because the score is strongly influenced by physical damage estimated from inundation depth. This limitation is particularly relevant for pluvial flooding, which is often characterised by shallow and localised ponding. In such cases, small changes in flood depth may not produce large changes in physical damage-based resilience scores, even though shallow flooding can still disrupt access, basement use, technical systems, and short-term building operation.

How can pluvial flood impact be simulated in Grasshopper to support building resilience scoring?

Because the resilience assessment is linked to a depth–damage relationship, the simulation focuses on estimating inundation depth as the main flood-impact input. This is done through a particle-based rainwater simulation in Grasshopper using Kangaroo, where particle accumulation is translated into flood-depth values and the resulting depth grid is smoothed using Gaussian smoothing. The findings show that this method can translate particle-based runoff accumulation into an approximate flood-depth input for building resilience scoring.

However, the depth-estimation method remains simplified. The main spatial spreading of runoff is already handled by the particle-based simulation, while Gaussian smoothing is only applied afterward to reduce the discretised appearance of the depth grid. Because this smoothing operates in the 2D grid domain and does not account for terrain elevation during smoothing, the method works more reasonably for the relatively flat site, but would need further development for sites with stronger topographic variation.

> “Building flood resilience can be assessed by linking simulated inundation depth with building vulnerability, but the resulting score is more useful for relative scenario comparison than exact damage prediction. The particle-based simulation provides the flood-depth input needed for this assessment, while also making the simplified nature of depth estimation clear.”

Blue Green Infrastructure

What defines the selection and rainwater regulation performance of BGI types for flood adaptation?

In this research, urban parks, bioswales, and permeable pavements are selected because they represent different ground-based adaptation types that can be applied in dense urban areas. Rainwater performance is represented through storage depth, which refers to the assumed depth of rainwater that a BGI patch can infiltrate and absorb per unit area. The findings show that BGI selection is a multidimensional decision and cannot be based on storage performance alone. Bioswales have higher storage depth and lower cost, but require dedicated planted space. Permeable pavement has lower storage depth, but can maintain hardscape functions such as pedestrian movement, plazas, or circulation areas. Therefore, BGI suitability depends on how rainwater performance, urban function, cost, and spatial feasibility are balanced. This adds nuance to the design process, because the most suitable BGI option is not always the one with the highest storage capacity, but the one that best fits both the hydrological need and how the designer intends the space to be used.

How can the selected BGI types be modelled in Grasshopper to evaluate their impact on building flood resilience?

In the workflow, each BGI area is assigned a type, area, storage depth, and cost parameter. This allows the workflow to calculate absorbed volume, remaining capacity, utilisation rate, and indicative implementation cost. The findings show that this parameter-based method is useful for early-stage scenario comparison, because BGI type, size, and location can be changed while keeping the rainfall, terrain, and building conditions constant. In addition, the recorded runoff movement paths help guide the interpretation of BGI placement by showing not only where water accumulates, but also where runoff moves across the site before reaching those accumulation areas. This is important because adaptation may not always be possible directly at the ponding location, especially in dense urban areas.

> “BGI placement is multidimensional: it depends not only on where water ponds, but also on where runoff can be intercepted before reaching ponding areas, what spatial quality the area needs to support, and which adaptation type is feasible there.”

Application to the Neighbourhood Scale

How can the simulation environment be applied to design and compare BGI strategies at the neighbourhood scale?

The workflow can be applied at the neighbourhood scale by integrating spatial data, building attributes, rainfall input, and BGI adaptation scenarios into one consistent Grasshopper environment. Its transferability depends on the availability and suitability of local data and parameters.

In the Lijnbaan case study, the workflow is applied by integrating 3DBAG building geometry, terrain data, BGT spatial context, building-class data, rainfall input, and selected BGI adaptation scenarios. These datasets are processed, aligned, and translated into Grasshopper, where rainwater simulation, BGI performance calculation, flood-depth estimation, and building resilience assessment are connected. The application shows that different BGI strategies can be compared by keeping the same rainfall condition, terrain model, and building dataset while changing the adaptation configuration.

The findings also suggest that the workflow has the potential to be transferred to other urban contexts. Its structure is not tied specifically to the Lijnbaan site, as the main input data can be replaced according to the selected study area. In addition, depth–damage relationships are available for different regions, allowing the resilience assessment component to be adapted to other contexts. However, reliable application depends strongly on the availability and suitability of local input data, including building geometry, terrain elevation, rainfall data, BGI performance values, damage curves, recovery parameters, and cost data. Therefore, data preparation is not only a technical preprocessing step, but an essential condition for reliable and transferable neighbourhood-scale application.

What insights can be gained from the simulation environment regarding the impact of BGI strategies on building flood resilience?

The scenario comparison shows that BGI adaptation can improve resilience outcomes, but the effect is spatially uneven. The improvement depends on the combination of BGI type, storage depth, surface coverage, and placement in relation to runoff pathways and vulnerable buildings. The results suggest that BGI effectiveness is not determined by adapted area or storage depth alone, but by how the adaptation is positioned within the site's water movement pattern. At the same time, the workflow's usability is affected by simulation resolution, particle size, computational load, terrain modification, and result communication. Rhino and Grasshopper are useful for spatial design exploration, but presentation figures such as legends, colour scales, labels, and scenario-comparison diagrams often require post-processing. Therefore, the workflow is useful as a comparative design-support environment, but its outputs need to be carefully interpreted and communicated.

> "The workflow can be applied to compare BGI strategies at the neighbourhood scale by integrating spatial datasets into one consistent simulation environment. Its insights show that BGI impact depends not only on type and storage capacity, but also on data reliability, spatial placement, runoff pathways, and the buildings affected."

5.2 | Recommendation

Use a smaller study area when a more refined simulation setting is needed

The workflow can be applied at neighbourhood scale, but the level of simulation detail depends on the user's objective and computational capacity. If the aim is to observe more refined runoff behaviour, a smaller study area may be more suitable because it allows smaller particle diameters, finer terrain meshes, or higher simulation settings without making the workflow too computationally heavy. However, this decision depends on the purpose of the analysis: a larger area may be useful for broader scenario comparison, while a smaller area may be better for more detailed local design exploration.

Improve result visualisation through post-processing outside Grasshopper

Rhino and Grasshopper are sufficient for design exploration because the impact of BGI adaptation can be checked directly through colours, geometry, and spatial feedback. However, they are less suitable for producing clear presentation outputs, especially for legends, colour scales, labels, BGI utilisation percentages, and scenario-comparison diagrams. A practical improvement would be to export simulation results as CSV files and continue the post-processing in Python, so that graphs, percentage summaries, and presentation-ready figures can be generated more consistently.

5.2 | Future Development

Incorporate more pluvial-specific damage and functionality-loss relationships

Future development should incorporate more pluvial-specific damage and functionality-loss relationships, especially for shallow urban flooding. This would allow the workflow to represent not only physical damage, but also disruptions to access, basement use, technical systems, ground-floor activity, and short-term building operation. These relationships could be adopted from more specific empirical studies, local recovery data, or expert-based adjustment factors when available.

Incorporate the temporal dimension of flooding and BGI performance

A stronger temporal representation of both flood behaviour and BGI performance could further improve the workflow if it is developed for more detailed assessment beyond the early design stage. In the current workflow, BGI performance is mainly represented through storage depth during a selected rainfall event. This simplification is suitable for early-stage scenario comparison, where the aim is to compare the relative influence of different BGI configurations rather than to reproduce detailed hydrological processes. However, real BGI systems respond over time through processes such as repeated absorption after emptying and evapotranspiration. Including these temporal processes would allow the workflow to better represent how BGI performance changes during and after rainfall, especially for longer events or repeated storm conditions.

Test the workflow under more varied site and rainfall conditions

The workflow should also be tested under more varied conditions to better understand its robustness and transferability. In the current research, the workflow is demonstrated through one relatively flat case-study area and one selected extreme rainfall scenario. Further testing could include sites with different terrain slopes and rainfall intensities. This would help evaluate whether the workflow remains reliable when applied to more complex urban contexts. It would also support a more detailed validation of the flood-depth distribution by comparing the simulated results with local observations, high-resolution hydraulic model outputs, or more detailed flood-depth datasets when available.

5.4 | Reflection

I began this thesis from a fascination with water: not just in its literal form as a natural element, but also as something that shapes experience, atmosphere, and spatial quality. However, working with water also means working with complexity. Water does not stay still, and its behaviour is influenced by many spatial, environmental, and technical conditions. In translating water into a design-support workflow, I found that it requires not only calculation, but also careful interpretation.

To connect the simulated water behaviour to the receiving building receptor, my thesis operates within a data-driven framework. One important reflection from this research is that data-driven design is not about just achieving the best numerical result. It is also about understanding the implications and consequences of design decisions. In the end, design is not determined by numbers alone, but also by how designers intend a space to function, be experienced, and respond to its context. This is also why the workflow does not reduce the qualitative assessment into one single score. Design choices are multidimensional, and different decisions may lead to different spatial, environmental, and resilience-related consequences. Therefore, the role of the tool is not to prescribe one 'best' solution, but to help designers reflect on multiple possible outcomes.

BGI performance in relation to flooding is also more complex than infiltration alone. It can influence runoff velocity, flow direction, temporary storage, water quality, microclimate, ecological value, and spatial experience. However, because this research focuses on early-stage design assessment, these processes are simplified to make the workflow more accessible and operational within Grasshopper. One key lesson from developing the workflow is that simplification turned out to be more difficult than I initially expected. The challenge lies in finding a balance between simplification and meaning, so that the results can still support design decision-making.

This thesis also made me reflect on the time required to work with data in design. As designers, we often want our decisions to be more data-driven, but working with data also takes time: to collect, clean, process, interpret, and question it. This makes me question whether designers always have the time and resources to work in such a data-intensive way. At the same time, this process reminded me that a well-thought-out design does take time.

In that sense, this thesis is not only about developing a computational workflow, but also about learning how far a designer-friendly tool can go in representing a complex environmental issue. It does not replace detailed hydrological modelling, and it is not intended to. Instead, it offers a way for designers to engage with water-related consequences earlier in the design process, when spatial decisions are still open to change. For me this becomes the main value of the workflow: not to give final answers, but to make the consequences of design choices more visible, discussable, and easier to reflect on.

Reference

Acosta, F., & Haroon, S. (2021). Memorial Parking Trees: Resilient Modular Design with Nature-Based Solutions in Vulnerable Urban Areas. Land, 10(3), 298. https://doi.org/10.3390/land10030298

Ahern, J. (2011). From fail-safe to safe-to-fail: Sustainability and resilience in the new urban world. Landscape and Urban Planning, 100(4), 341–343. https://doi.org/10.1016/j.landurbplan.2011.02.021

Al-Ghobari, H., Dewidar, A., & Alataway, A. (2020). Estimation of Surface Water Runoff for a Semi-Arid Area Using RS and GIS-Based SCS-CN Method. Water, 12(7), 1924. https://doi.org/10.3390/w12071924

Andriessen, L., Agugiaro, G., Borgers, A., & Pauwels, P. (2024). Semantic 3D city models as support for urban flood resilience: Experiences from Rotterdam. ISPRS Annals of the Photogrammetry, Remote Sensing and Spatial Information Sciences, X-4/W4-2024, 5–12. https://doi.org/10.5194/isprs-annals-X-4-W4-2024-5-2024

Armson, D., Stringer, P., & Ennos, A. R. (2013). The effect of street trees and amenity grass on urban surface water runoff in Manchester, UK. Urban Forestry & Urban Greening, 12(3), 282–286. https://doi.org/10.1016/j.ufug.2013.04.001

Barsley, E. (2020). Retrofitting for Flood Resilience: A Guide to Building & Community Design (E. Barsley, Ed.; 1st ed.). RIBA Publishing. https://doi.org/10.4324/9780429347986

Bertilsson, L., Wiklund, K., De Moura Tebaldi, I., Rezende, O. M., Veról, A. P., & Miguez, M. G. (2019). Urban flood resilience – A multi-criteria index to integrate flood resilience into urban planning. Journal of Hydrology, 573, 970–982. https://doi.org/10.1016/j.jhydrol.2018.06.052

Bianchi, S., Kim, K., Matteoni, M., Koniari, A. M., Koning, K., Costache, R.-D., Ciobotaru, N., Luna-Navarro, A., Peng, Z., Ciurlanti, J., Shahriari, H., Mittal, D., Stavridou, E., Silva, A., Petrini, F., Palmieri, M., Pampanin, S., & Overend, M. (2025). Resilience Readiness Levels for Buildings: Establishing Multi-Hazard Resilience Metrics and Rating Systems. SSRN. https://doi.org/10.2139/ssrn.5177406

Bona, S., Silva-Afonso, A., Gomes, R., Matos, R., & Rodrigues, F. (2023). Nature-Based Solutions in Urban Areas: A European Analysis. Applied Sciences, 13(1), 168. https://doi.org/10.3390/app13010168

Boogaard, F., Bruins, G., & Wentink, R. (2006). Wadi's: Aanbevelingen voor ontwerp, aanleg en beheer: gebaseerd op zes jaar onderzoek van de wadi's in Enschede gecombineerd met overige binnen- en buitenlandse ervaringen. Stichting RIONED.

Brolsma, R. (2024, January 22). Tables construction and maintenance cost (Dutch prices). Deltares Public Wiki, Climate Resilient City Tool. https://publicwiki.deltares.nl/spaces/AST/pages/289702255/Tables+construction+and+maintenance+cost+Dutch+prices

Bruneau, M., Chang, S. E., Eguchi, R. T., Lee, G. C., O'Rourke, T. D., Reinhorn, A. M., Shinozuka, M., Tierney, K., Wallace, W. A., & Von Winterfeldt, D. (2003). A Framework to Quantitatively Assess and Enhance the Seismic Resilience of Communities. Earthquake Spectra, 19(4), 733–752. https://doi.org/10.1193/1.1623497

Burns, M. J., Fletcher, T. D., Walsh, C. J., Ladson, A. R., & Hatt, B. E. (2012). Hydrologic shortcomings of conventional urban stormwater management and opportunities for reform. Landscape and Urban Planning, 105(3), 230–240. https://doi.org/10.1016/j.landurbplan.2011.12.012

Chen, Y., Samuelson, H. W., & Tong, Z. (2016). Integrated design workflow and a new tool for urban rainwater management. Journal of Environmental Management, 180, 45–51. https://doi.org/10.1016/j.jenvman.2016.04.059

Church, S. P. (2015). Exploring Green Streets and rain gardens as instances of small scale nature and environmental learning tools. Landscape and Urban Planning, 134, 229–240. https://doi.org/10.1016/j.landurbplan.2014.10.021

Climate Impact Atlas. (2026). Viewer. Climate Adaptation Services. Retrieved June 1, 2026, from https://www.klimaateffectatlas.nl/en/viewer

Crowe, S., Dawson, S., & AlWaer, H. (2025). Placemaking and Blue Green Infrastructure for Liveable, Resilient Places: Insights from Dundee, Scotland. International Journal of Water Governance, 12. https://doi.org/10.59490/ijwg.12.2025.8031

De Bruijn, K., Wagenaar, D., Slager, K., De Bel, M., & Burzel, A. (2015). Updated and improved method for flood damage assessment: SSM2015 (version 2). Deltares.

Eisenberg, B., & Polcher, V. (2019). Nature Based Solutions -Technical Handbook. https://doi.org/10.13140/RG.2.2.24970.54726

Ekka, S. A., Rujner, H., Leonhardt, G., Blecken, G.-T., Viklander, M., & Hunt, W. F. (2021). Next generation swale design for stormwater runoff treatment: A comprehensive approach. Journal of Environmental Management, 279, 111756. https://doi.org/10.1016/j.jenvman.2020.111756

Fletcher, T. D., Shuster, W., Hunt, W. F., Ashley, R., Butler, D., Arthur, S., Trowsdale, S., Barraud, S., Semadeni-Davies, A., Bertrand-Krajewski, J.-L., Mikkelsen, P. S., Rivard, G., Uhl, M., Dagenais, D., & Viklander, M. (2015). SUDS, LID, BMPs, WSUD and more – The evolution and application of terminology surrounding urban drainage. Urban Water Journal, 12(7), 525–542. https://doi.org/10.1080/1573062X.2014.916314

Gonzalez, R. C., & Woods, R. E. (2018). Digital image processing. Pearson.

Hadimlioglu, I. A., King, S. A., & Starek, M. J. (2020). FloodSim: Flood Simulation and Visualization Framework Using Position-Based Fluids. ISPRS International Journal of Geo-Information, 9(3), 163. https://doi.org/10.3390/ijgi9030163

Hadimlioglu, I., & King, S. (2019). Visualization of Flooding Using Adaptive Spatial Resolution. ISPRS International Journal of Geo-Information, 8(5), 204. https://doi.org/10.3390/ijgi8050204

Federal Emergency Management Agency. (2025). Hazus 7.0 flood model technical manual. U.S. Department of Homeland Security.

Huizinga, J., Moel, H. de, & Szewczyk, W. (2017). Global flood depth-damage functions. Methodology and the database with guidelines. Publications Office. https://doi.org/10.2760/16510

Hogan, J., Almufti, I., & Ackerson, M. (2023). REDi™: Resilience-based design guidelines for floods. Arup.

Intergovernmental Panel On Climate Change (Ipcc). (2023). Climate Change 2022 – Impacts, Adaptation and Vulnerability: Working Group II Contribution to the Sixth Assessment Report of the Intergovernmental Panel on Climate Change (1st ed.). Cambridge University Press. https://doi.org/10.1017/9781009325844

Jia, J., Zhang, K., Liu, H., & Zlatanova, S. (2024). A framework supporting green stormwater management for urban designers. Journal of Environmental Management, 370, 122650. https://doi.org/10.1016/j.jenvman.2024.122650

Jia, J., Zlatanova, S., Zhang, K., & Liu, H. (2022). INTEGRATED STORMWATER ANALYSIS MODEL TO SUPPORT SUSTAINABLE URBAN GREEN SPACE DESIGN. ISPRS Annals of the Photogrammetry, Remote Sensing and Spatial Information Sciences, X-4/W2-2022, 153–160. https://doi.org/10.5194/isprs-annals-X-4-W2-2022-153-2022

Jørgensen, G., Fryd, O., Lund, A. A., Andersen, P. S., & Herslund, L. (2022). Nature-based climate adaptation projects, their governance and transitional potential-cases from Copenhagen. Frontiers in Sustainable Cities, 4, 906960. https://doi.org/10.3389/frsc.2022.906960

Joshi, P. K., Rao, K. S., Bhadouria, R., Tripathi, S., & Singh, R. (Eds.). (2024). Blue-Green Infrastructure for Sustainable Urban Settlements: Implications for Developing Countries Under Climate Change. Springer Nature Switzerland. https://doi.org/10.1007/978-3-031-62293-9

Kondratenko, J., Boogaard, F. C., Rubulis, J., & Maļinovskis, K. (2024). Spatial and Temporal Variability in Bioswale Infiltration Rate Observed during Full-Scale Infiltration Tests: Case Study in Riga Latvia. Water, 16(16), 2219. https://doi.org/10.3390/w16162219

Kuruppu, U., Rahman, A., & Rahman, M. A. (2019). Permeable pavement as a stormwater best management practice: A review and discussion. Environmental Earth Sciences, 78(10), 327. https://doi.org/10.1007/s12665-019-8312-2

Lemieux, C., Gar, S. L., Bichai, F., Ciari, F., & Boisjoly, G. (2025). Green stormwater infrastructure and active mobility: A case study investigating the effects of bioswales on individuals' perceptions. Travel Behaviour and Society, 41, 101042. https://doi.org/10.1016/j.tbs.2025.101042

Liu, W., Feng, Q., Engel, B. A., Yu, T., Zhang, X., & Qian, Y. (2023). A probabilistic assessment of urban flood risk and impacts of future climate change. Journal of Hydrology, 618, 129267. https://doi.org/10.1016/j.jhydrol.2023.129267

Luo, J., Lei, Z., & Cao, L. (2020). VISUAL SIMULATION METHOD OF RUNOFF IN LANDSCAPE SPACE BASED ON UAV TILT PHOTOGRAPHY. 363–373. https://doi.org/10.2495/SC200301

Morschek, J., König, R., & Schneider, S. (2019). An Integrated Urban Planning and Simulation Method to Enforce Spatial Resilience Towards Flooding Hazards.

P, A., N.R, C., & Firoz C, M. (2024). A framework for urban pluvial flood resilient spatial planning through blue-green infrastructure. International Journal of Disaster Risk Reduction, 103, 104342. https://doi.org/10.1016/j.ijdrr.2024.104342

Rotterdams WeerWoord. (2023). Programme framework 2030. Municipality of Rotterdam. https://rotterdamsweerwoord.nl/content/uploads/2023/03/Programmakader-Rotterdams-Weerwoord-2030-EN.pdf

Sayers, P. (2013). Flood risks management: A strategic approach. Asian Development Bank.

Science for Environment Policy (2021) The solution is in nature. Future Brief 24. Brief produced for the European Commission DG Environment. Bristol: Science Communication Unit, UWE Bristol.

Son, J., & Kwon, T. (2022). Evaluation and Improvement Measures of the Runoff Coefficient of Urban Parks for Sustainable Water Balance. Land, 11(7), 1098. https://doi.org/10.3390/land11071098

Soulis, K. X. (2021). Soil Conservation Service Curve Number (SCS-CN) Method: Current Applications, Remaining Challenges, and Future Perspectives. Water, 13(2), 192. https://doi.org/10.3390/w13020192

Tingsanchali, T. (2012). Urban flood disaster management. Procedia Engineering, 32, 25–37. https://doi.org/10.1016/j.proeng.2012.01.1233

United Nations, Department of Economic and Social Affairs, Population Division. (2025). World Urbanization Prospects 2025. United Nations Population Division

United Nations Office for Disaster Risk Reduction. (2017). Disaster resilience scorecard for cities: Detailed level assessment. UNDRR. https://mcr2030.undrr.org/disaster-resilience-scorecard-cities

United Nations Office for Disaster Risk Reduction. (2024). Forensic insights for future resilience: Learning from past disasters (GAR Special Report 2024). United Nations.

Zhu, Y., Burlando, P., Tan, P. Y., Blagojevic, J., & Fatichi, S. (2024). Investigating the influence of urban morphology on pluvial flooding: Insights from urban catchments in England (UK). Science of The Total Environment, 953, 176139. https://doi.org/10.1016/j.scitotenv.2024.176139

Watson, D., & Adams, M. (2011). Design for flooding: Architecture, landscape, and urban design for resilience to flooding and climate change. John Wiley & Sons.

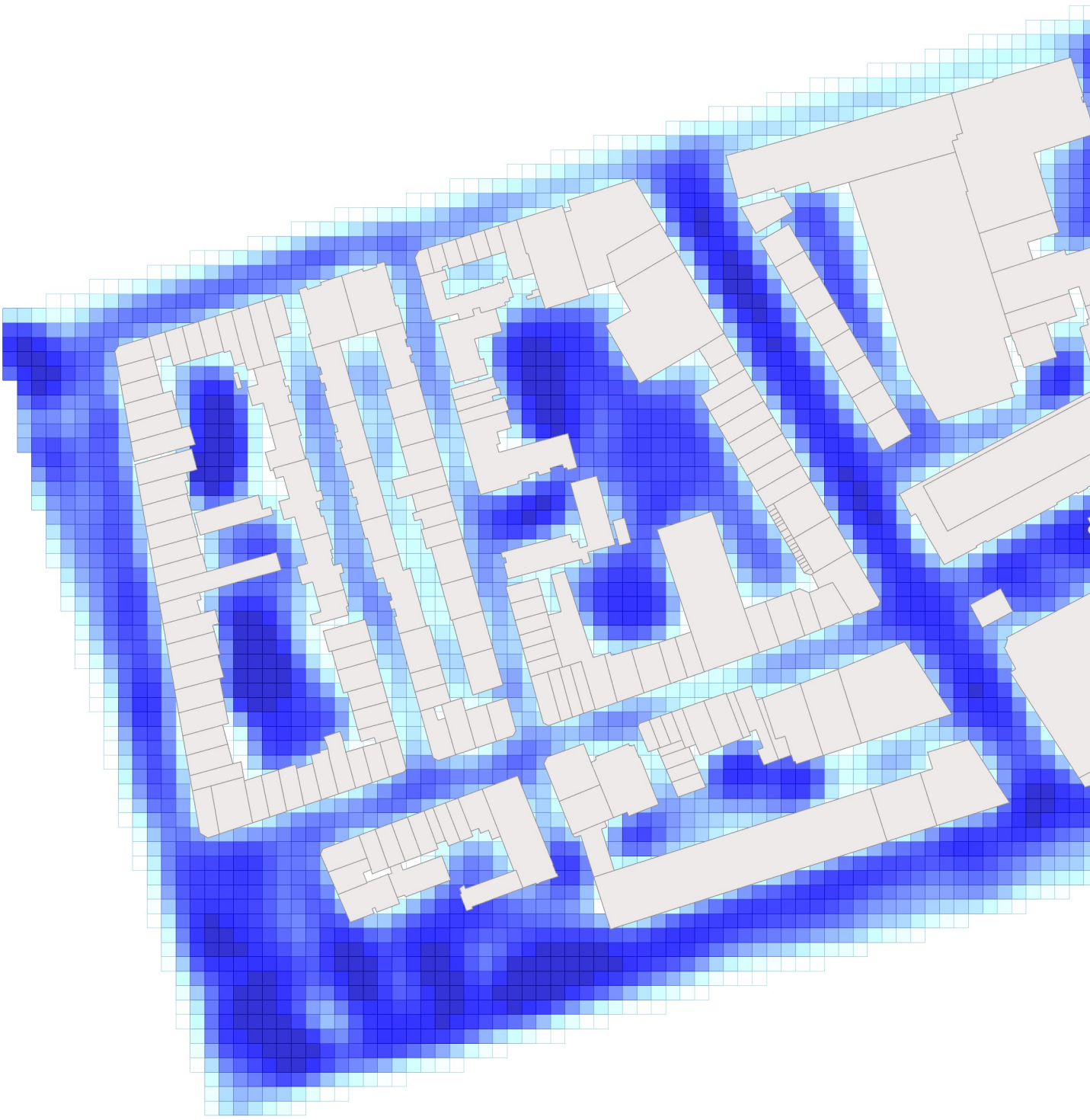

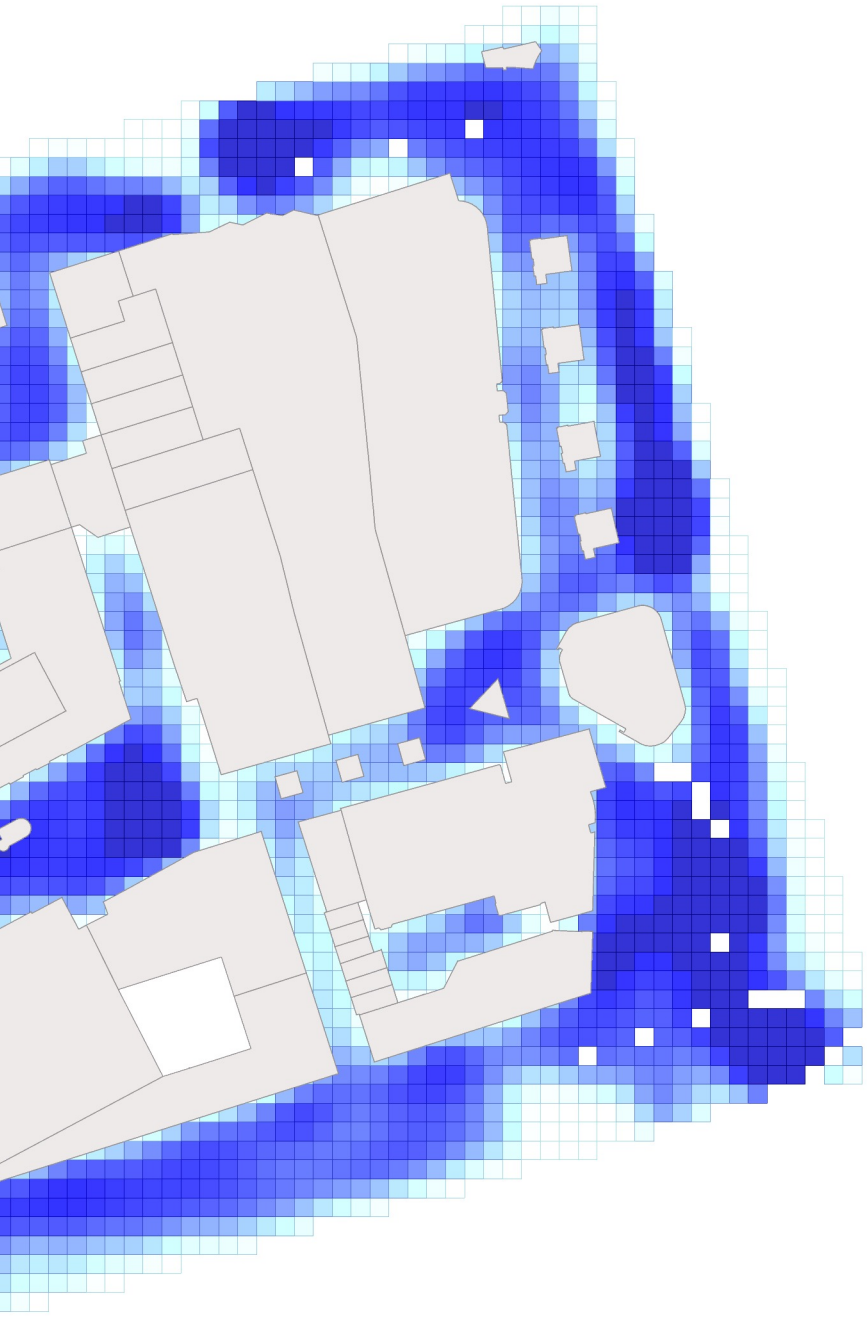

FLOOD DEPTH MAP

Area: Lijnbaan, Rotterdam

Condition: No BGI Adaptation

LEGENDS

0 20 40 80 120 m

Depth Distribution

> 0.3 m

< 0.05 m

North

Grounded Resilience

MSc Architecture, Urbanism, and Building Sciences

Vadya Dzauqiah | 6184030

APPENDIX

FM 01


7
6
5
4
3
2
1
A
B
C
D
E
Karel Doormanstraat

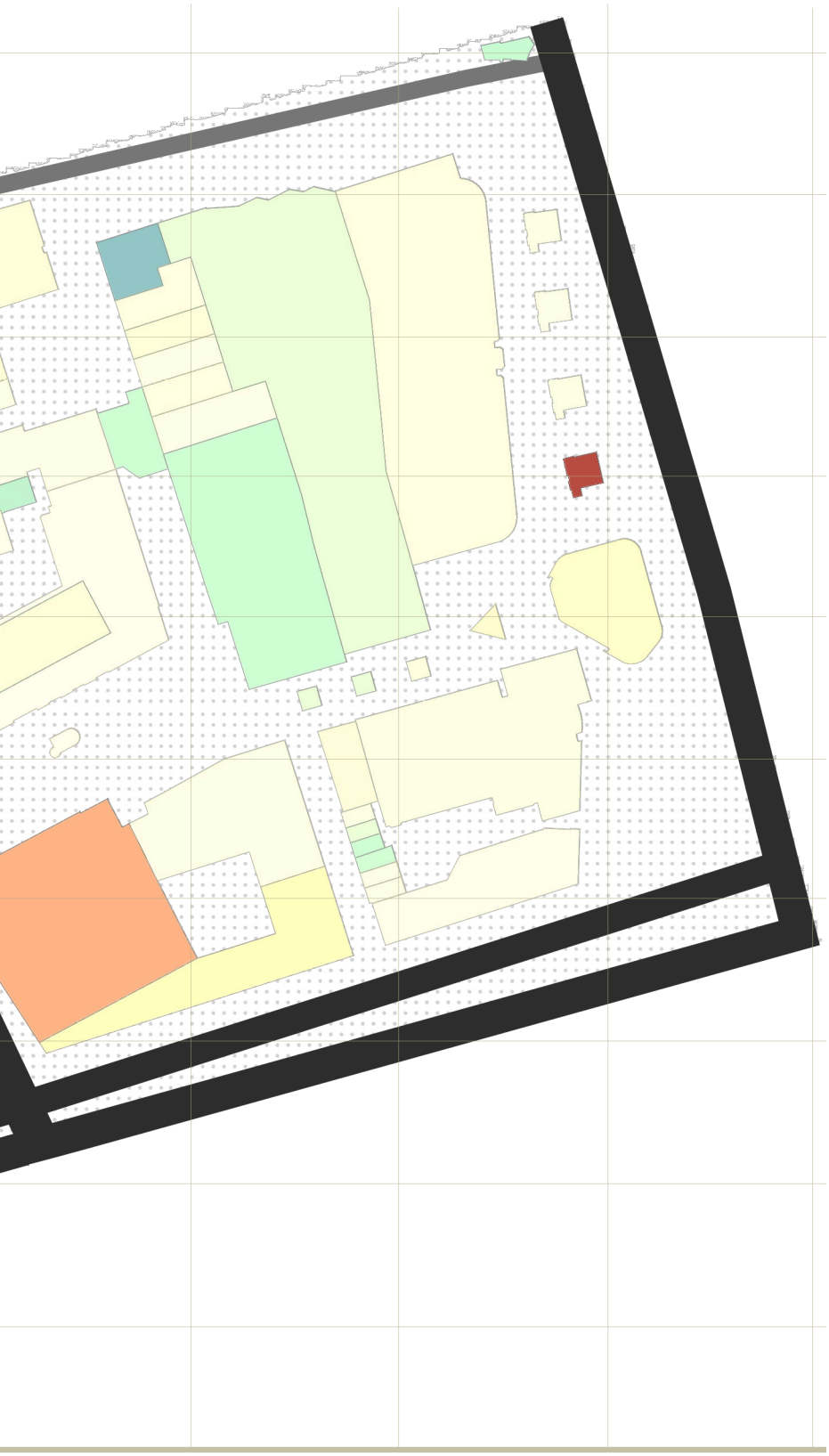

F G H

RESILIENCE SCORE MAP

Area: Lijnbaan, Rotterdam

Condition: No BGI Adaptation

LEGENDS

0 20 40 80 120 m

Score Distribution

> 0.94

< 0.82

North

Grounded Resilience

MSc Architecture, Urbanism, and Building Sciences

Vadya Dzauqiah | 6184030

APPENDIX

RS 01

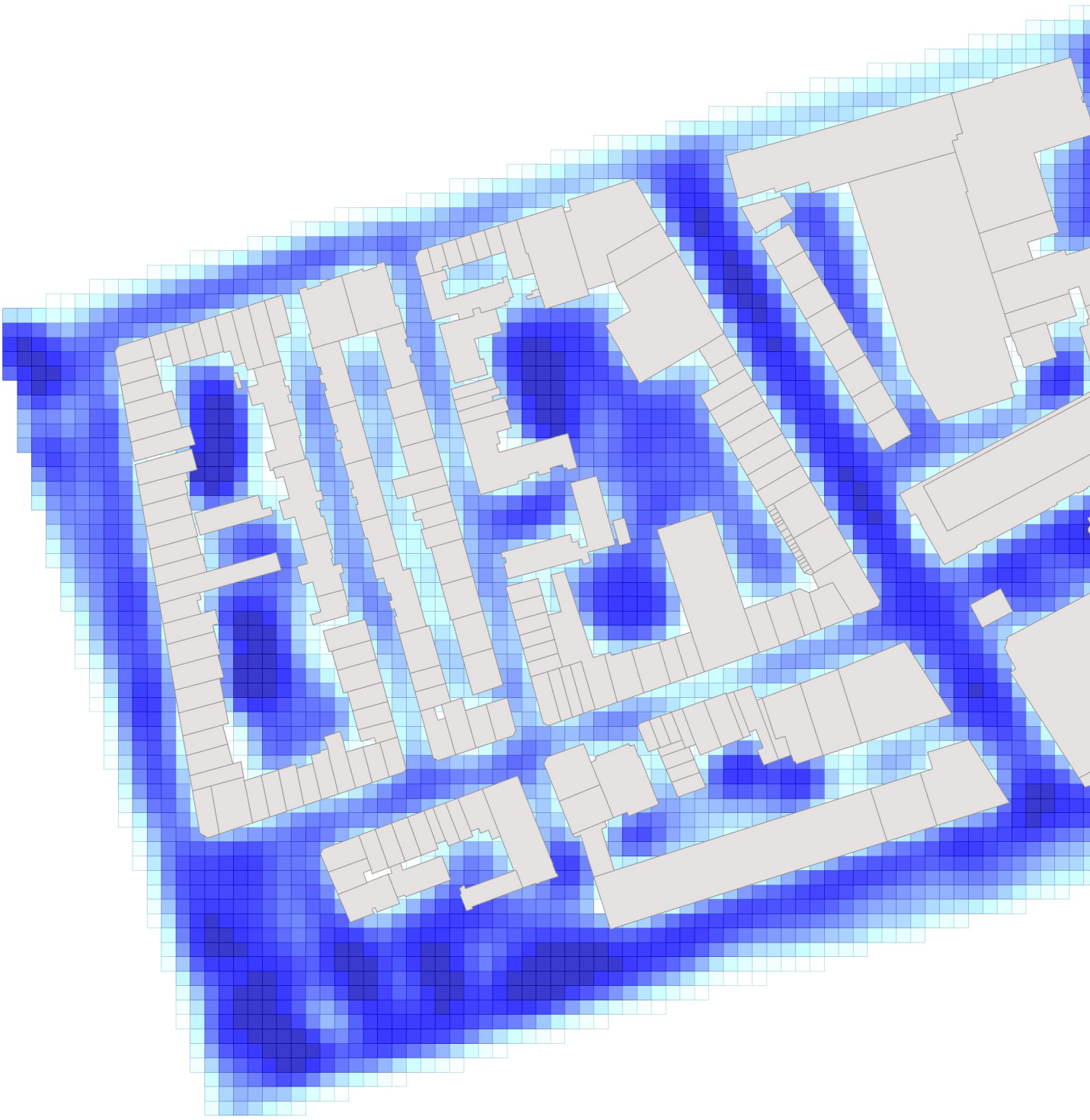

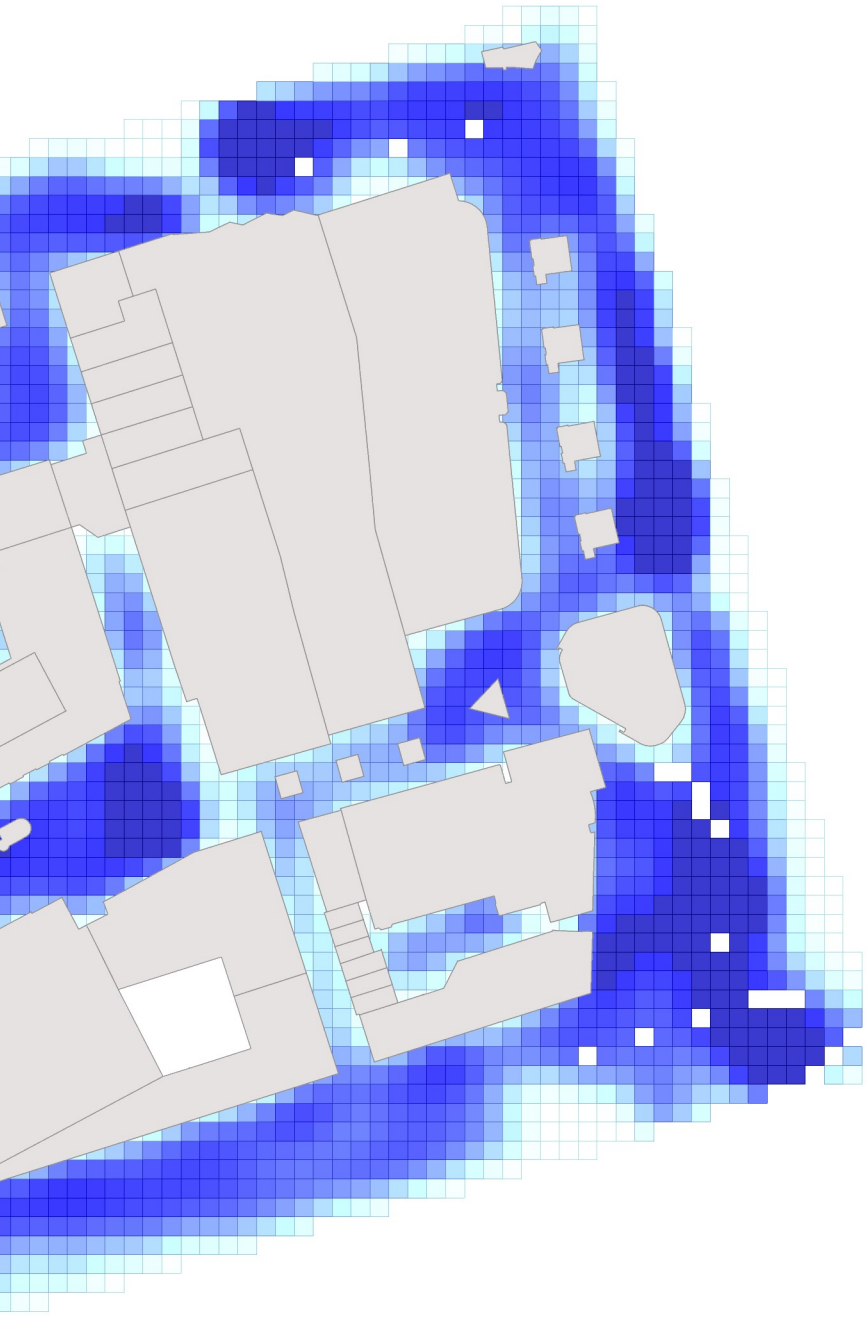

FLOOD DEPTH MAP

Area: Lijnbaan, Rotterdam

Condition: Existing BGI Adaptation

LEGENDS

0 20 40 80 120 m

Depth Distribution

> 0.3 m

< 0.05 m

North

Grounded Resilience

MSc Architecture, Urbanism, and Building Sciences

Vadya Dzauqiah | 6184030

APPENDIX

FM 02


7
6
5
4
3
2
1
A
B
C
D
E
UP1
UP2
UP3
UP4
UP5
UP6
UP7
UP8
UP9
UP10
UP11
UP12
UP 13
Karel Doormanstraat

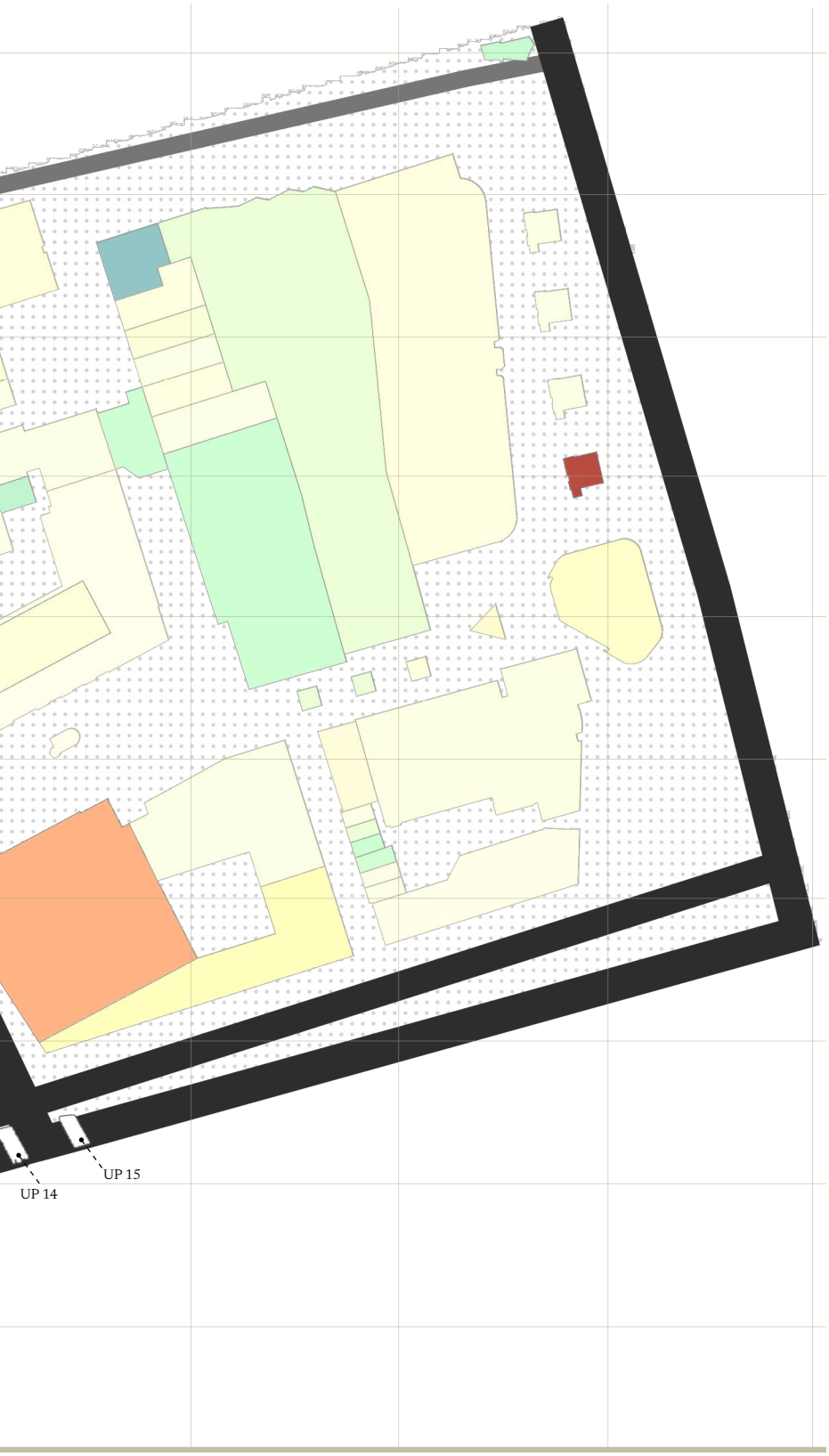

F G H

RESILIENCE SCORE MAP

Area: Lijnbaan, Rotterdam

Condition: Existing BGI Adaptation

LEGENDS

0 20 40 80 120 m

Score Distribution

> 0.94

< 0.82

North

Grounded Resilience

MSc Architecture, Urbanism, and Building Sciences

Vadya Dzauqiah | 6184030

APPENDIX

RS 02

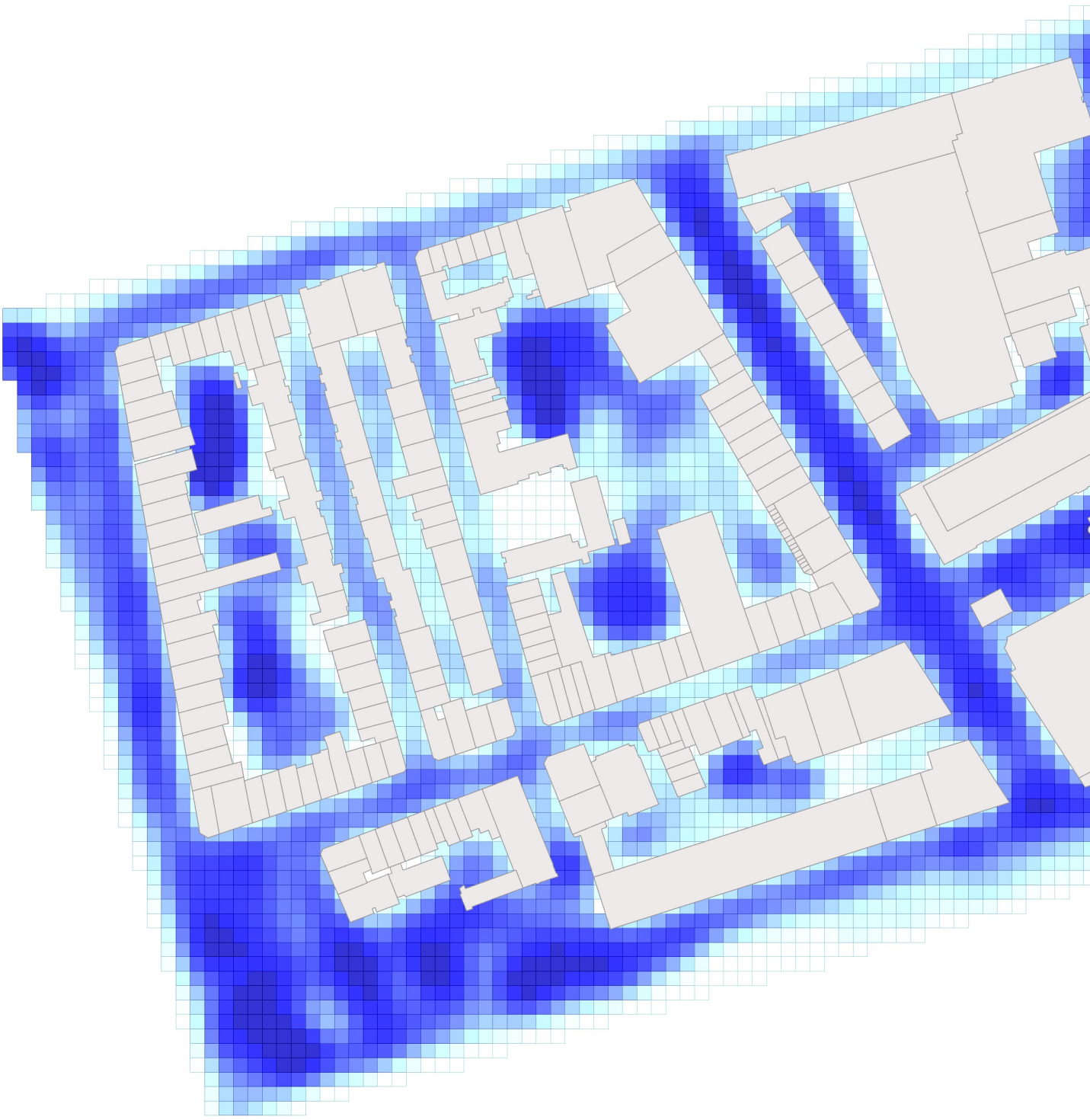

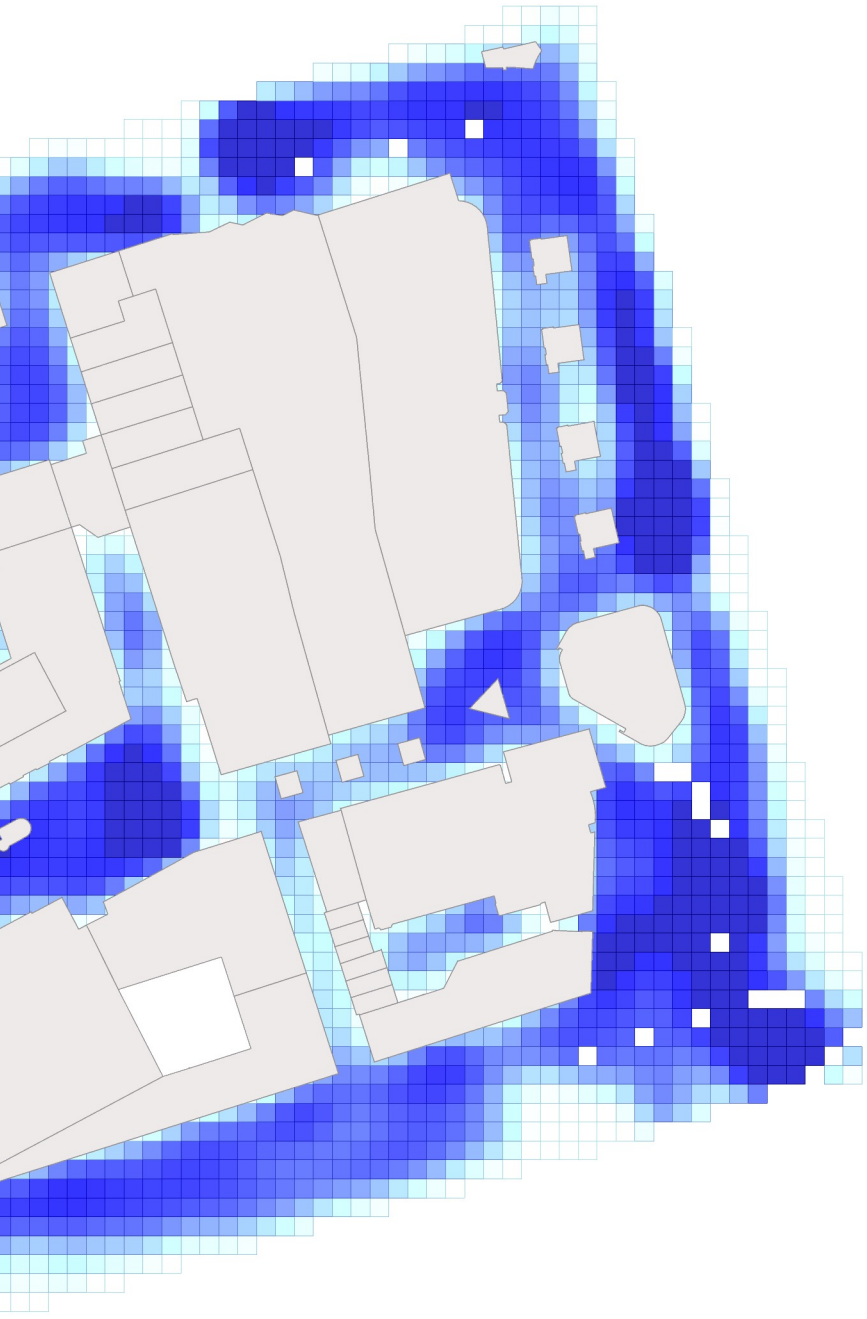

FLOOD DEPTH MAP

Area: Lijnbaan, Rotterdam

Condition: BGI Adaptation - Scenario 1

LEGENDS

0 20 40 80 120 m

Depth Distribution

> 0.3 m

< 0.05 m

North

Grounded Resilience

MSc Architecture, Urbanism, and Building Sciences

Vadya Dzauqiah | 6184030

APPENDIX

FM 03


7
6
5
4
3
2
1
A
B
C
D
E
UP1
BS1
BS2
BS3
BS4
BS5
BS6
BS7
BS8
BS9
BS10
PP1
Karel Doormanstraat

F G H

RESILIENCE SCORE MAP

Area: Lijnbaan, Rotterdam

Condition: BGI Adaptation - Scenario 1

LEGENDS

0 20 40 80 120 m

Score Distribution

> 0.94

< 0.82

North

Grounded Resilience

MSc Architecture, Urbanism, and Building Sciences

Vadya Dzauqiah | 6184030

APPENDIX

RS 03

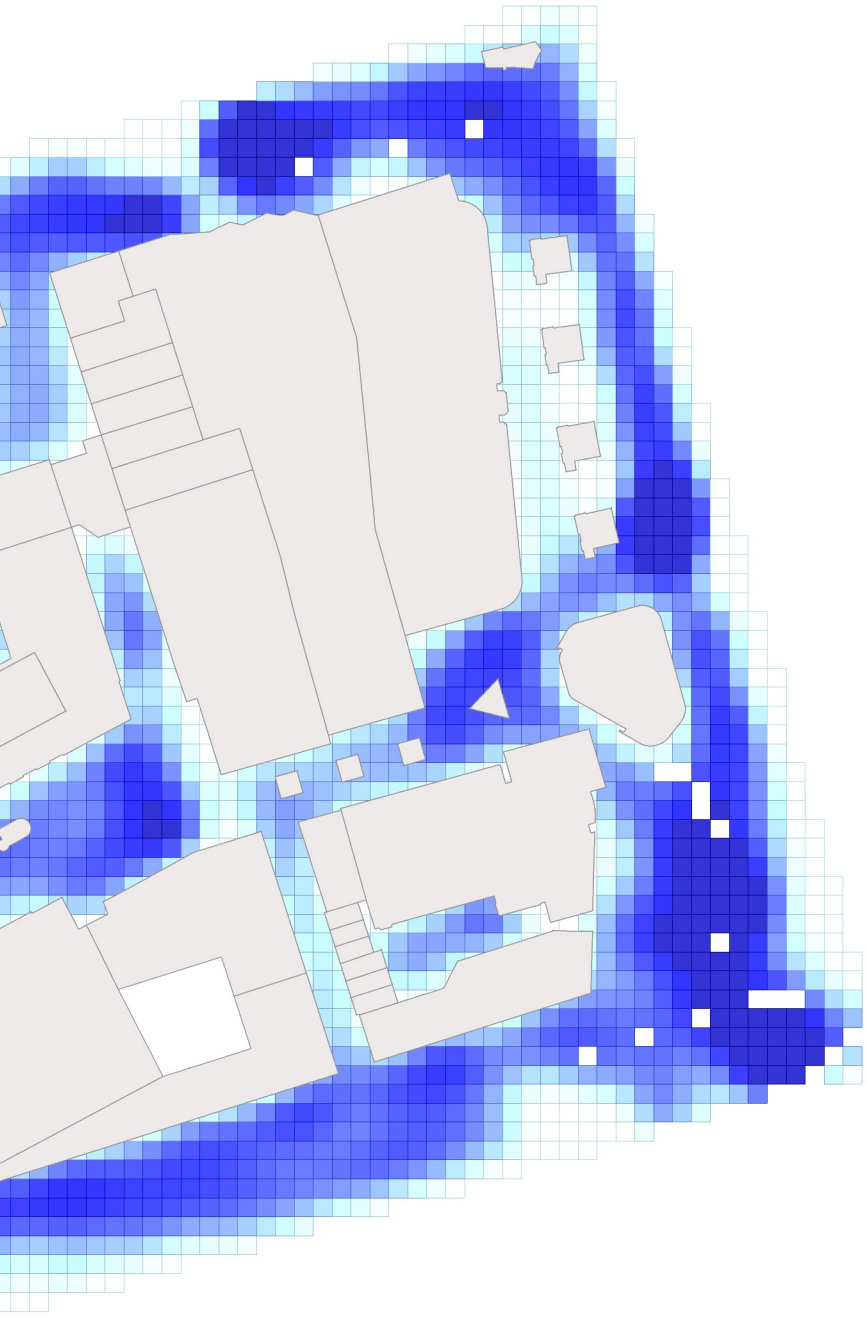

FLOOD DEPTH MAP

Area: Lijnbaan, Rotterdam

Condition: BGI Adaptation - Scenario 2

LEGENDS

0 20 40 80 120 m

Depth Distribution

> 0.3 m

< 0.05 m

North

Grounded Resilience

MSc Architecture, Urbanism, and Building Sciences

Vadya Dzauqiah | 6184030

APPENDIX

FM 04


7
6
5
4
3
2
1
A
B
C
D
E
UP1
PP 1
PP 2
PP 3
Karel Doormanstraat
BS 1
BS 2

RESILIENCE SCORE MAP

Area: Lijnbaan, Rotterdam

Condition: BGI Adaptation - Scenario 2

F G H

LEGENDS

0 20 40 80 120 m

Score Distribution

> 0.94

< 0.82

North

Grounded Resilience

MSc Architecture, Urbanism, and Building Sciences

Vadya Dzauqiah | 6184030

APPENDIX

RS 04